

**Project Report**

**EO-1-11**

**Earth Observing-1 Advanced Land Imager Flight  
Performance Assessment: Noise and Dark  
Current Stability During the First Year On Orbit**

**J.A. Mendenhall**

**M.D. Gibbs**

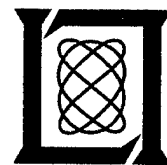
**19 August 2002**

---

**Lincoln Laboratory**

MASSACHUSETTS INSTITUTE OF TECHNOLOGY

*LEXINGTON, MASSACHUSETTS*



---

**Prepared for the National Aeronautics and Space Administration  
under Air Force Contract F19628-00-C-0002.**

**Approved for public release; distribution is unlimited.**

**20020905 029**


This report is based on studies performed at Lincoln Laboratory, a center for research operated by Massachusetts Institute of Technology. This work was sponsored by NASA/Goddard Space Flight Center under Air Force Contract F19628-00-C-0002. Opinions, interpretations, conclusions, and recommendations are those of the authors and are not necessarily endorsed by the United States Air Force.

This report may be reproduced to satisfy needs of U.S. Government agencies.

The ESC Public Affairs Office has reviewed this report, and it is releasable to the National Technical Information Service, where it will be available to the general public, including foreign nationals.

This technical report has been reviewed and is approved for publication.

FOR THE COMMANDER

  
Gary Tutungian  
Administrative Contracting Officer  
Plans and Programs Directorate  
Contracted Support Management

Non-Lincoln Recipients

PLEASE DO NOT RETURN

Permission is given to destroy this document  
when it is no longer needed.

Massachusetts Institute of Technology  
Lincoln Laboratory

**Earth Observing-1 Advanced Land Imager Flight Performance Assessment:  
Noise and Dark Current Stability During the First Year On Orbit**

*J.A. Mendenhall*  
*Group 99*  
*M.D. Gibbs*  
*Group 91*

Project Report EO-1-11

19 August 2002

Approved for public release; distribution is unlimited.

## ABSTRACT

The noise and dark current stability of the Advanced Land Imager during the first year on orbit (November 21, 2000 – November 21, 2001) are presented. Data have been separated into short-term and long-term periods. The analysis of short-term data indicate some SWIR detectors may drift up to ten digital numbers between the pre and post dark observations of a given data collection event. Analysis of long-term data suggest the VNIR dark current has deviated by less than ten digital numbers and some SCA SWIR dark current have increased by up to 200 digital numbers during the first year on orbit.

## TABLE OF CONTENTS

Abstract	iii
List of Illustrations	vii
List of Tables	xi
•	
1. INTRODUCTION	1
-	
2. DARK CURRENT	3
2.1 Short-Term	3
2.2 Long-Term	12
3. NOISE	53
3.1 Trending	53
4. DISCUSSION	65
REFERENCES	67

## LIST OF ILLUSTRATIONS

Figure No.		Page
1	Band 1p drift between pre and post dark current collections for January 15, 2001.	4
2	Band 1 drift between pre and post dark current collections for January 15, 2001.	4
3	Band 2 drift between pre and post dark current collections for January 15, 2001.	5
4	Band 3 drift between pre and post dark current collections for January 15, 2001.	5
5	Band 4 drift between pre and post dark current collections for January 15, 2001.	6
6	Band 4p drift between pre and post dark current collections for January 15, 2001.	6
7	Band 5p drift between pre and post dark current collections for January 15, 2001.	7
8	Band 5 drift between pre and post dark current collections for January 15, 2001.	7
9	Band 7 drift between pre and post dark current collections for January 15, 2001.	8
10	Panchromatic Band drift between pre and post dark current collections for January 15, 2001.	8
11	Band 7 drift between pre and post dark current collections for January 15, 2001.	9
12	Band 7 drift between pre and post dark current collections for January 15, 2001.	10
13	Band 7 drift between pre and post dark current collections for January 15, 2001.	10
14	Dark current trending for Band 1p odd detectors.	13
15	Dark current trending for Band 1p even detectors.	14
16	Dark current trending for Band 1 odd detectors.	15
17	Dark current trending for Band 1 even detectors.	16
18	Dark current trending for Band 2 odd detectors.	17
19	Dark current trending for Band 2 even detectors.	18
20	Dark current trending for Band 3 odd detectors.	19
21	Dark current trending for Band 3 even detectors.	20
22	Dark current trending for Band 4 odd detectors.	21
23	Dark current trending for Band 4 even detectors.	22

## LIST OF ILLUSTRATIONS (CONTINUED)

Figure No.		Page
24	Dark current trending for Band 4p odd detectors.	23
25	Dark current trending for Band 4p even detectors.	24
26	Dark current trending for Band 5p odd detectors.	25
27	Dark current trending for Band 5p even detectors.	26
28	Dark current trending for Band 5 odd detectors.	27
29	Dark current trending for Band 5 even detectors.	28
30	Dark current trending for Band 7 odd detectors.	29
31	Dark current trending for Band 7 even detectors.	30
32	Dark current trending for Panchromatic Band tri-read #1 odd detectors.	31
33	Dark current trending for Panchromatic Band tri-read #2 odd detectors.	32
34	Dark current trending for Panchromatic Band tri-read #3 odd detectors.	33
35	Dark current trending for Panchromatic Band tri-read #1 even detectors.	34
36	Dark current trending for Panchromatic Band tri-read #2 even detectors.	35
37	Dark current trending for Panchromatic Band tri-read #3 even detectors.	36
38	Dark current drifting for Band 1p over 10 day period after an on-orbit bakeout.	38
39	Dark current drifting for Band 1 over 10 day period after an on-orbit bakeout.	39
40	Dark current drifting for Band 2 over 10 day period after an on-orbit bakeout.	40
41	Dark current drifting for Band 3 over 10 day period after an on-orbit bakeout.	41
42	Dark current drifting for Band 4 over 10 day period after an on-orbit bakeout.	42
43	Dark current drifting for Band 4p over 10 day period after an on-orbit bakeout.	43
44	Dark current drifting for Band 5p over 10 day period after an on-orbit bakeout.	44
45	Dark current drifting for Band 5 over 10 day period after an on-orbit bakeout.	45
46	Dark current drifting for Band 7 over 10 day period after an on-orbit bakeout.	46
47	Dark current drifting for the panchromatic band over 10 day period after an on-orbit bakeout	47

## LIST OF ILLUSTRATIONS (CONTINUED)

Figure No.		Page
48	Dark current drifting for Band 5p between Jan. 2001 and Nov. 2001.	48
49	Dark current drifting for Band 5 between Jan. 2001 and Nov. 2001.	49
50	Dark current drifting for Band 7 odd detectors between Jan. 2001 and Nov. 2001.	50
51	Dark current drifting for Band 7 even detectors between Jan. 2001 and Nov. 2001.	51
52	Noise trending for Band 1p.	54
53	Dark current and noise scatter plot for Band 1p.	54
54	Noise trending for Band 1.	55
55	Dark current and noise scatter plot for Band 1.	55
56	Noise trending for Band 2.	56
57	Dark current and noise scatter plot for Band 2.	56
58	Noise trending for Band 3.	57
59	Dark current and noise scatter plot for Band 3.	57
60	Noise trending for Band 4.	58
61	Dark current and noise scatter plot for Band 4.	58
62	Noise trending for Band 4p.	59
63	Dark current and noise scatter plot for Band 4p.	59
64	Noise trending for Band 5p.	60
65	Dark current and noise scatter plot for Band 5p.	60
66	Noise trending for Band 5.	61
67	Dark current and noise scatter plot for Band 5.	61
68	Noise trending for Band 7.	62
69	Dark current and noise scatter plot for Band 7.	62
70	Noise trending for the Panchromatic Band.	63
71	Dark current and noise scatter plot for the Panchromatic Band.	63



## LIST OF TABLES

Table No.		Page
1	Relative Time Sequence For a Typical DCE	12

## 1. INTRODUCTION

The Advanced Land Imager (ALI) is a technology demonstration instrument for future wide field-of-view, pushbroom, land-imaging systems<sup>1,2</sup>. An important aspect of this demonstration is instrument stability. This document provides the trending of detector noise and dark current during the first 12 months on-orbit (November 21, 2000 – November 21, 2001). Data will be trended for each of the ten spectral bands and each of the four sensor chip assemblies.

Dark current trending for the first sixty days on orbit have been presented previously<sup>3</sup>.

## **2. DARK CURRENT**

The dark current stability of the Advanced Land Imager has been analyzed using dark current data collected as a part of daily Earth scene observations. During a typical data collection event or DCE, two seconds of dark current are collected before and after the Earth scene is imaged. These data are used to establish dark current baselines for all detectors for the corresponding observation and are also used to monitor the noise of the focal plane over time. The stability of the ALI dark current has been divided into two epochs, short-term and long-term.

### **2.1 SHORT-TERM**

The short-term dark current stability of any instrument is important for accurate dark current subtraction as a part of the radiometric calibration of a scientific observation. Ideally, the dark current of an instrument will be absolutely stable during an observation, requiring a single correction for each detector to account for dark current levels. The short-term dark current stability of the Advanced Land Imager has been examined by comparing levels at the beginning of a data collection event to levels at the end of a data collection event. Initial dark current levels are defined as the mean levels of each detector during the dark reference period prior to the science data acquisition. Final dark current levels are defined as the mean levels of each detector during the dark reference period after the science data acquisition. The differences between the two periods have been calculated for a DCE on January 15, 2001, one day after the focal plane was purged of contamination through boil-off. The results are presented in Figures 1–10. When reading the values in these figures, it should be recalled that the saturation level for all detectors is 4096 digital counts.

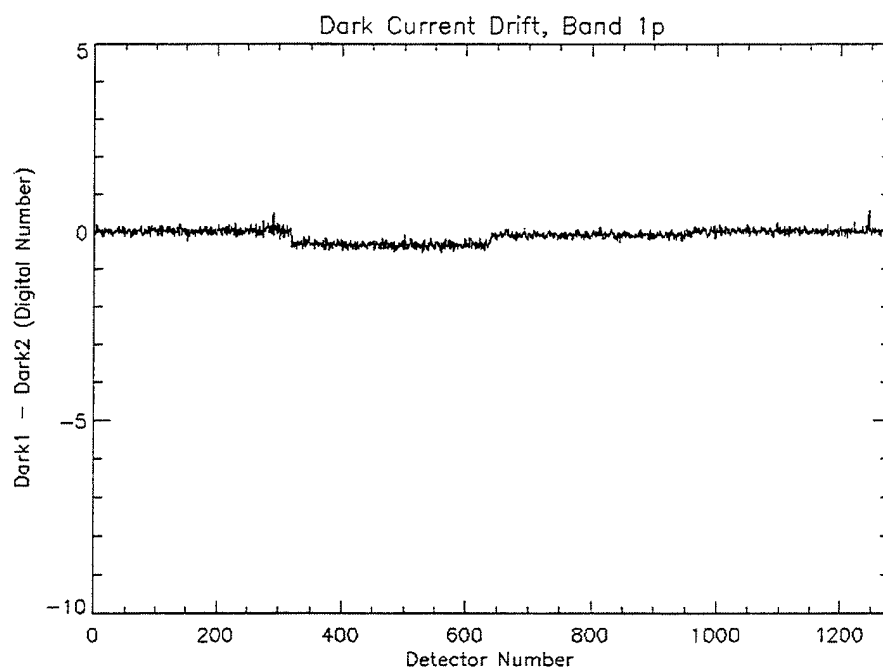


Figure 1. Band 1p drift between pre and post dark current collections for January 15, 2001.

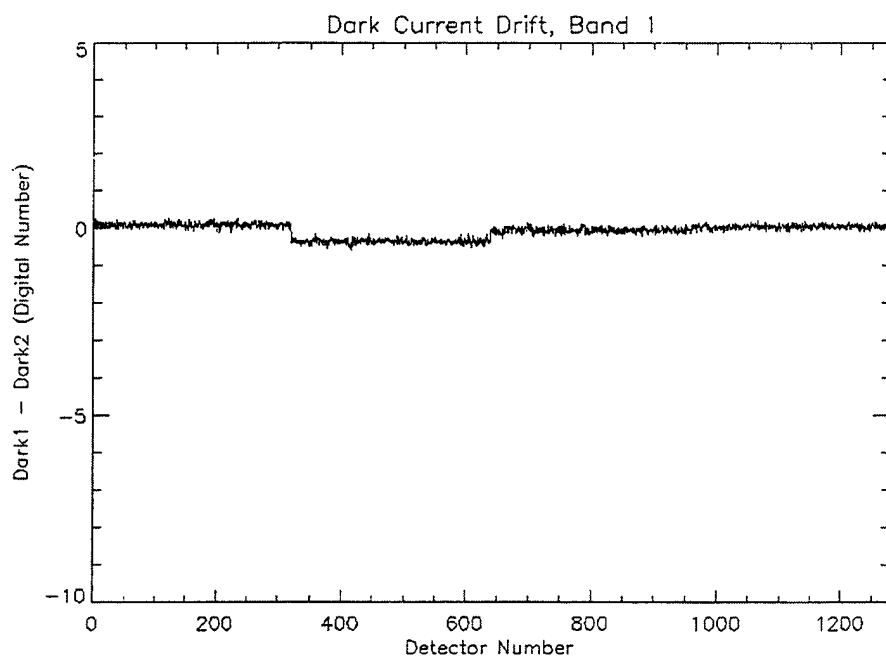


Figure 2. Band 1 drift between pre and post dark current collections for January 15, 2001.

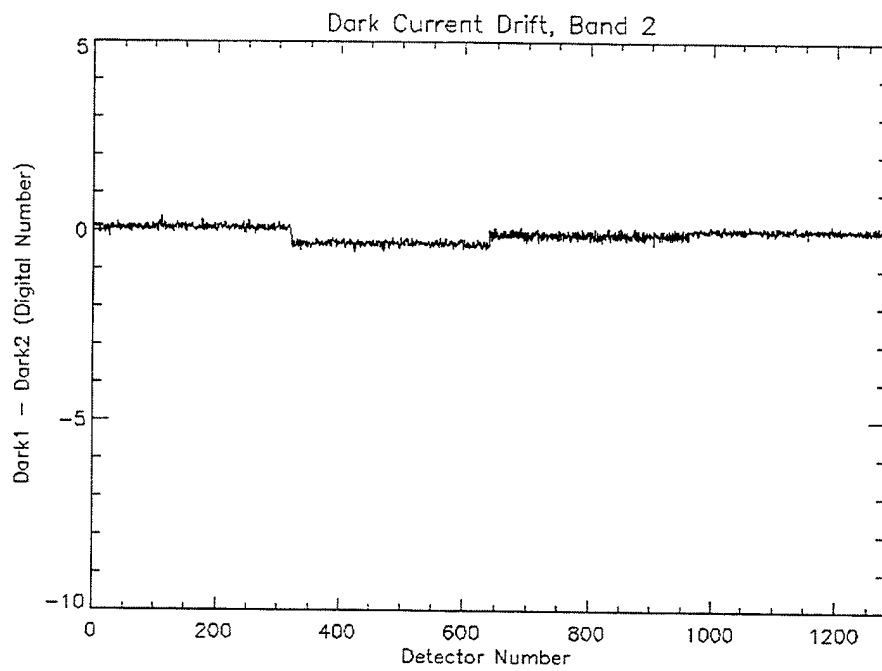


Figure 3. Band 2 drift between pre and post dark current collections for January 15, 2001.

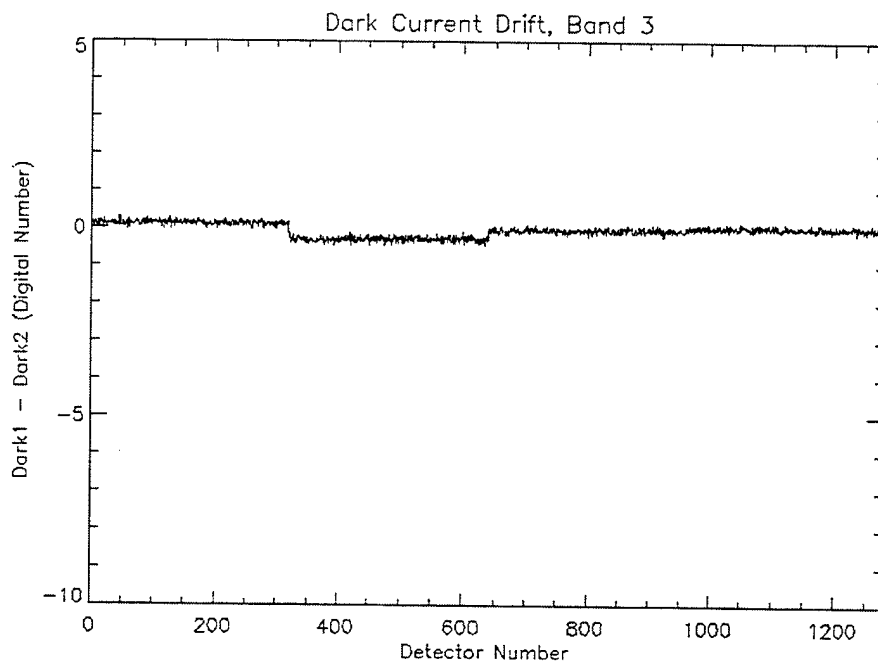


Figure 4. Band 3 drift between pre and post dark current collections for January 15, 2001.

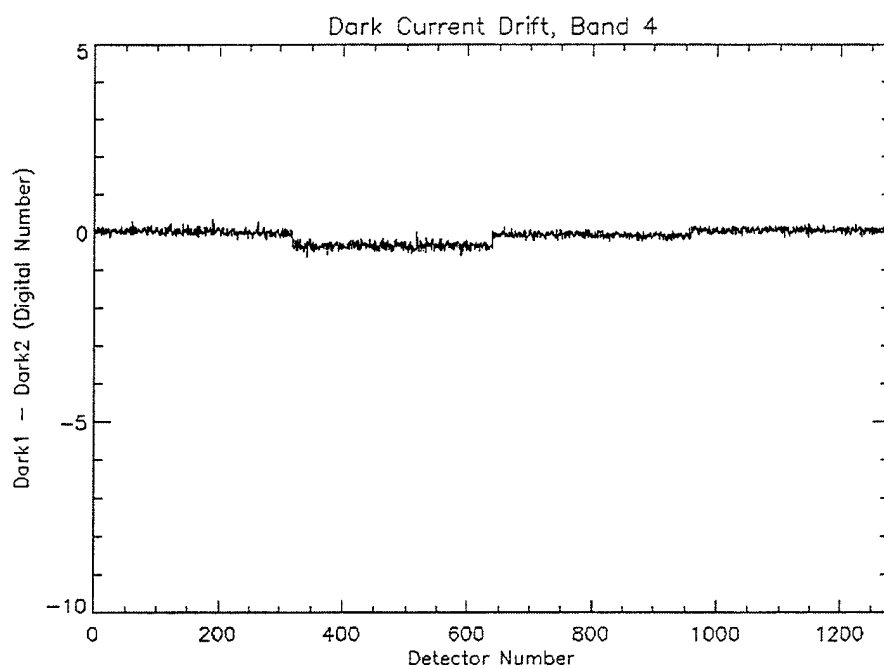


Figure 5. Band 4 drift between pre and post dark current collections for January 15, 2001.

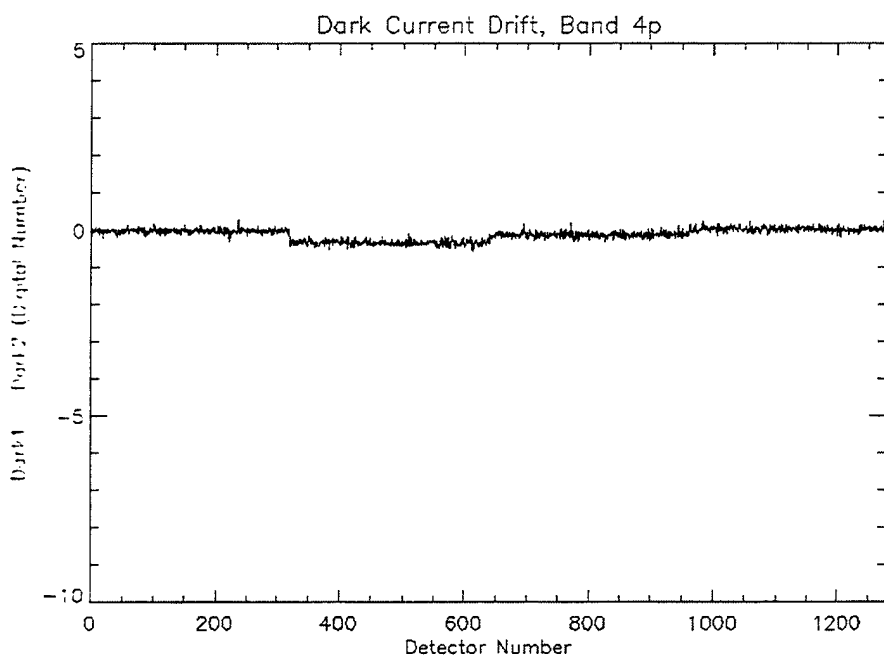


Figure 6. Band 4p drift between pre and post dark current collections for January 15, 2001.

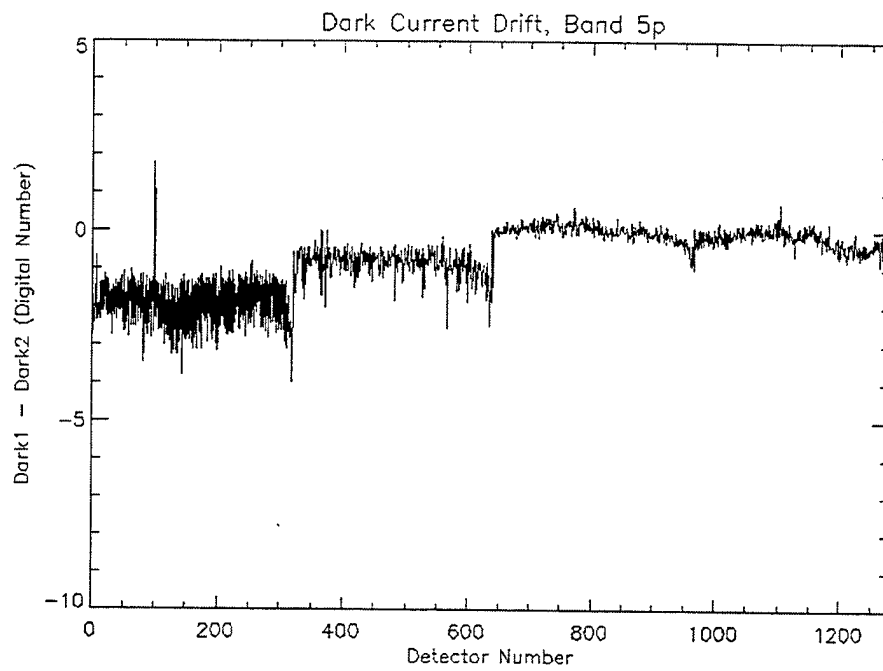


Figure 7. Band 5p drift between pre and post dark current collections for January 15, 2001.

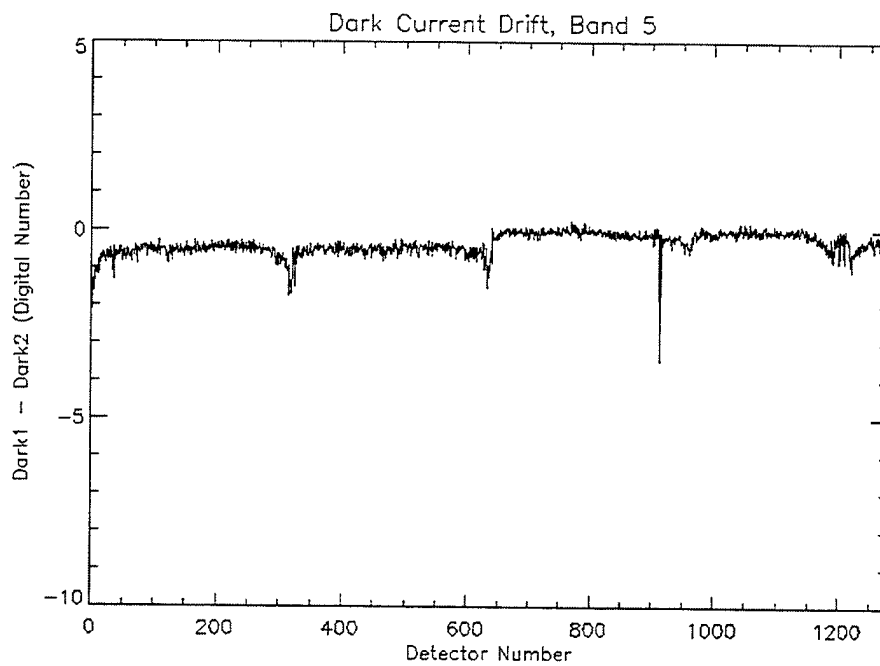


Figure 8. Band 5 drift between pre and post dark current collections for January 15, 2001.

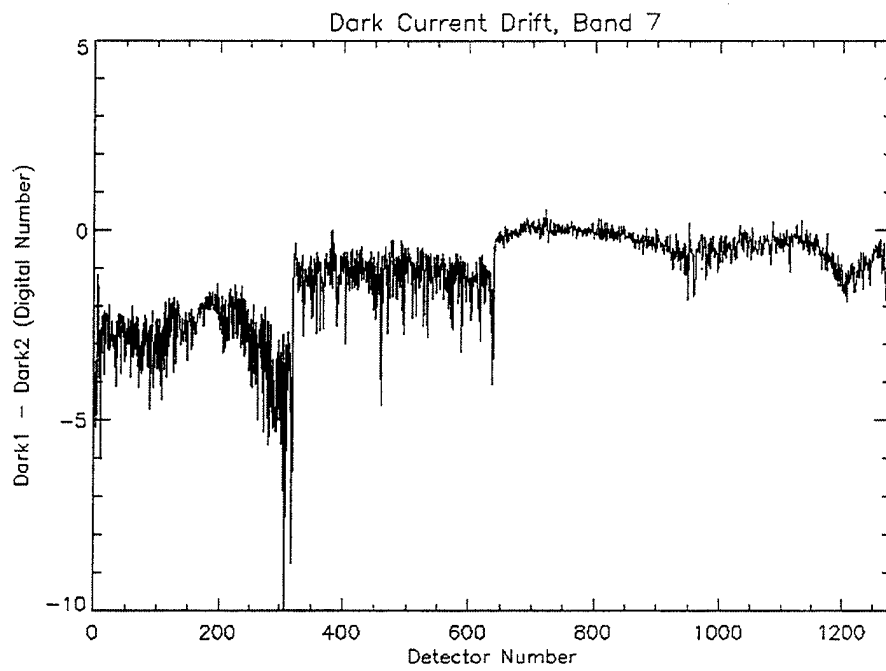


Figure 9. Band 7 drift between pre and post dark current collections for January 15, 2001.

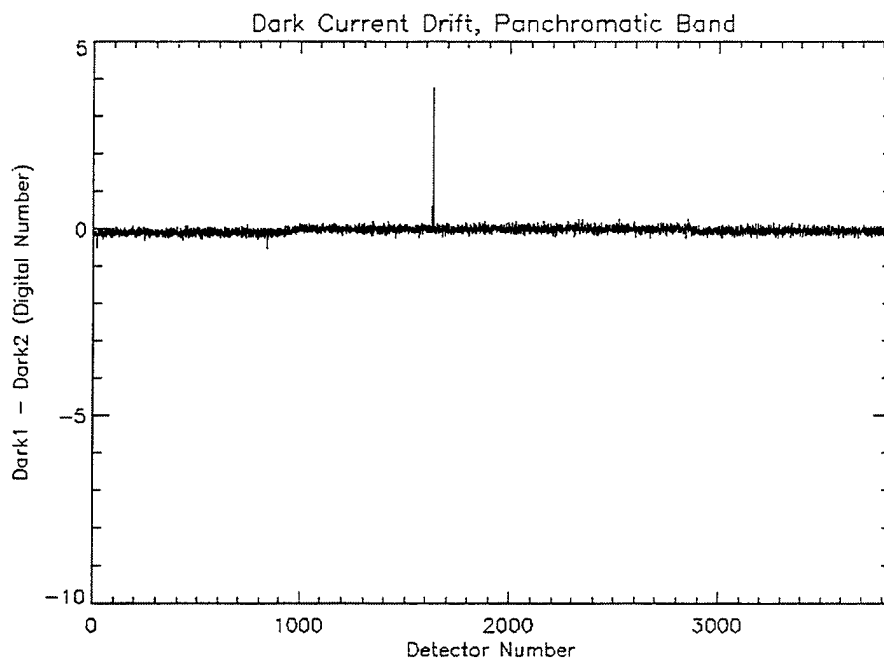


Figure 10. Panchromatic Band drift between pre and post dark current collections for January 15, 2001.



The data demonstrate excellent stability ( $<1$  DN) of the VNIR and Panchromatic detectors between dark current collection periods. Band 5p detectors drift up to 3 DN in SCA 1 and 2 DN in SCA 2. Band 5 exhibits little drifting, with slight increases towards the edges of SCA 1 and 2. Detectors 911 and 913 also show  $\sim 4$  DN variability but have been previously identified as anomalous detectors with excess dark current and noise<sup>4</sup>. Band 7 exhibits the largest dark current drift: 1-2 DN for SCA 3 and 4, 2-3 DN for SCA 2, and 2-5 DN for SCA 1.

To investigate the source of this drifting, a special dark current collection sequence, obtained on February 3, 2001, was analyzed. This test consisted of powering the ALI focal plane over the north pole of the Earth and taking dark current readings every 5 minutes over the course of  $\frac{1}{2}$  orbit<sup>5</sup>. The mean dark current values for each detector of every band were calculated for two of the dark current collections, separated by five minutes. The differences between VNIR means are less than 1 DN. The differences between SWIR means are presented in Figures 11–13.

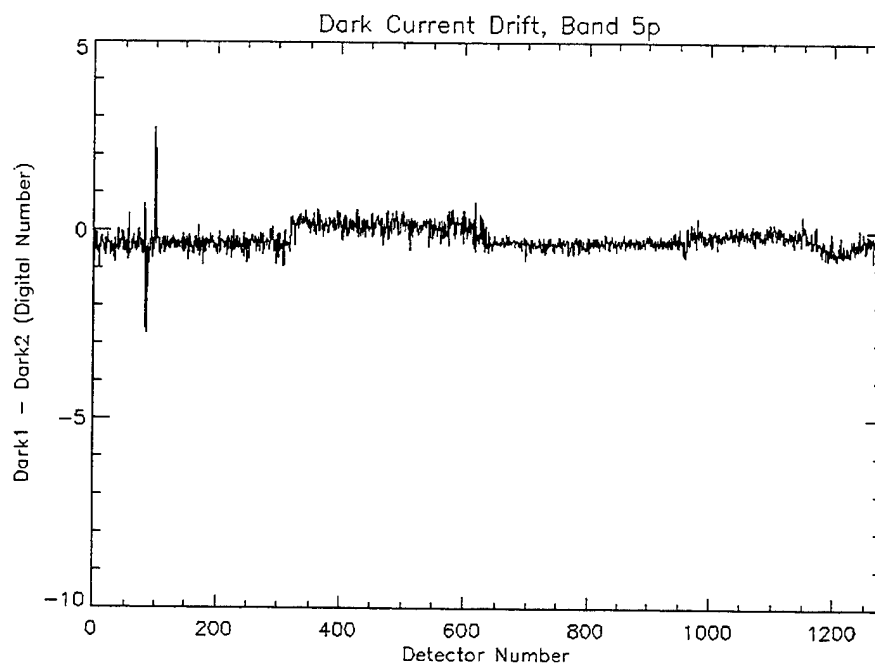


Figure 11. Band 5p drift between two dark current measurements from the February 3, 2001 special dark collection.

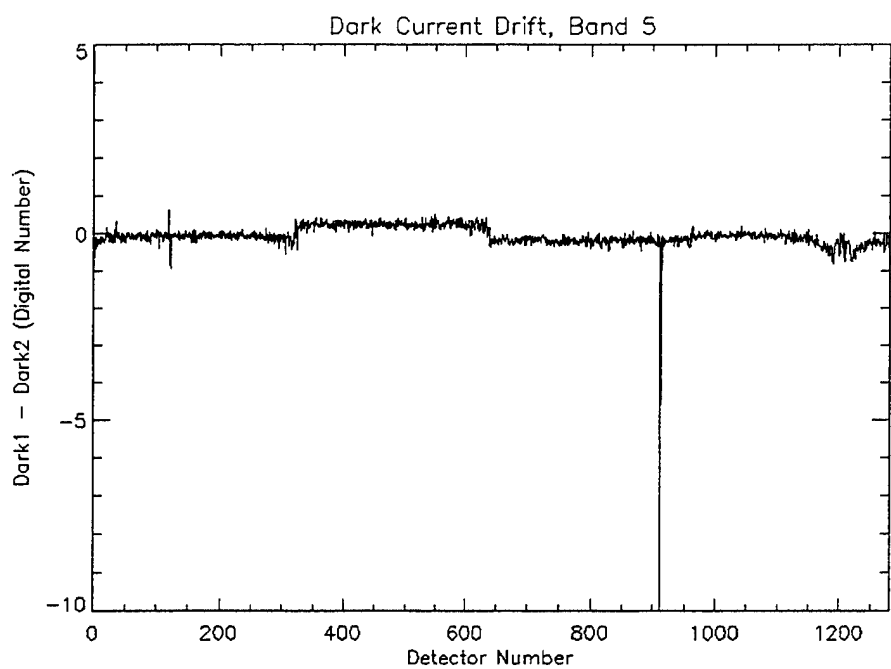


Figure 12. Band 5 drift between two dark current measurements from the February 3, 2001 special dark collection.

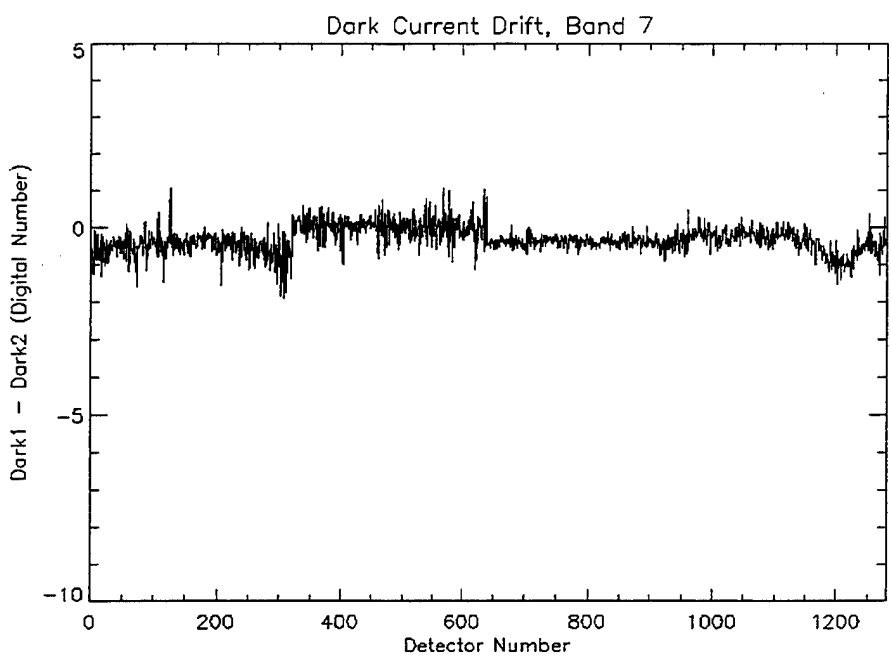


Figure 13. Band 7 drift between two dark current measurements from the February 3, 2001 special dark collection.

The VNIR and panchromatic data, obtained from the special dark current collection, demonstrate excellent stability between observations. This is in agreement with the nominal DCE dark current drift between pre and post-science dark current collections. However, the special dark collections also indicate little dark current drift for the SWIR bands as well. These data indicate much better dark current stability for this observation, when contrasted to the nominal DCE data.

A possible source of the different behavior of the SWIR detectors during nominal DCEs is heating of the focal plane by reflected sunlight. Table 1 provides a timing sequence for a typical ALI data collection event. This sequence has been normalized such that the beginning of the science data collection occurs at time 0:00. For a typical DCE, the first dark collection occurs three minutes and eight seconds before the Earth observation begins. The significant delay is the time required for the EO-1 Attitude Control System to stabilize the spacecraft after the ALI aperture cover is opened. The second dark collection occurs fifty-seven seconds after the Earth observation ends. Between the -3:05 and 0:39 periods, the focal plane is illuminated by reflected sunlight. During the special dark collections, the aperture cover remains closed, eliminating this source of heating. However, a good instrument thermal control system would compensate for any heating effects by reducing the heat load on the focal plane through whatever cooling mechanism is available. Unfortunately, the ALI does not have the ability to adjust the focal plane temperature while the focal plane is powered. Shortly after instrument assembly, it was discovered that when the Focal Plane Electronics (FPE) Operational Power is turned on, the FPA temperature control loop is effectively disabled because the feedback signal is corrupted by noise generated in the FPE. It is assumed that this comes about because the DT570 diode temperature sensor on the FPA rectifies AC noise and a large offset is imposed on the signal. The FPE thermal control system reacts by reducing the FPA conductor bar heater power to zero. In order to overcome this, the ALI thermal control software has been modified to induce the FPA thermal control system to supply an amount of power during stand-by mode (when the focal plane is not powered), which is equal to the electronic dissipation in the FPA resulting from the operation of the SCAs (data collection mode). This level is 0.4 W. When the focal plane is powered, the heat lost by disabling the FPA temperature control loop is replaced by the electronic dissipation in the FPA. In addition, the last state of the ALI thermal control system, when the focal plane is powered, is frozen. Thus, the power provided to the FPA remains constant during data collection and during stand-by mode, thereby maintaining the thermal stability of the instrument throughout an orbit. In laboratory measurements, it was established that 5 to 6 minutes after focal plane activation, the worst case of dark current drift (Band 7) was 0.5 counts. However, it is postulated that the thermal load created by reflected sunlight during a nominal DCE is not properly accounted for by this system, resulting in the slight dark current drifting of some SWIR detectors during an Earth observation.

In order to minimize the effects of SWIR baseline drifting during Earth observing portions of a DCE, dark current values obtained from the second dark reference period or an interpolation between the first and second periods should be used when accounting for detector biases. Bias levels obtained solely from the first reference period should not be used.

**TABLE 1**  
**Relative Time Sequence For a Typical DCE**

Time (Relative to DCE)	Event
-7:08	Power Focal Plane
-3:08	Dark #1
-3:05	Open Aperture Cover
0:00	Start Earth Observation
0:28	Stop Earth Observation
0:39	Close Aperture Cover
0:57	Dark #2
1:06	Reference Lamp Observation
1:26	Power Off Focal Plane

## 2.2 LONG-TERM

The long-term dark current stability of the instrument has been examined by trending dark current data from all DCEs during the first year the ALI was in-orbit. For each data collection event, the data from the second dark period is used for the dark current trending.

The focal plane has been divided into several sections for this analysis, owing to the different dark current produced by different detectors. Odd and even detectors are treated separately for all bands. Results for the Panchromatic band have been additionally divided by tri-reads (each Panchromatic detector is read three times for each Multispectral detector read and each tri-read results in a different dark current value for each detector.). SCA 4 for the SWIR bands has been divided into four sections to account for the enhanced dark current values observed near detector 1200. Finally, the dark current has been calculated as the mean of individual detector dark current values.

The results of the ALI focal plane dark current trending for Bands 1p, 1, 2, 3, 4, 4p are provided in Figures 14–25. Each figure depicts the results of an individual band. Within each figure, the results of odd and even detectors for each sensor chip assembly are provided. The results of dark current trending for Bands 5p, 5, and 7 are provided in Figures 26–31. Each figure depicts the results of an individual band. Within each figure, the results of odd and even detectors for each sensor chip assembly are provided. SCA 4 is further divided into four quadrants, owing to the rapid change in dark current near the previously identified ‘hot spot’ near detector 1200<sup>4</sup>. Finally, the results of dark current trending for the Panchromatic Band are provided in Figures 32–37. Each figure depicts the results of an individual tri-read. Within each figure, the results of odd and even detectors for each sensor chip assembly are provided.

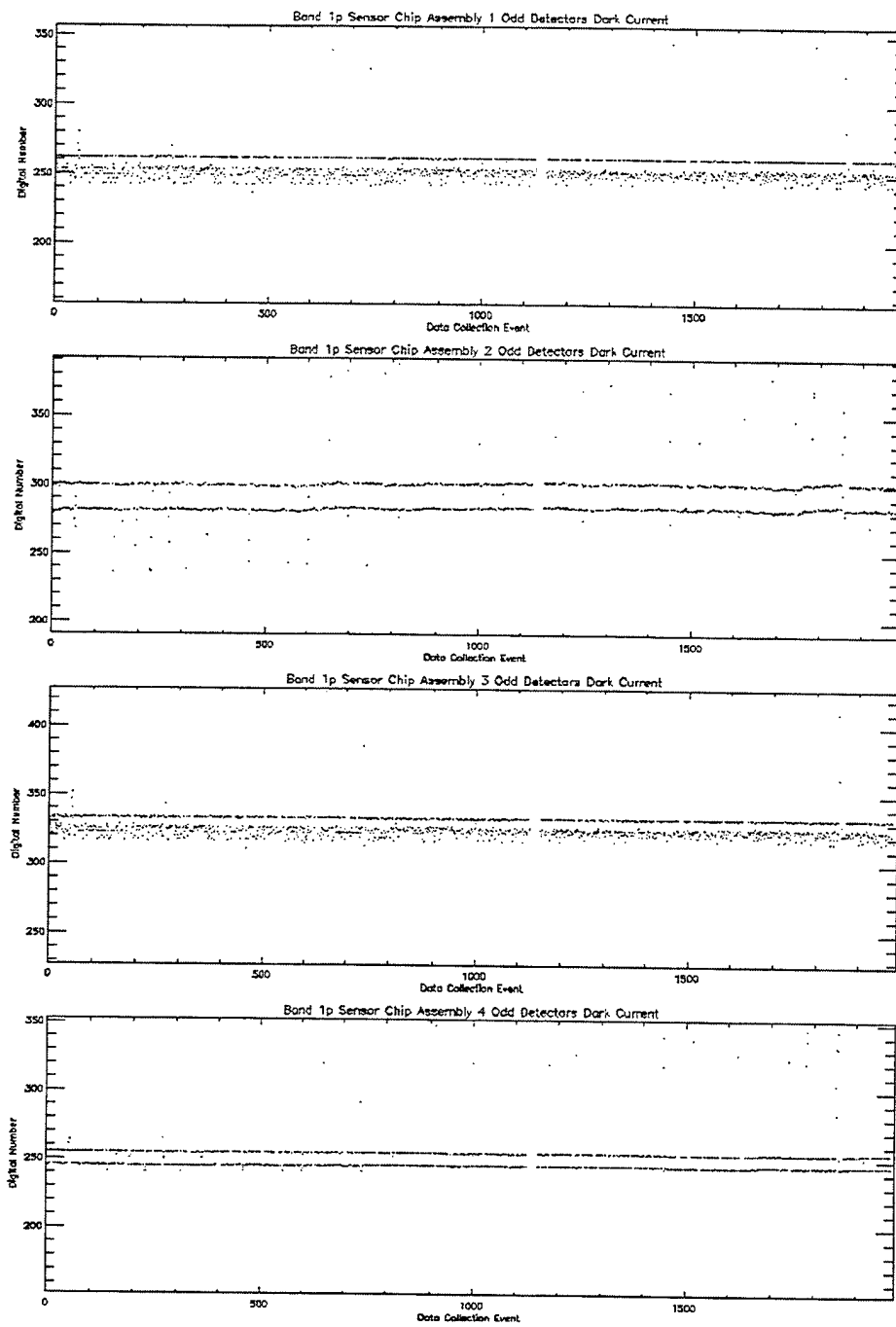
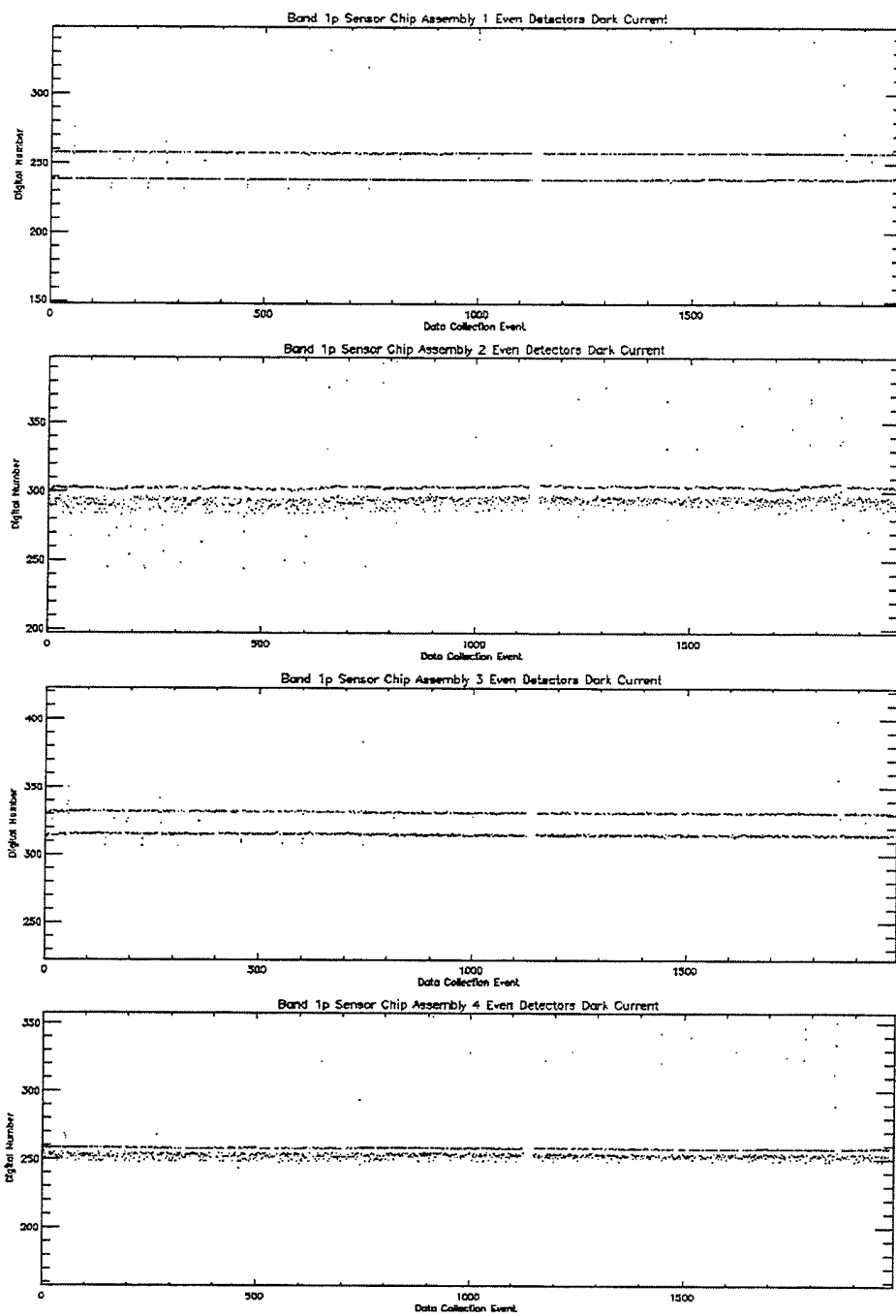


Figure 14. Dark current trending for Band 1p odd detectors.



*Figure 15. Dark current trending for Band 1p even detectors.*

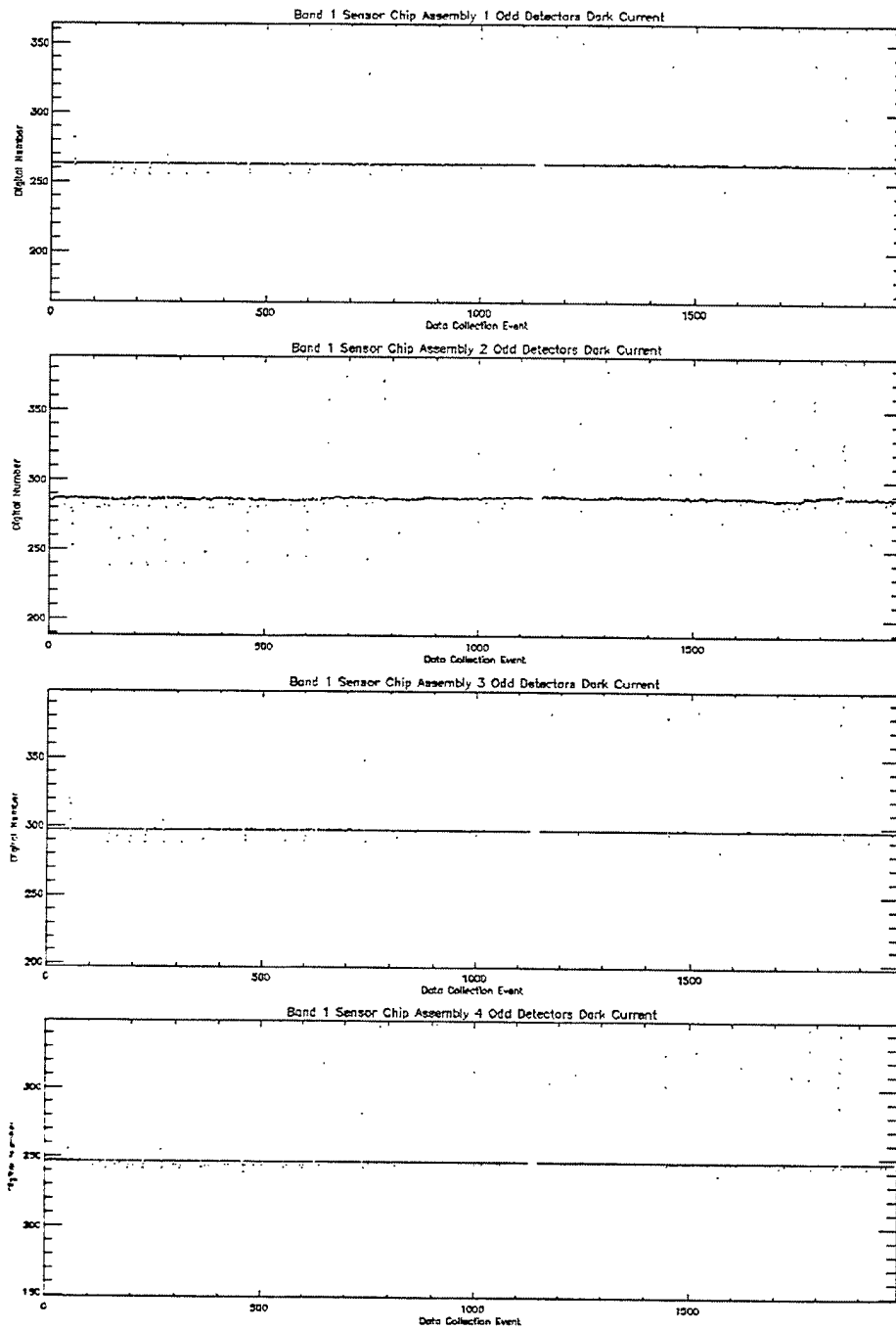
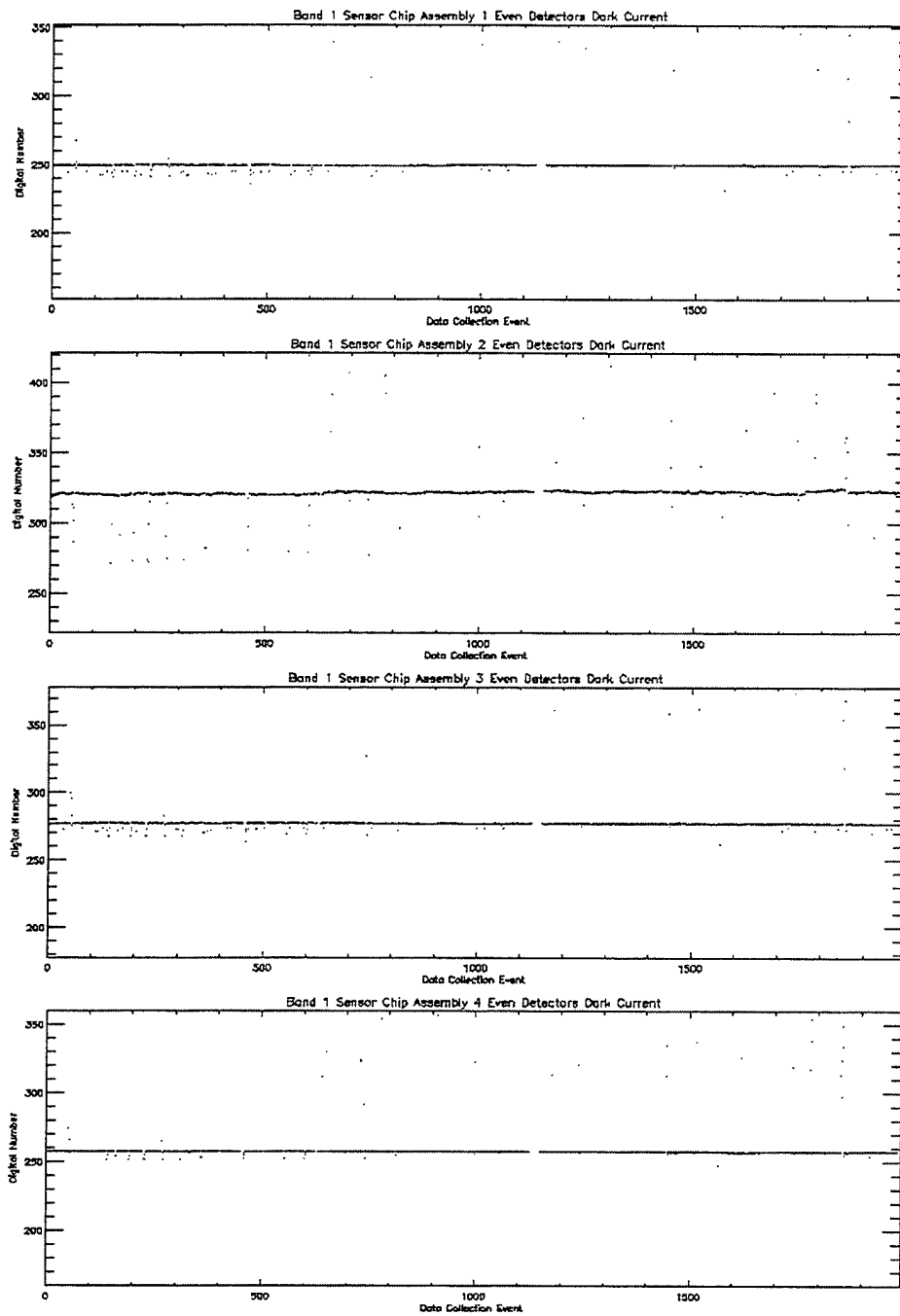


Figure 16. Dark current trending for Band 1 odd detectors.



*Figure 17. Dark current trending for Band 1 even detectors.*



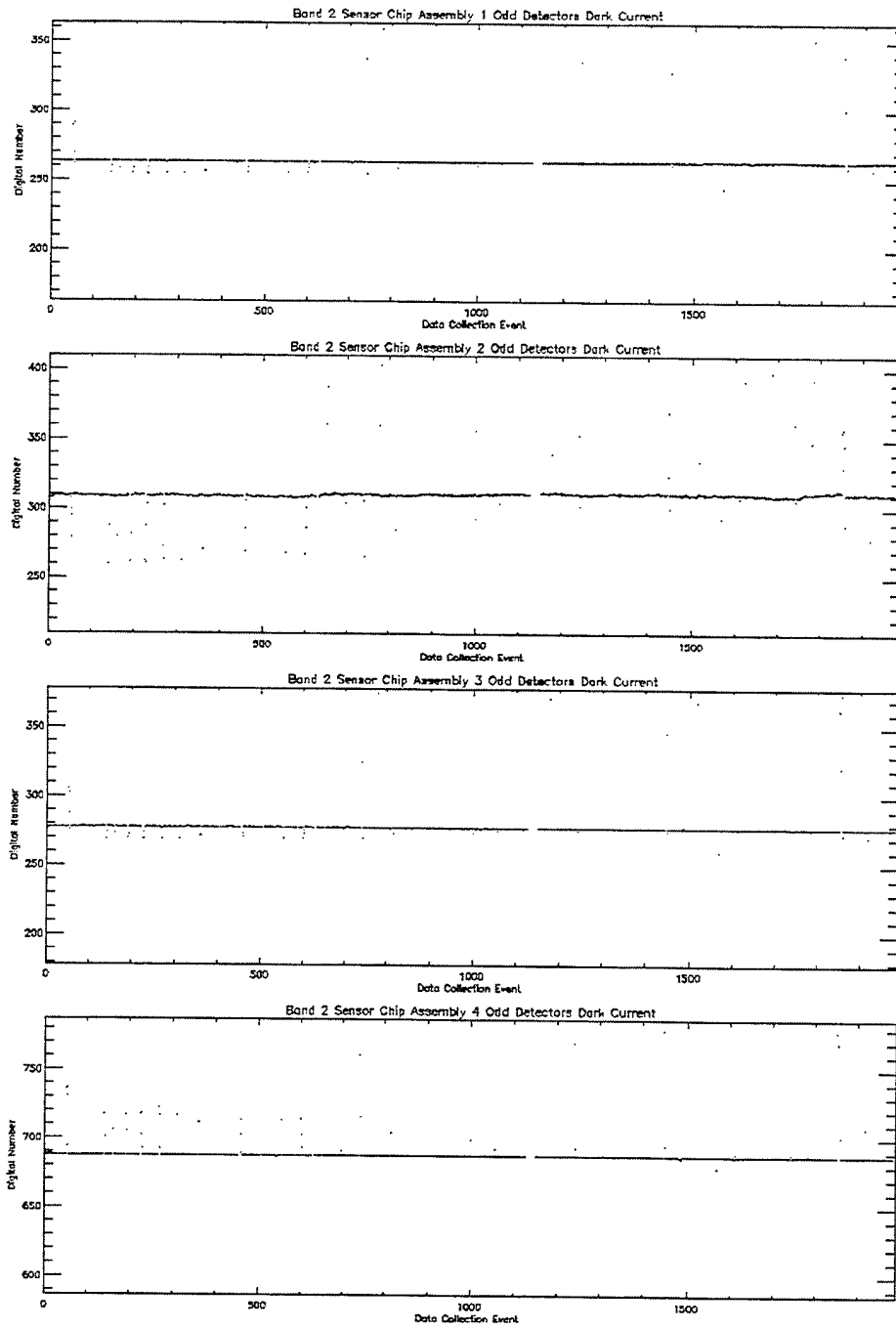


Figure 18. Dark current trending for Band 2 odd detectors.

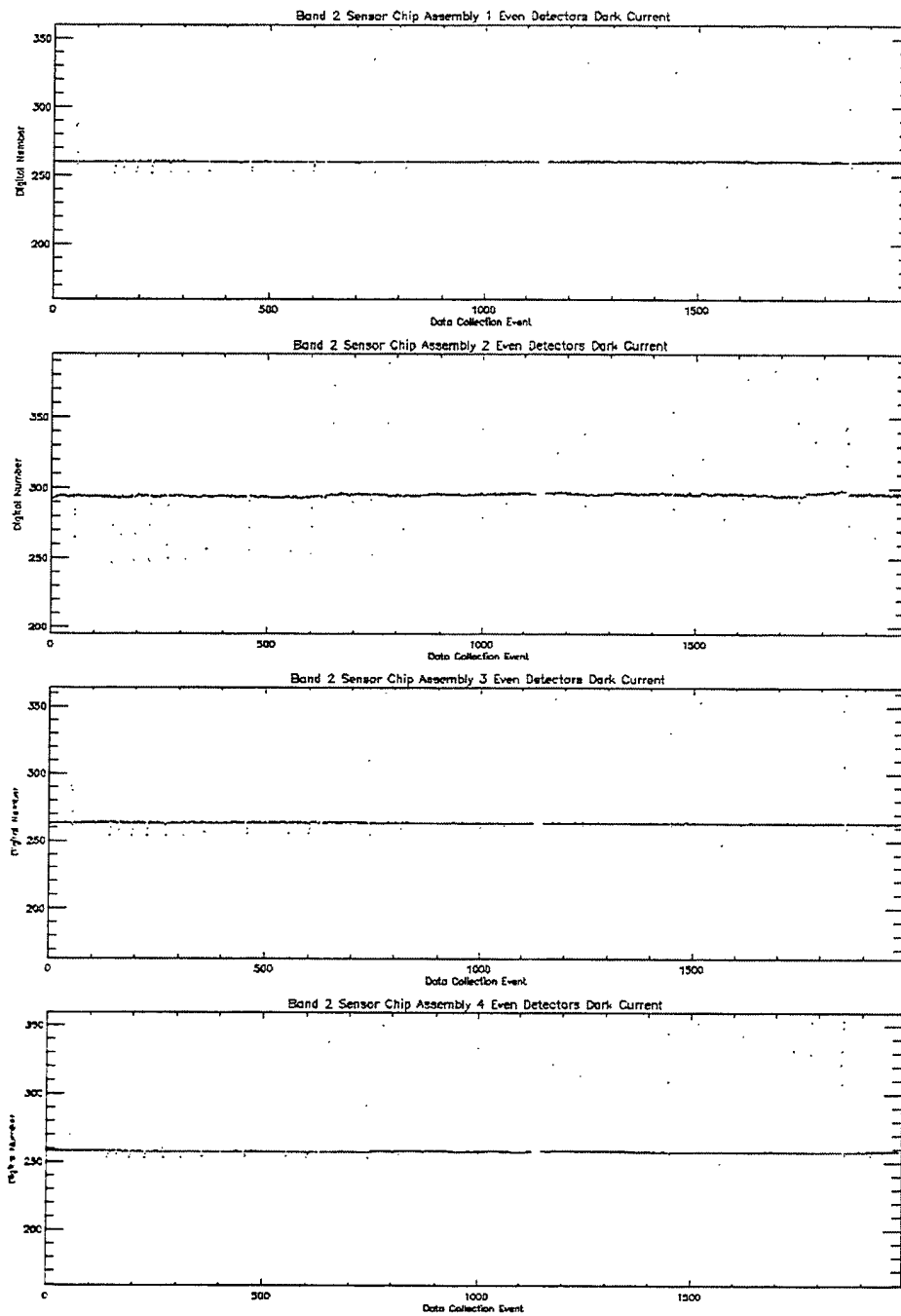


Figure 19. Dark current trending for Band 2 even detectors.

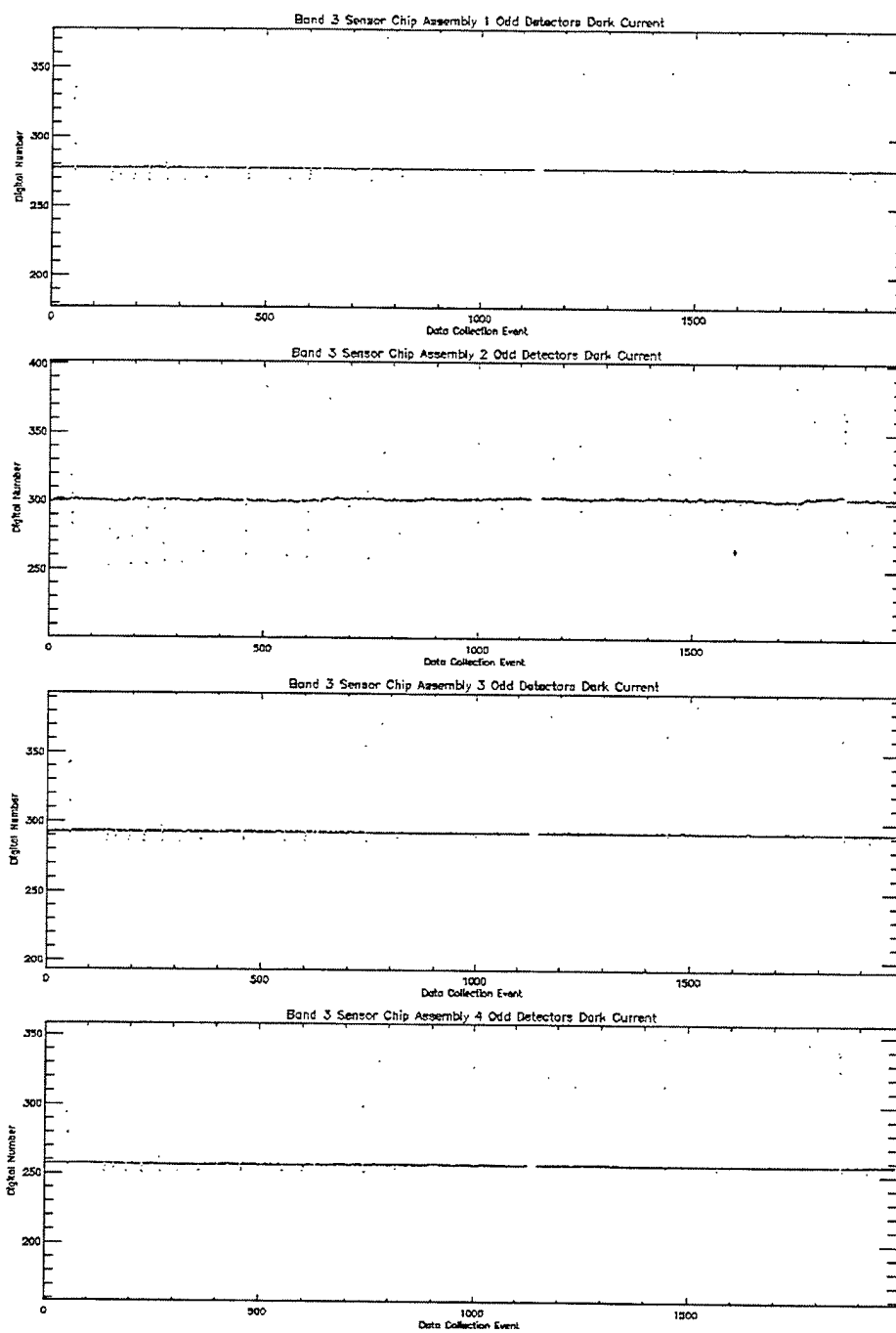


Figure 20. Dark current trending for Band 3 odd detectors.

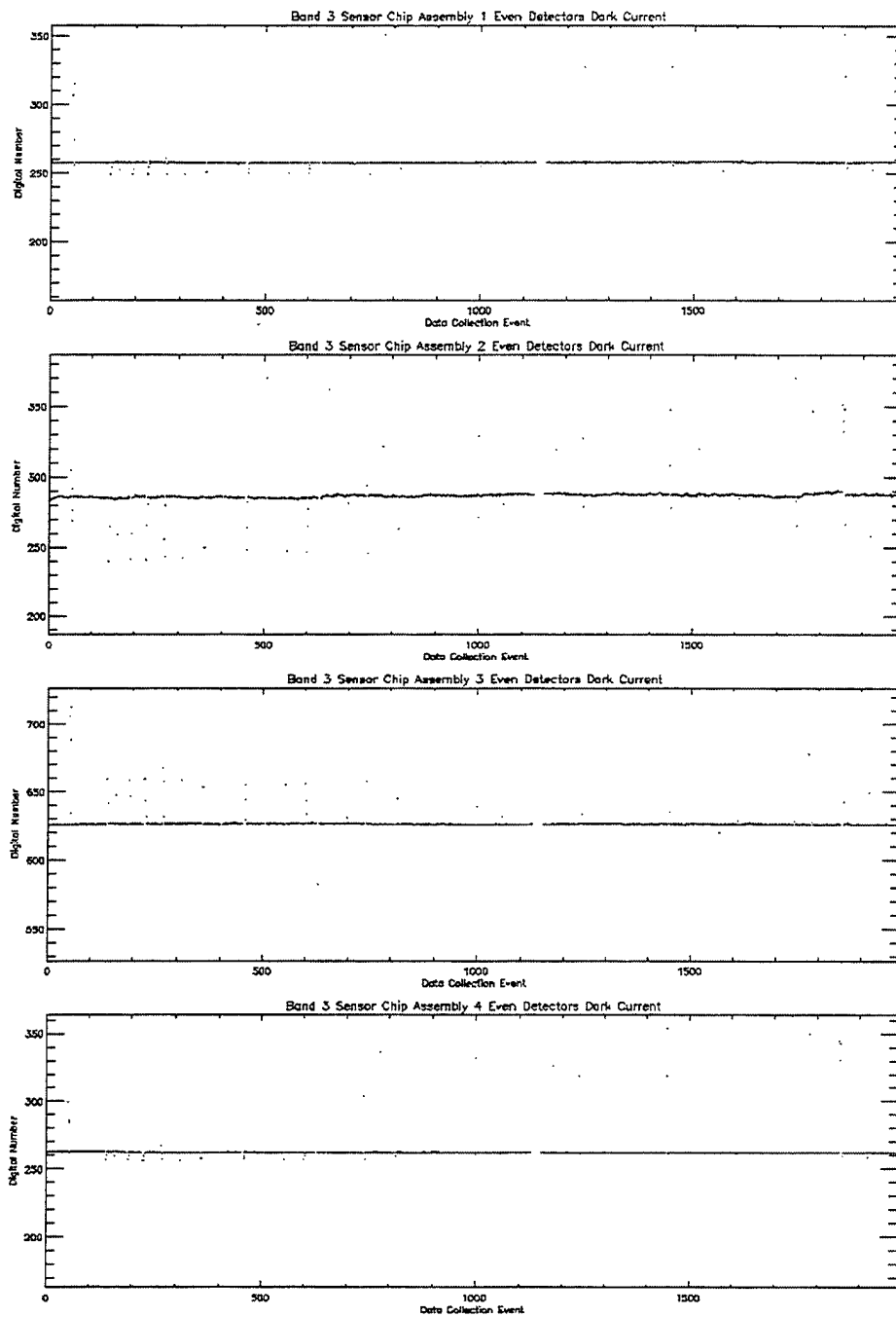


Figure 21. Dark current trending for Band 3 even detectors.

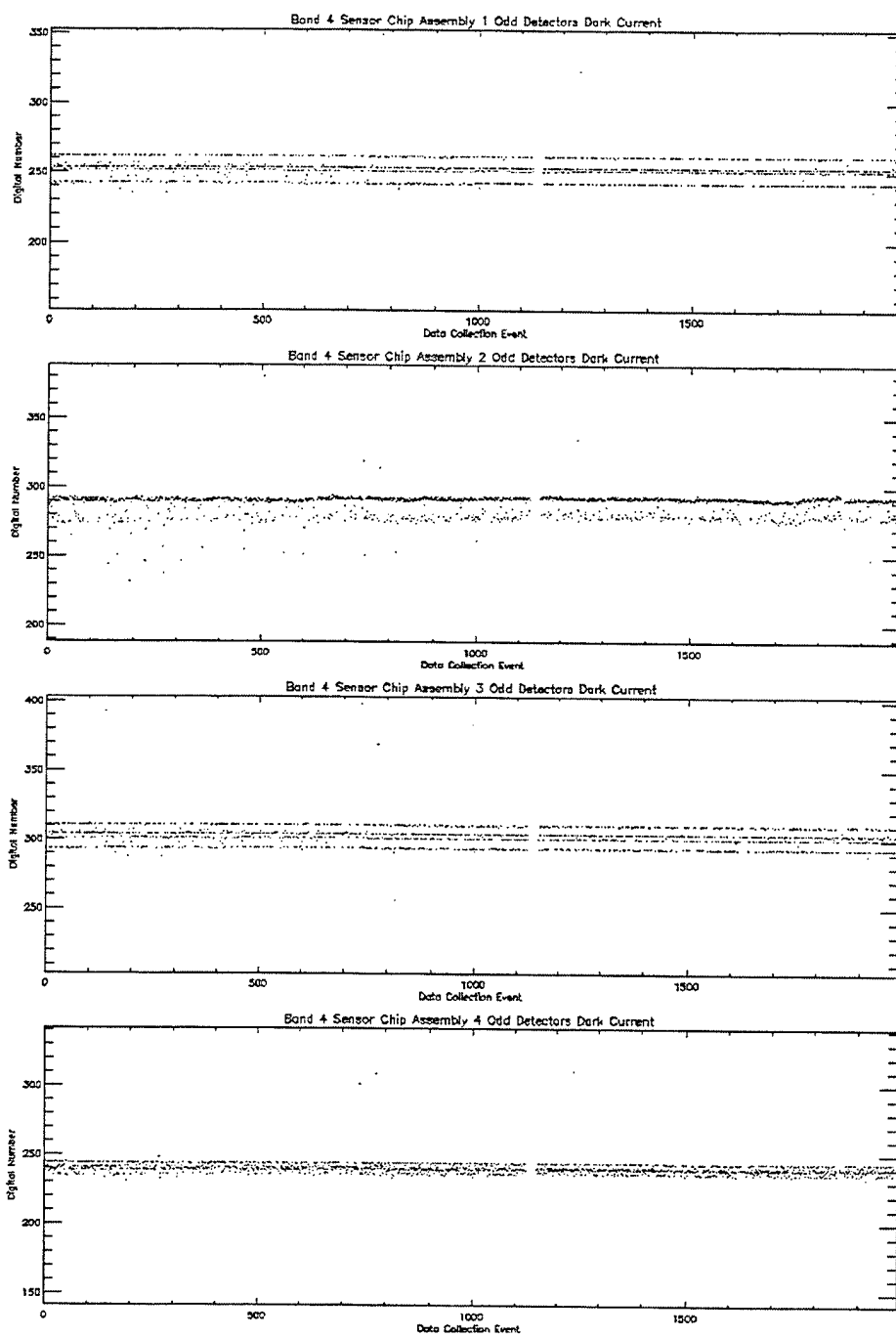
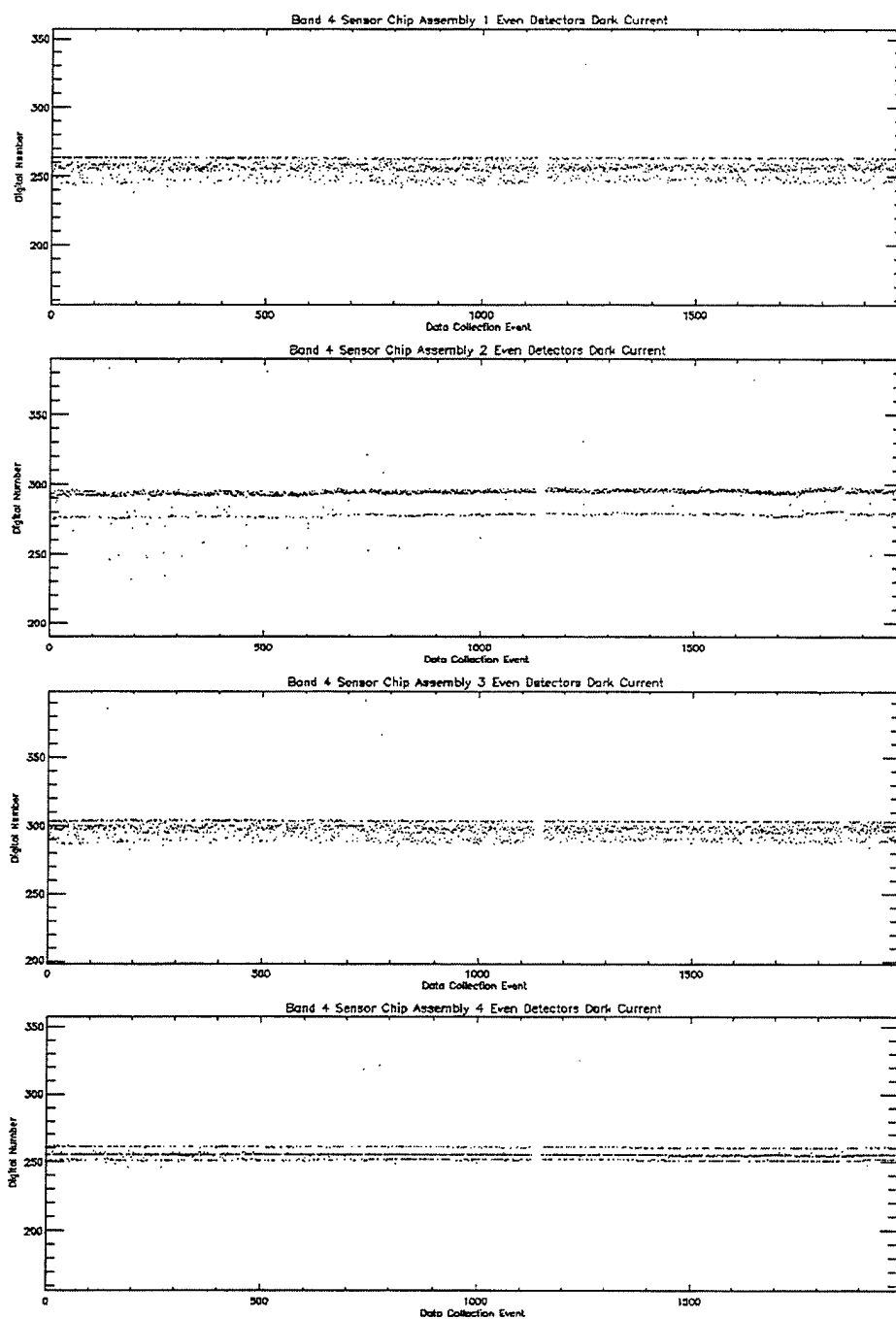


Figure 22. Dark current trending for Band 4 odd detectors.



*Figure 23. Dark current trending for Band 4 even detectors.*

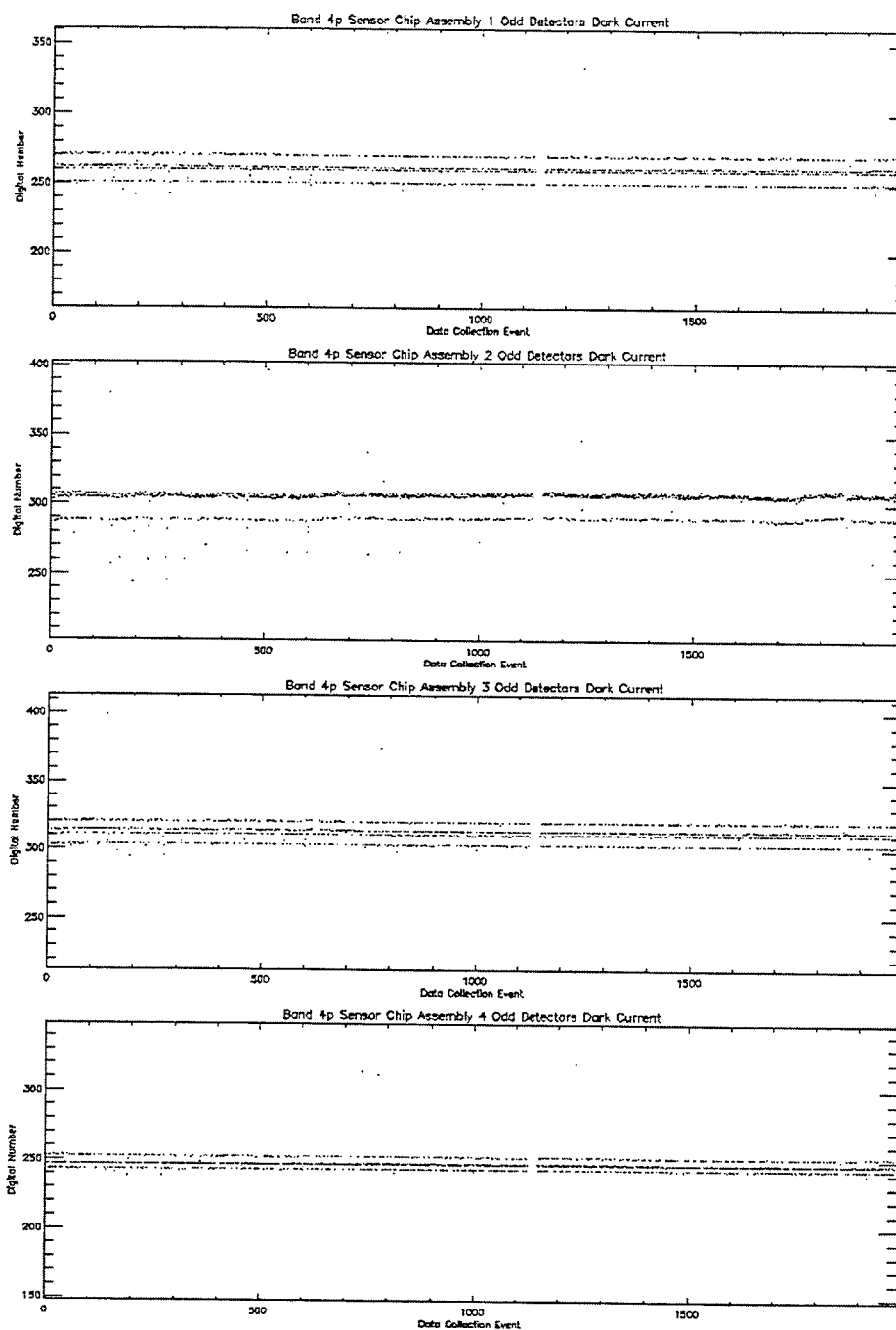


Figure 24. Dark current trending for Band 4p odd detectors.

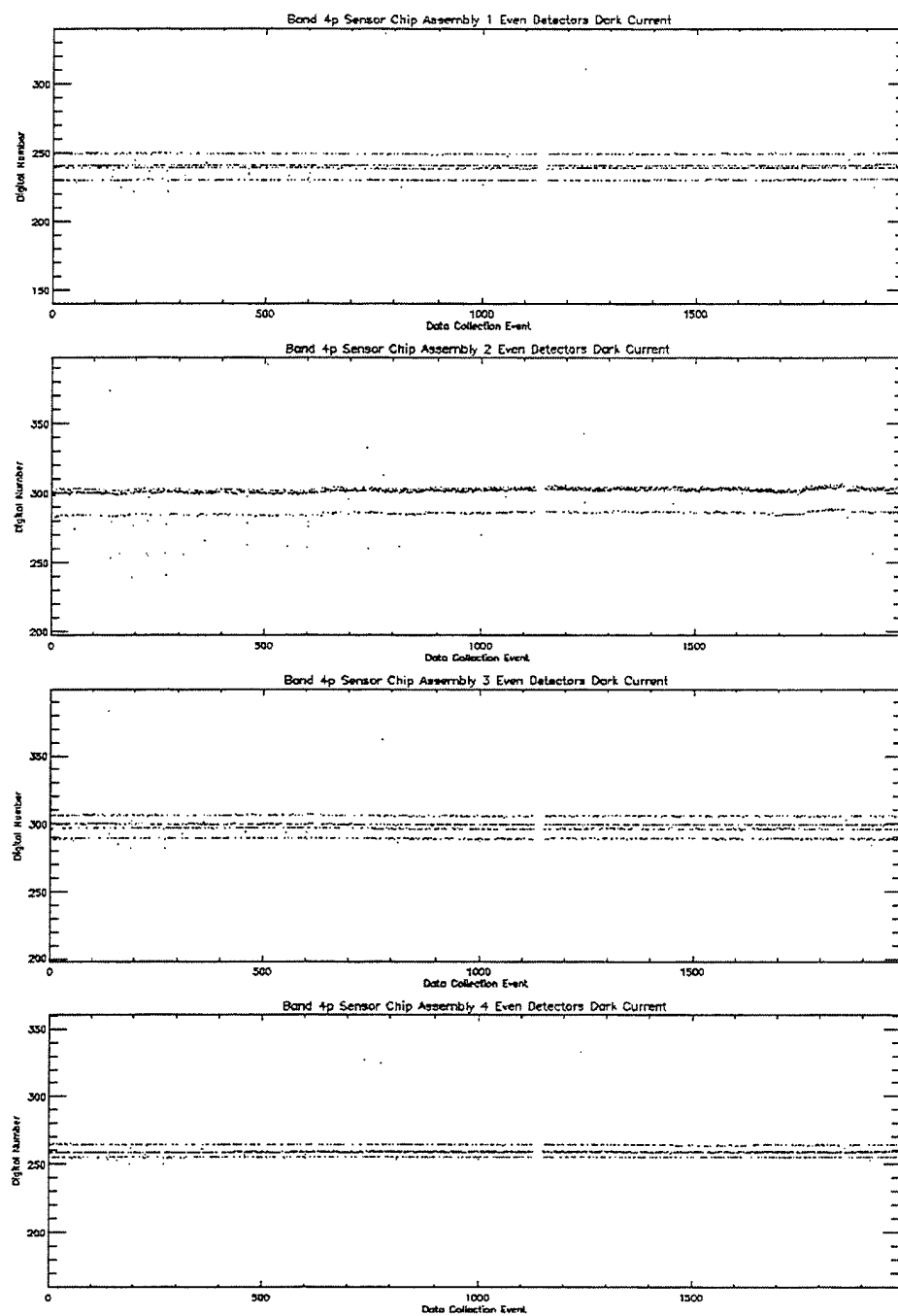


Figure 25. Dark current trending for Band 4p even detectors.



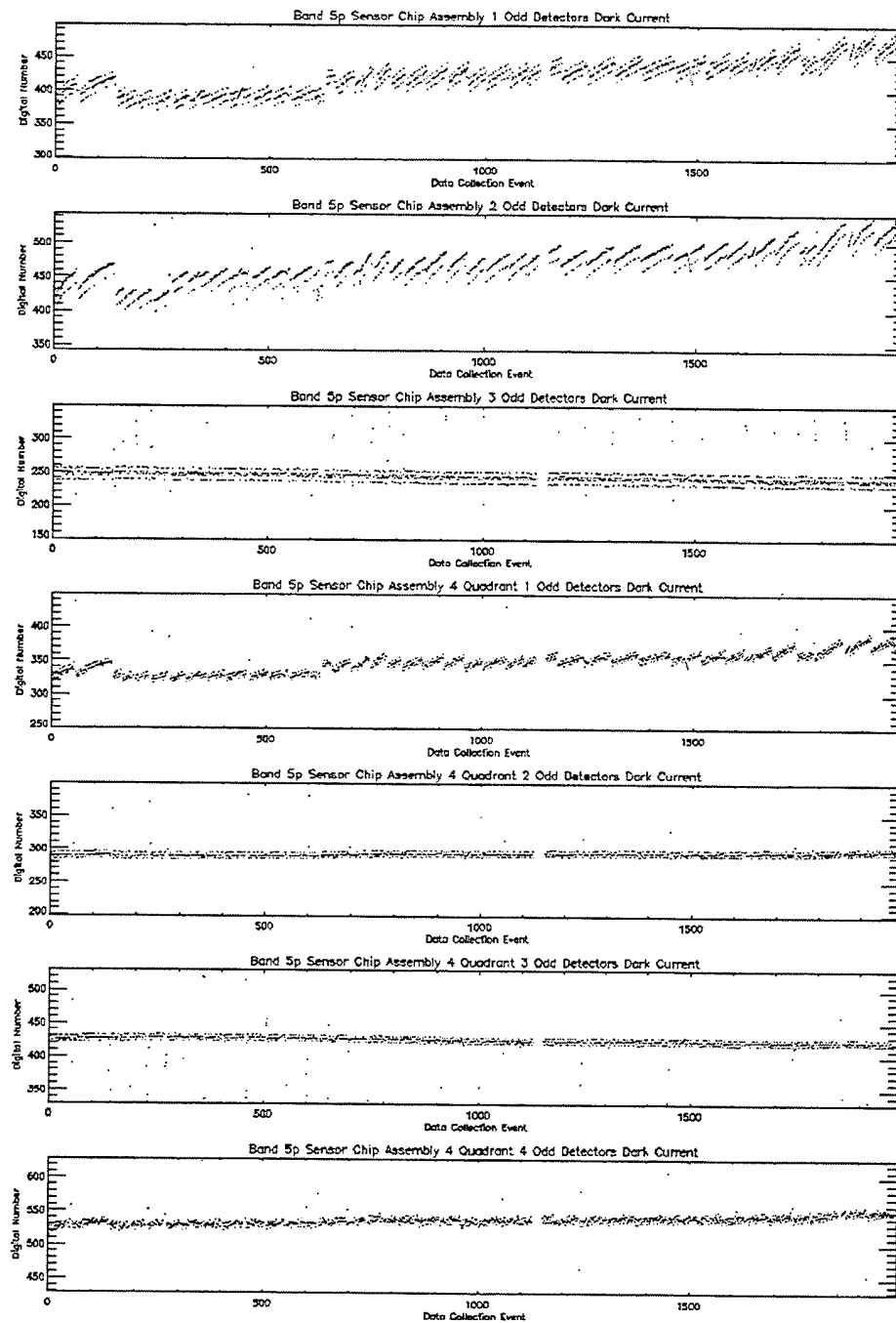


Figure 26. Dark current trending for Band 5p odd detectors.

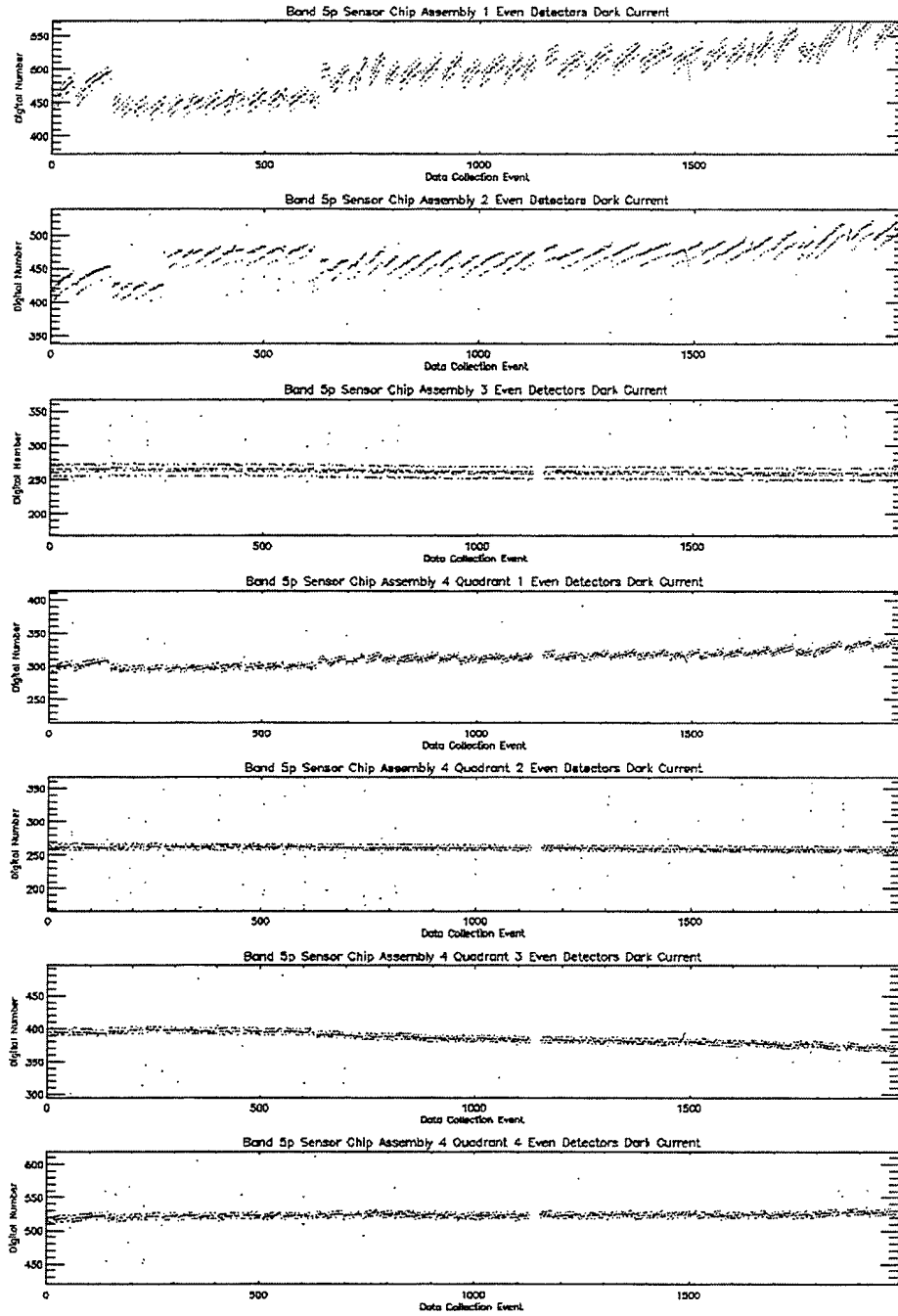


Figure 27. Dark current trending for Band 5p even detectors.

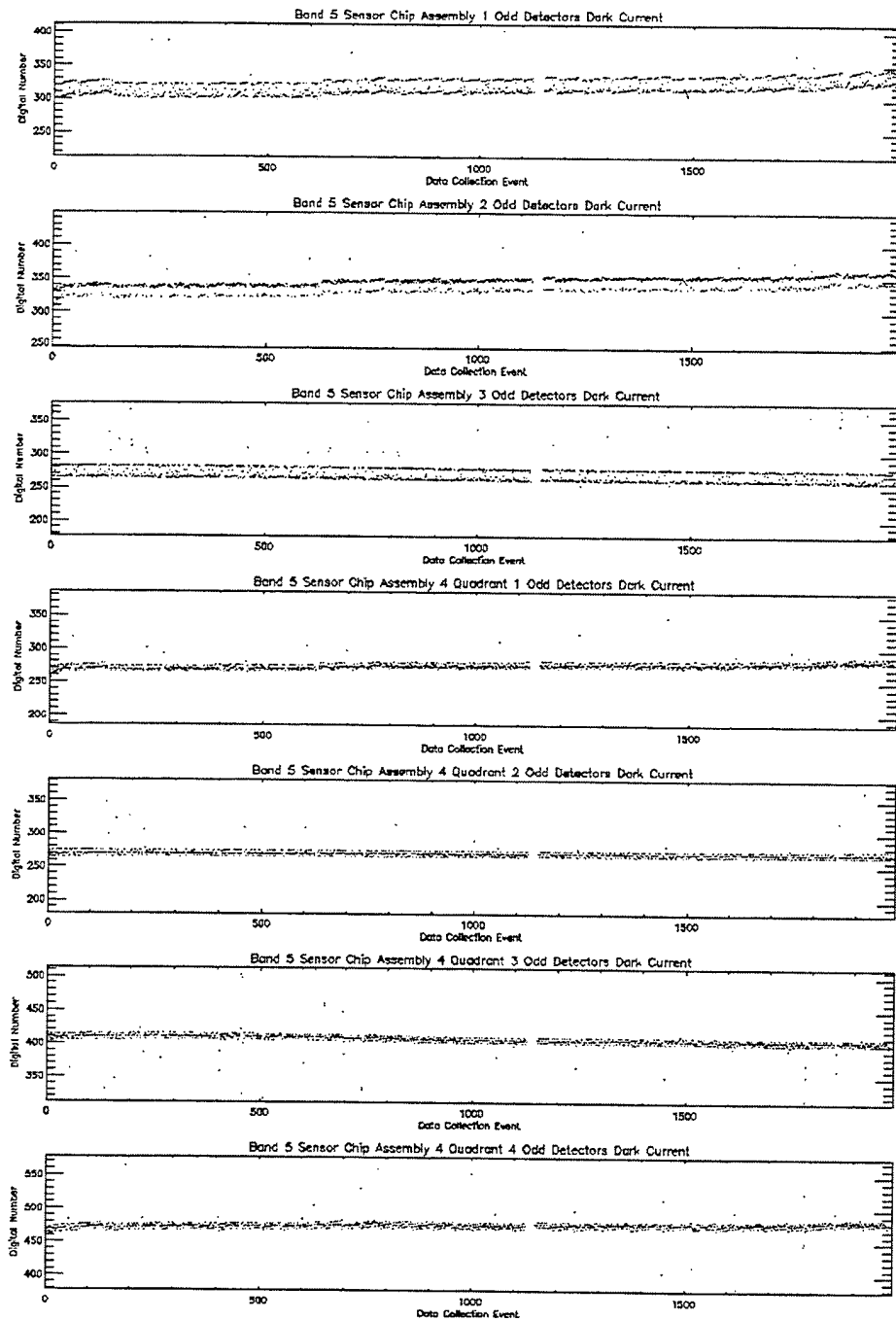


Figure 28. Dark current trending for Band 5 odd detectors.

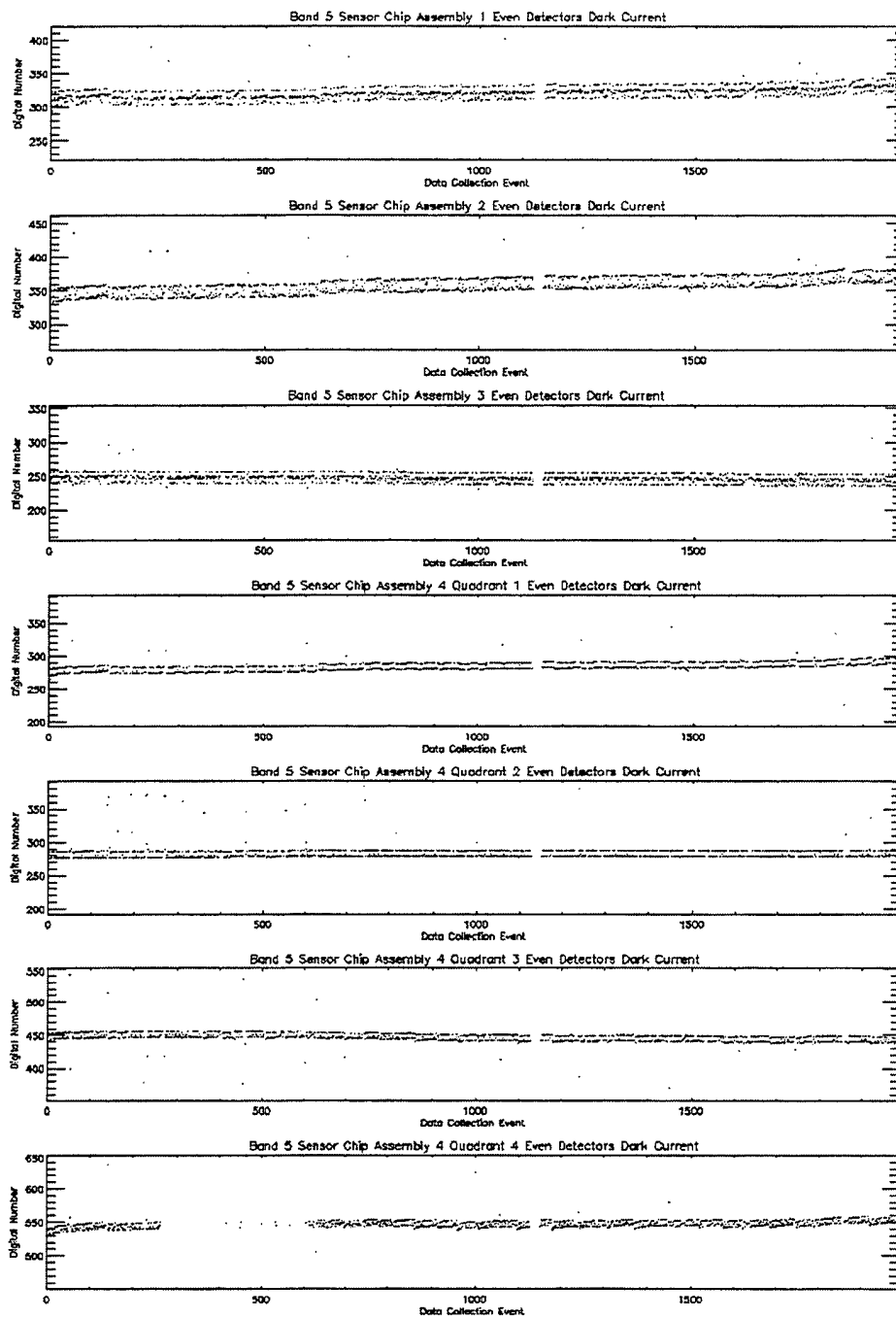


Figure 29. Dark current trending for Band 5 even detectors.

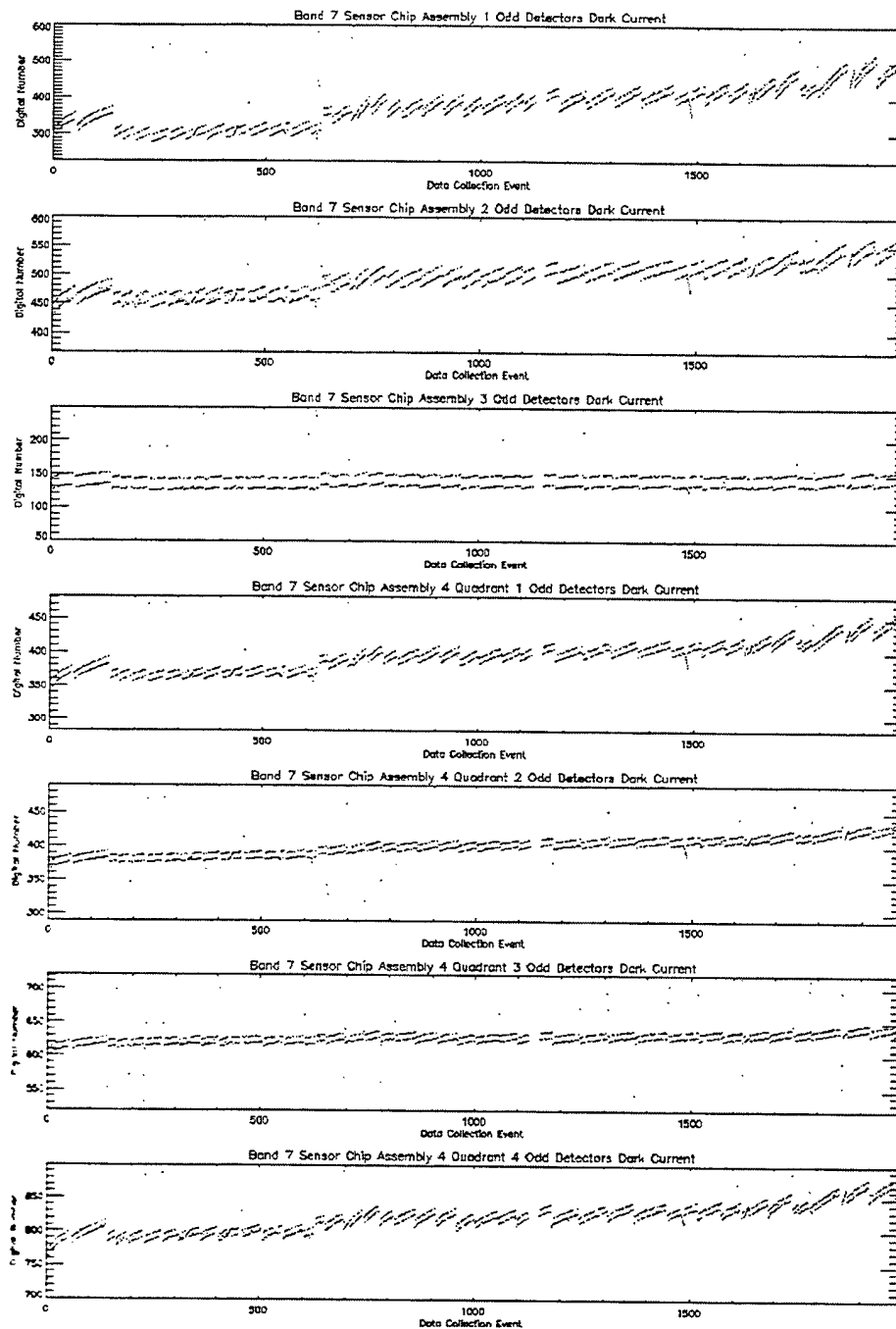


Figure 30. Dark current trending for Band 7 odd detectors.

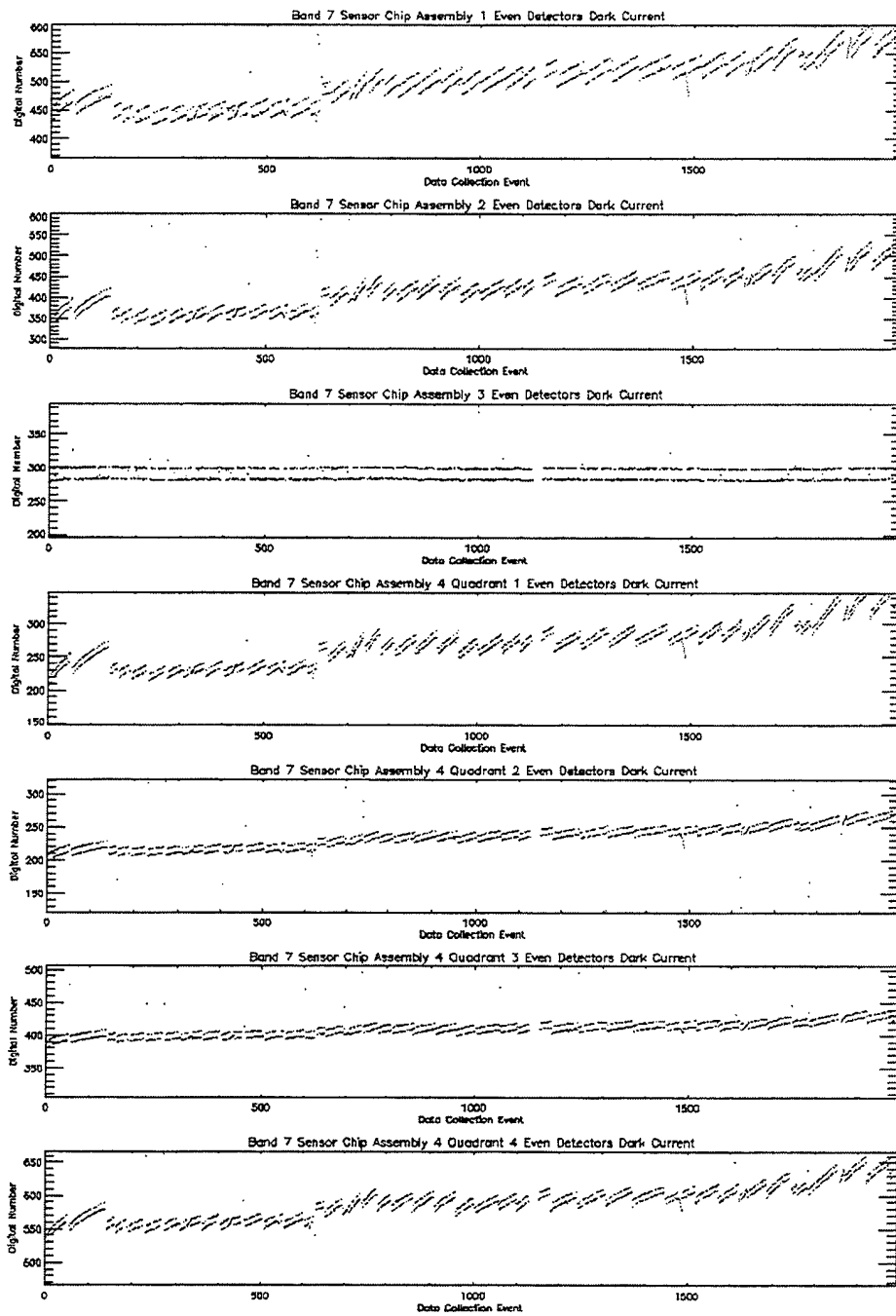


Figure 31. Dark current trending for Band 7 even detectors.

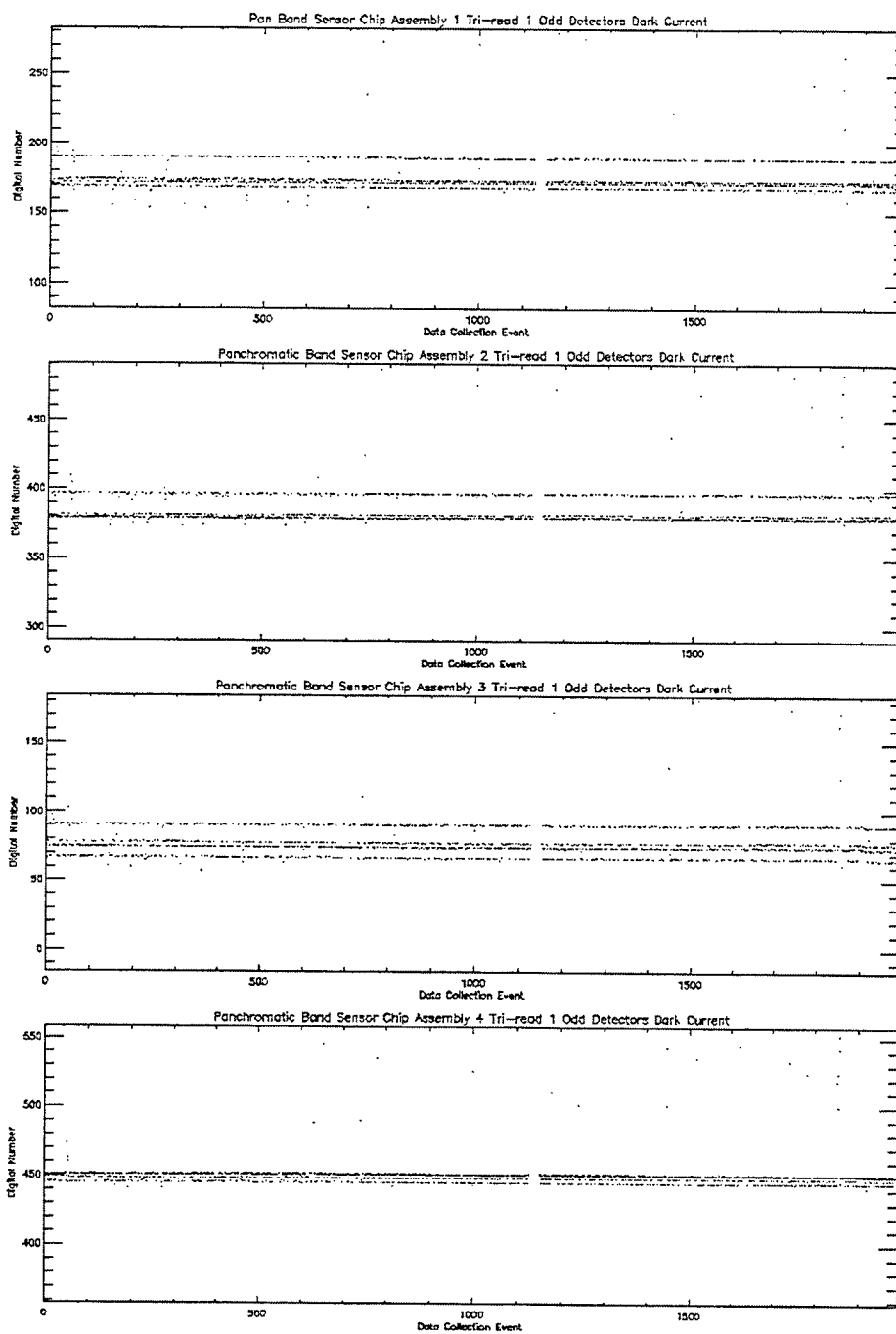


Figure 32. Dark current trending for Panchromatic Band tri-read #1 odd detectors.

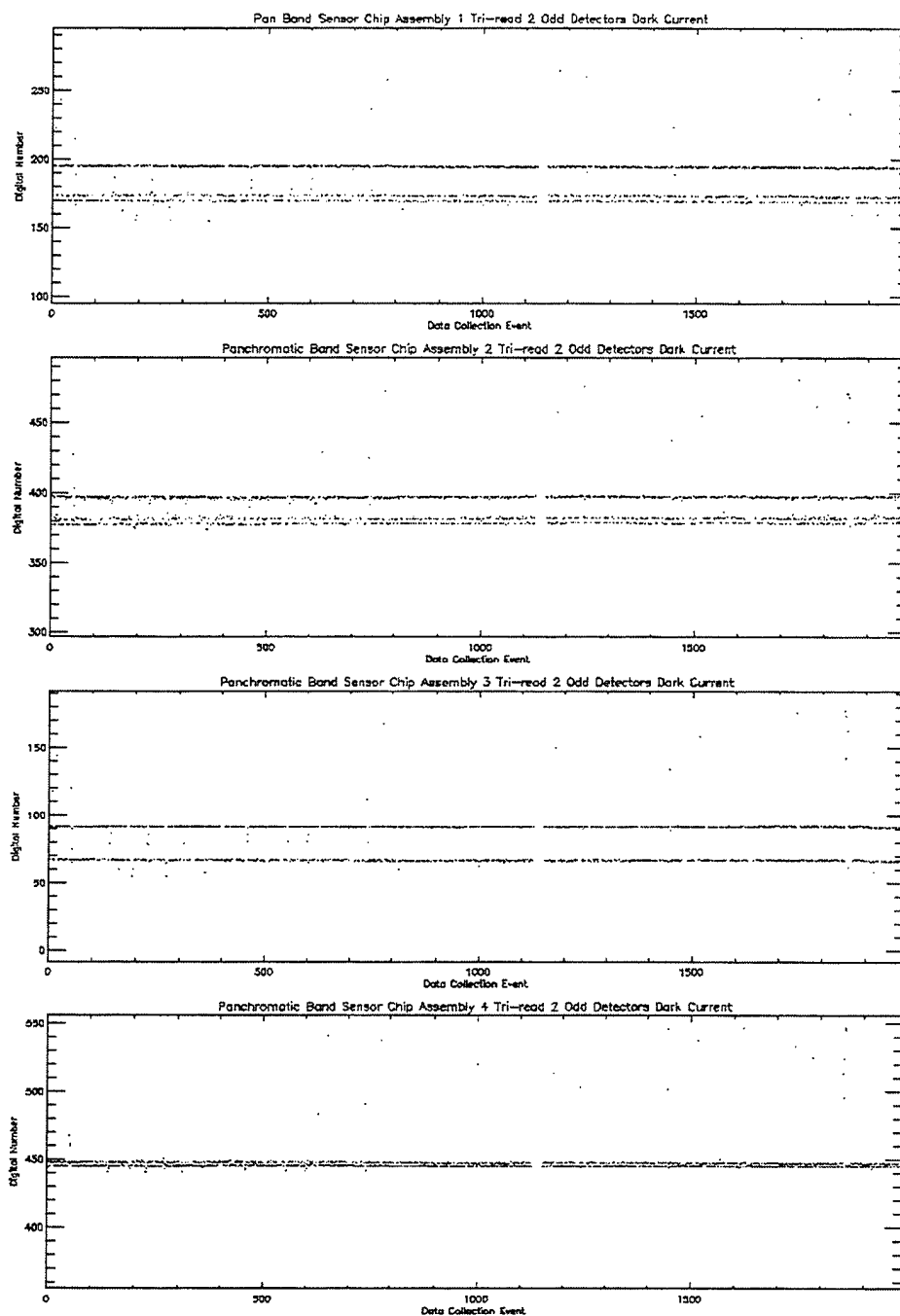


Figure 33. Dark current trending for Panchromatic Band tri-read #2 odd detectors.



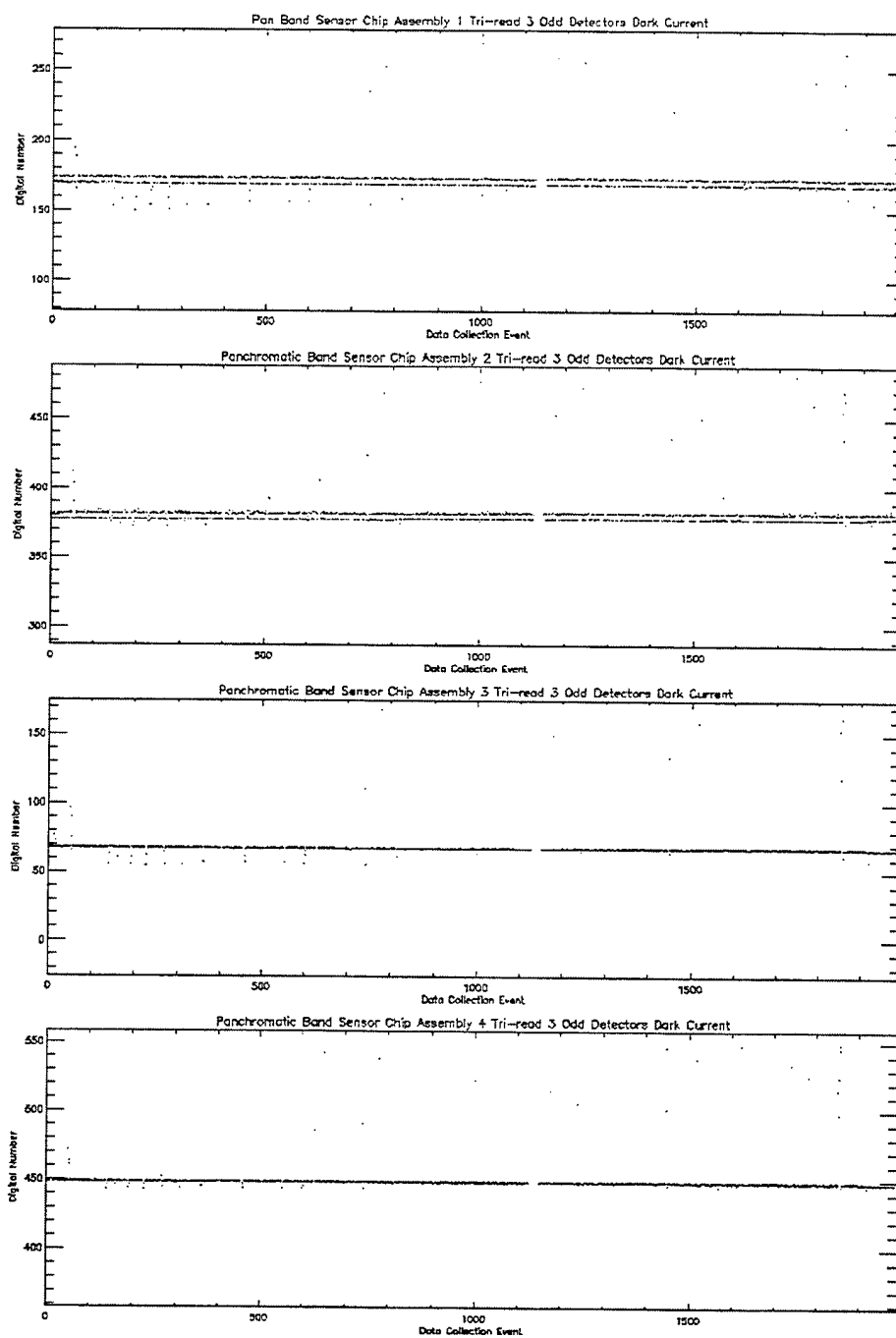


Figure 34. Dark current trending for Panchromatic Band tri-read #3 odd detectors.

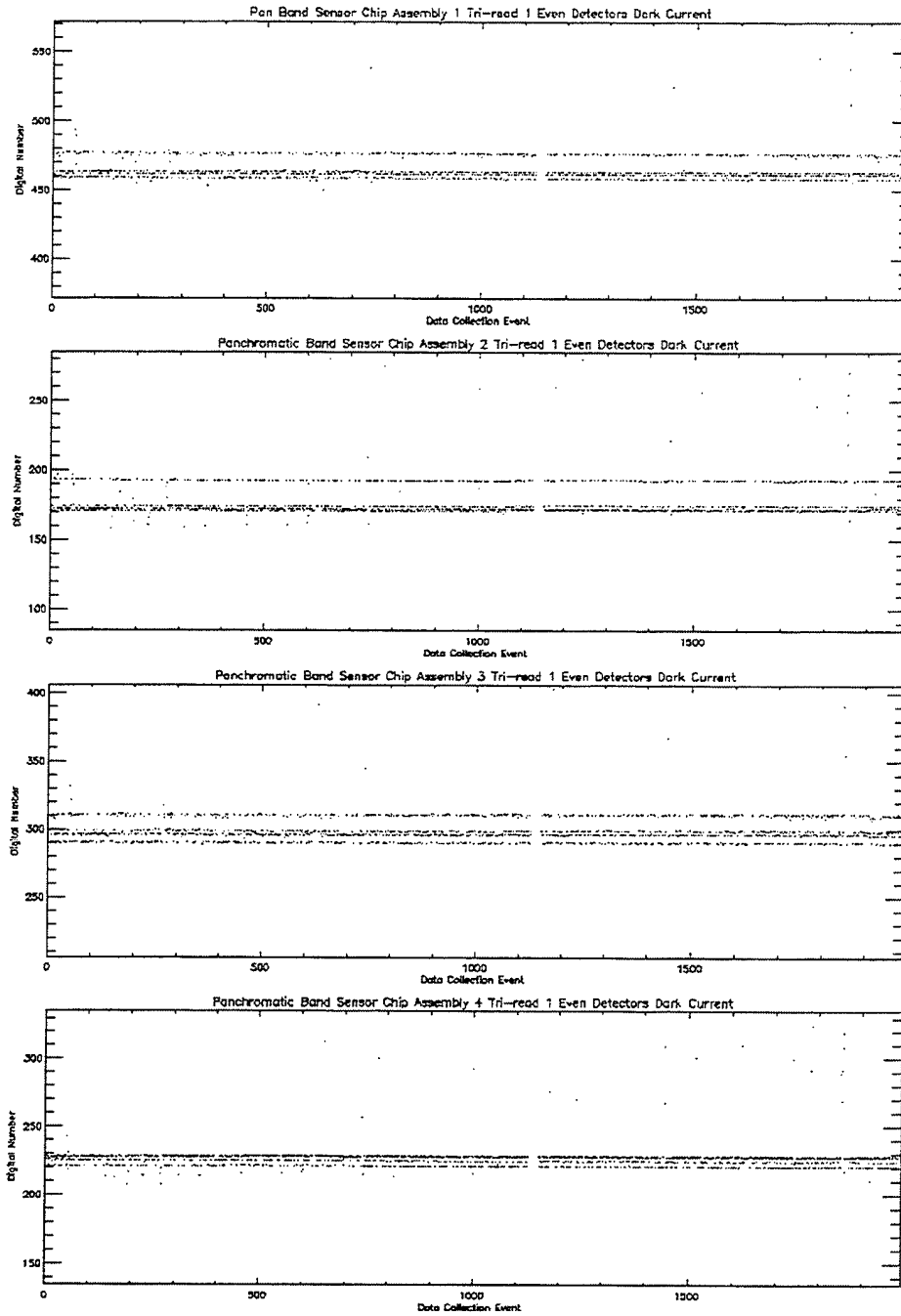


Figure 35. Dark current trending for Panchromatic Band tri-read #1 even detectors.

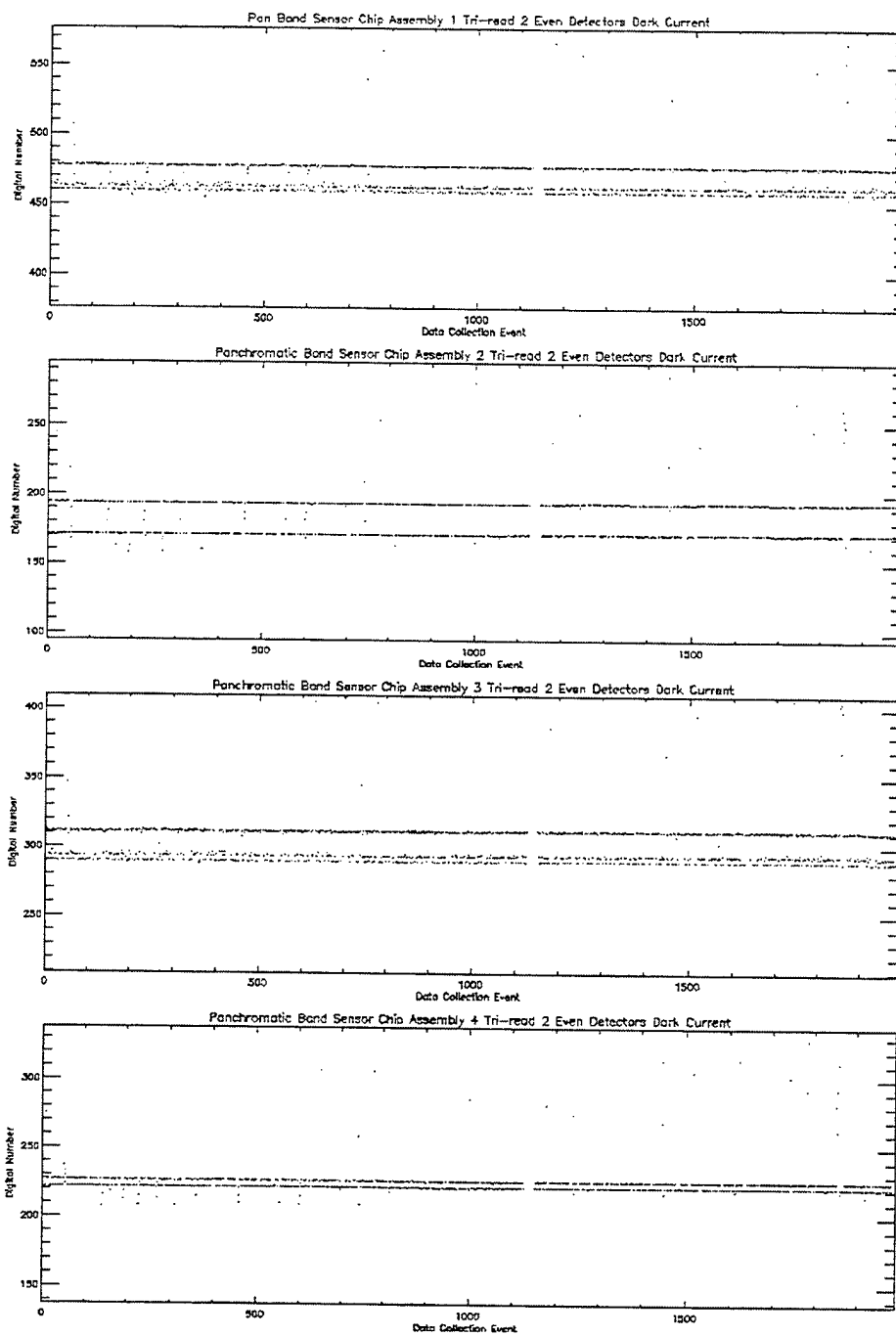


Figure 36. Dark current trending for Panchromatic Band tri-read #2 even detectors.

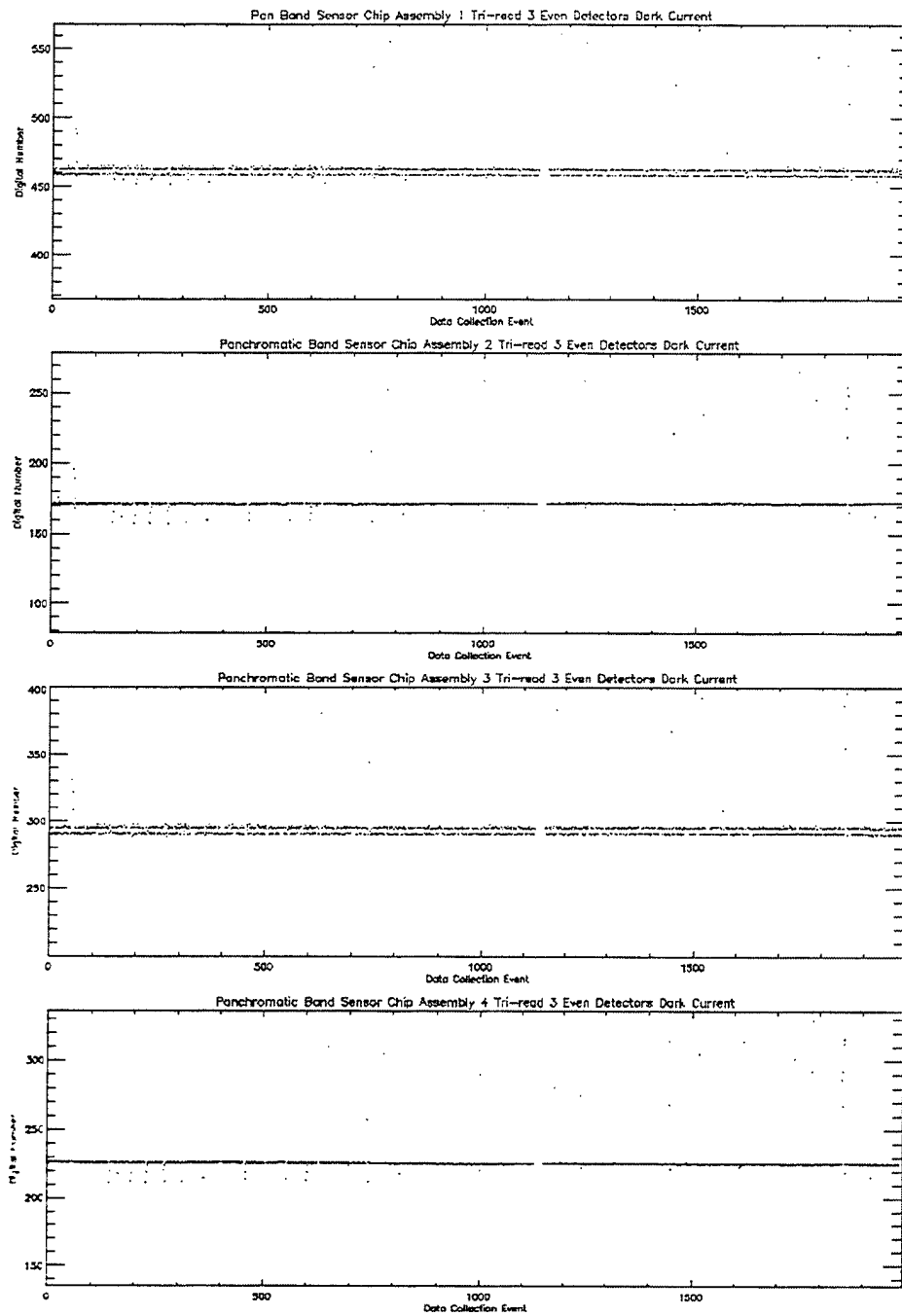


Figure 37. Dark current trending for Panchromatic Band tri-read #3 even detectors.

The magnitudes of the VNIR dark current levels, shortly after launch, are consistent with those calculated during pre-flight calibration of the instrument<sup>4</sup>. Band 2 SCA4 odd detectors and Band 3 SCA 3 even detectors have increased dark current levels compared to the corresponding even and odd detectors respectively. This is due to the influence of previously identified leaky detectors in these bands. Additionally, all SWIR bands exhibit enhanced dark current levels for a region of SCA 4 that is associated with a previously identified 'hot spot' in the focal plane. Finally, focal plane bakeout periods are associated with the apparent periodic resetting of the dark current levels in the SWIR bands.

Aside from the above known peculiarities, dark current trending during the first year on orbit has identified two new focal plane behaviors: differing dark current levels or states between observations and an increase in SWIR dark current levels between bakeouts and over the course of the year.

Differing states manifests itself as different dark current levels for Bands 1p, 4, 4p, 5p, 5, 7, and the Panchromatic band *from one observation to another*. This variability is very repeatable and appears to be different dark current *states* that the focal plane *locks into* during data collection events.

An increase in dark current levels for some SWIR bands has also been observed between bakeout periods. This increase appears to be largely reset after a bakeout occurs, but long-term trending indicates a gradual increase in dark current levels for the SWIR bands, particularly Bands 5p and 7.

To investigate the dark current *states* and SWIR drifting effects, the mean dark current level for each detector of every band has been calculated over a ten-day period, beginning on July 27, 2001. This period is bracketed by two ALI bakeout sequences. The difference in dark current levels for each band, relative to a baseline level obtained immediately after the first bakeout, is provided in Figures 38–47.

Band 1p exhibits at least four different, repeatable, dark current states over the course of the ten-day period. Bands 1-3, which seemed to have only one state during long-term trending, have two dark current states. Interestingly, the odd and even detectors appear to have offsetting states which, when averaged, appear to reduce to a single state. Band 4 exhibits four states, Bands 4p and 5 each exhibit 3 states, and the panchromatic band exhibits 4 states. It is difficult to identify different dark levels states for Bands 5p and 7, due to the evolving structure of the dark current levels over time. This structure, when averaged, results in the apparent increase in dark current levels between bakeout sequences.

Finally, the detector level structure of the long-term increase in SWIR dark current levels have been derived by subtracting mean dark current levels obtained from a January 2001 observation from mean dark current levels obtained from a November 2001 observation. These observations were obtained soon after a bakeout. The results of this comparison are presented in Figures 48–51. For clarity, odd and even detectors for Band 7 have been plotted separately. Inspection of these data reveal a significant increase in dark current levels for SCAs 1 and 2 of Band 5p and 7, consistent with long-term trending presented earlier. Similarly, little increase in dark current levels are observed for SCAs 3 and 4.

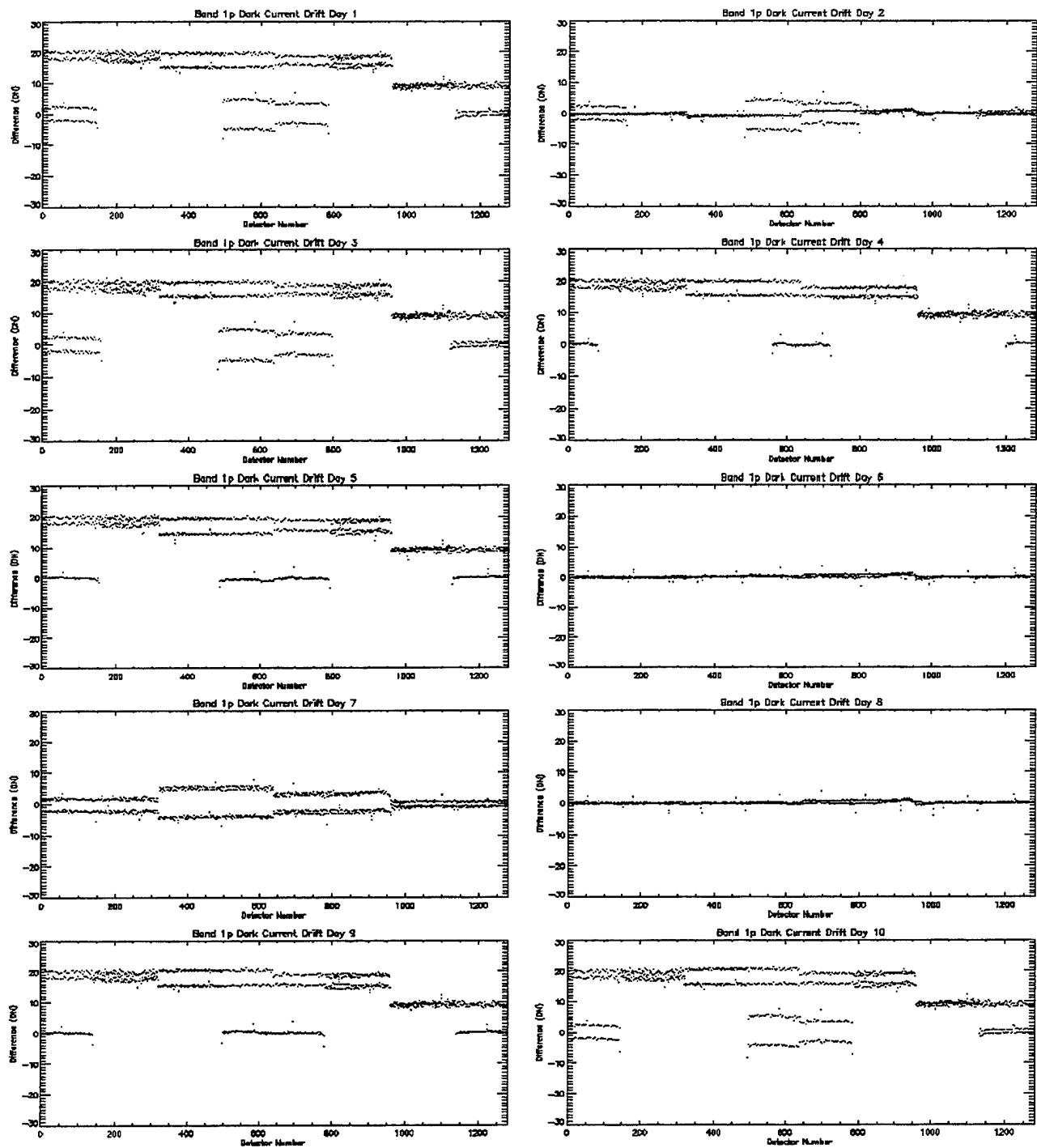


Figure 38. Dark current drifting for Band 1p over 10 day period after an on-orbit bakeout.

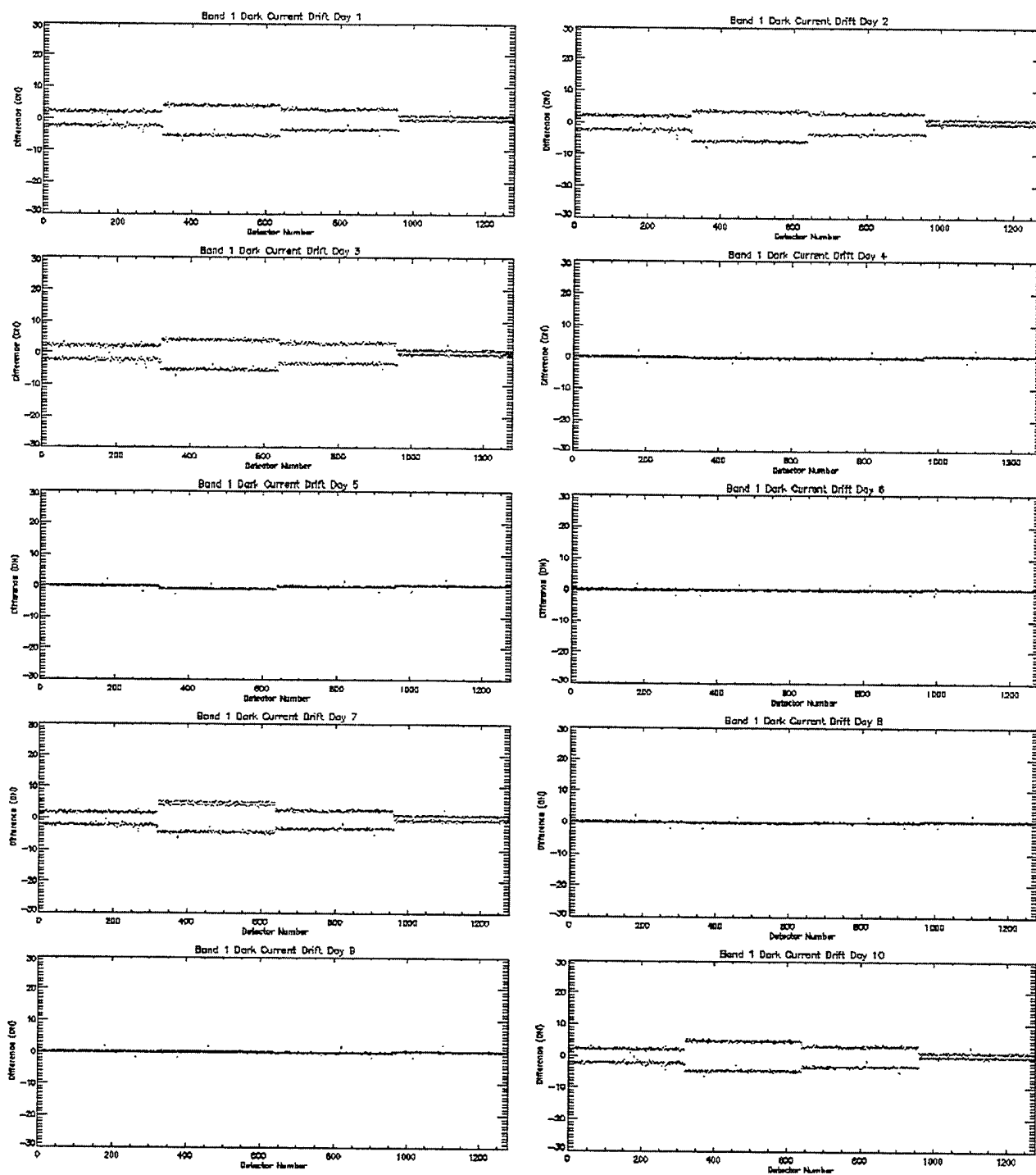


Figure 39. Dark current drifting for Band 1 over 10 day period after an on-orbit bakeout.

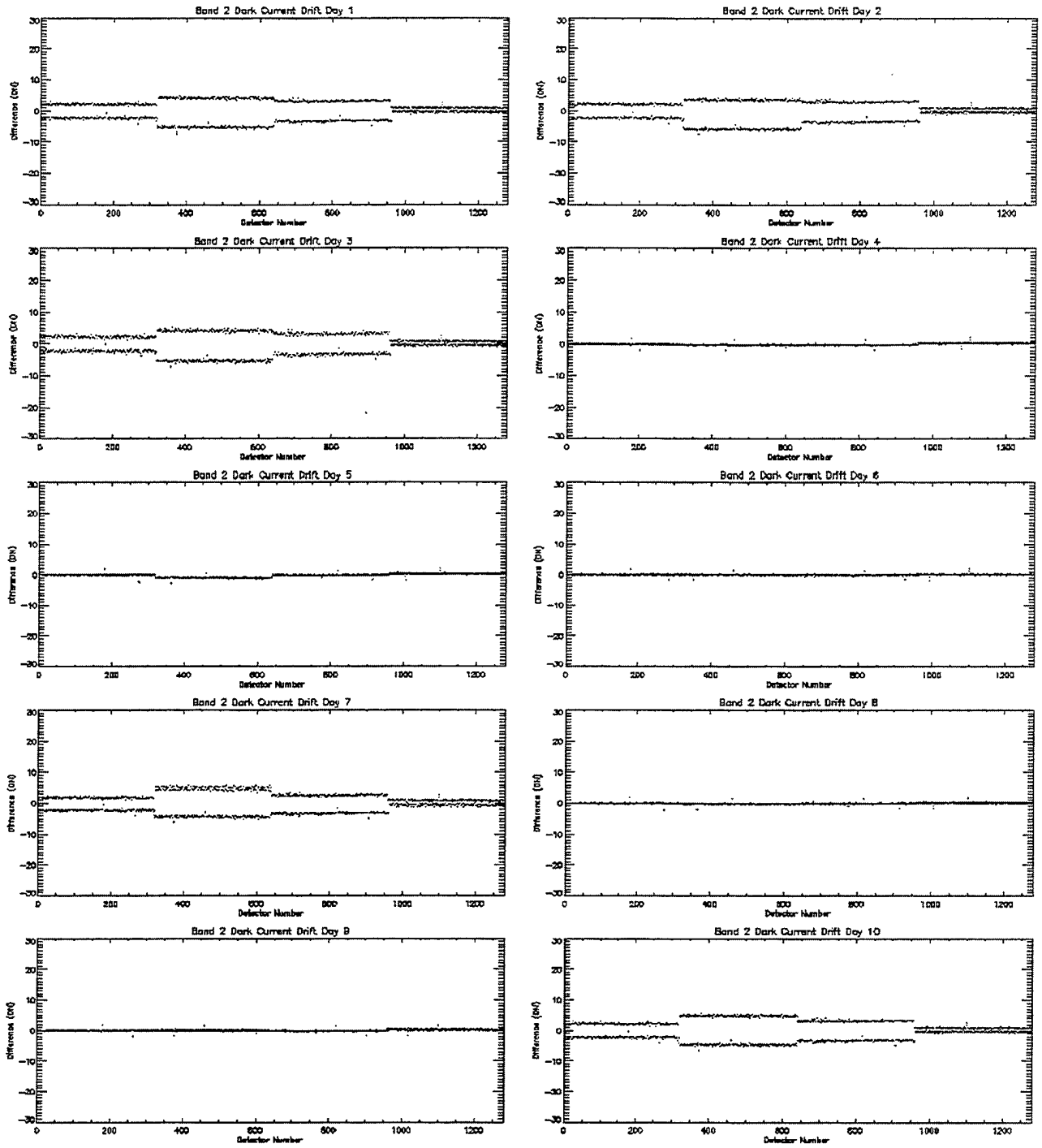


Figure 40. Dark current drifting for Band 2 over 10 day period after an on-orbit bakeout.



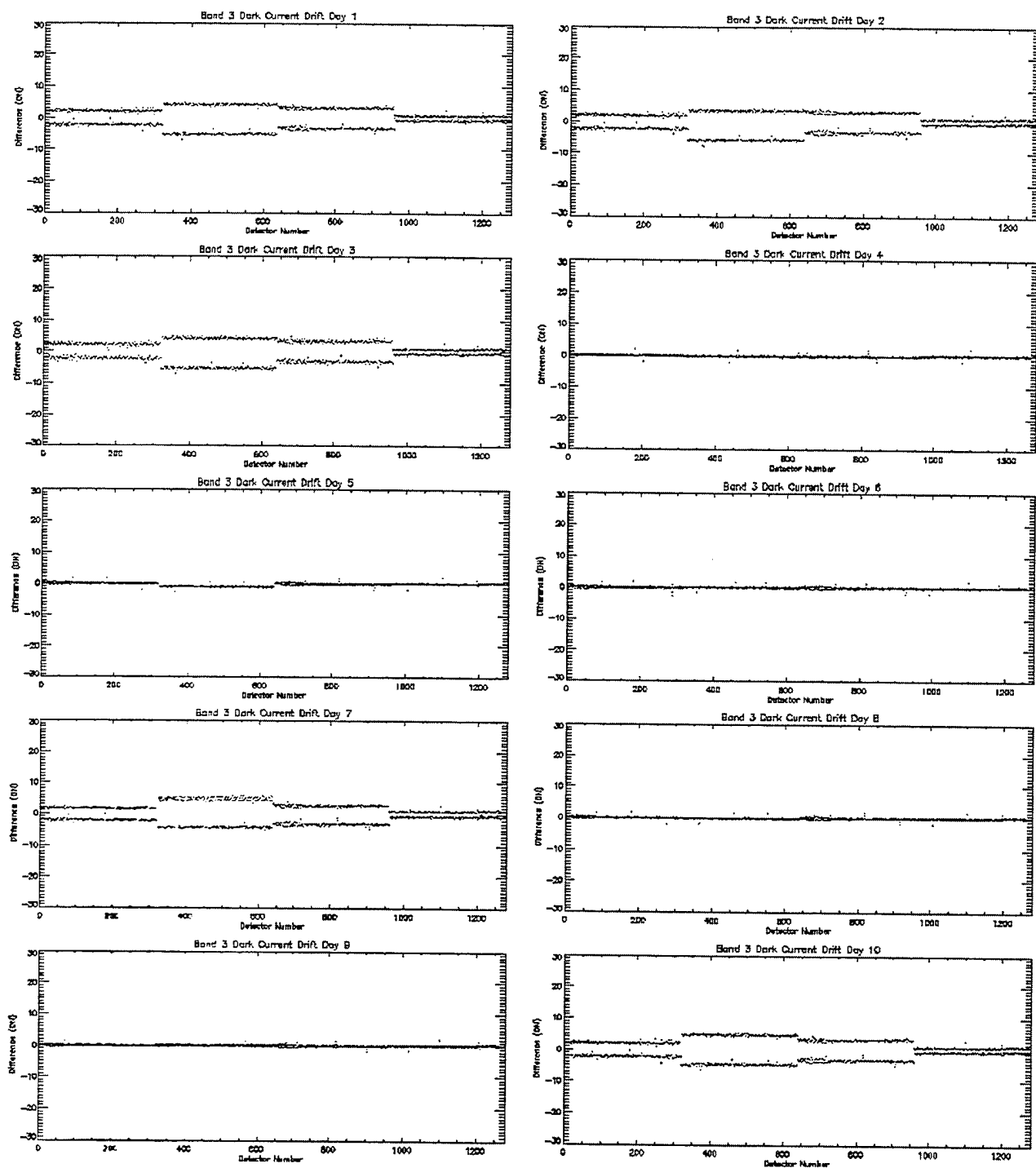


Figure 41. Dark current drifting for Band 3 over 10 day period after an on-orbit bakeout.

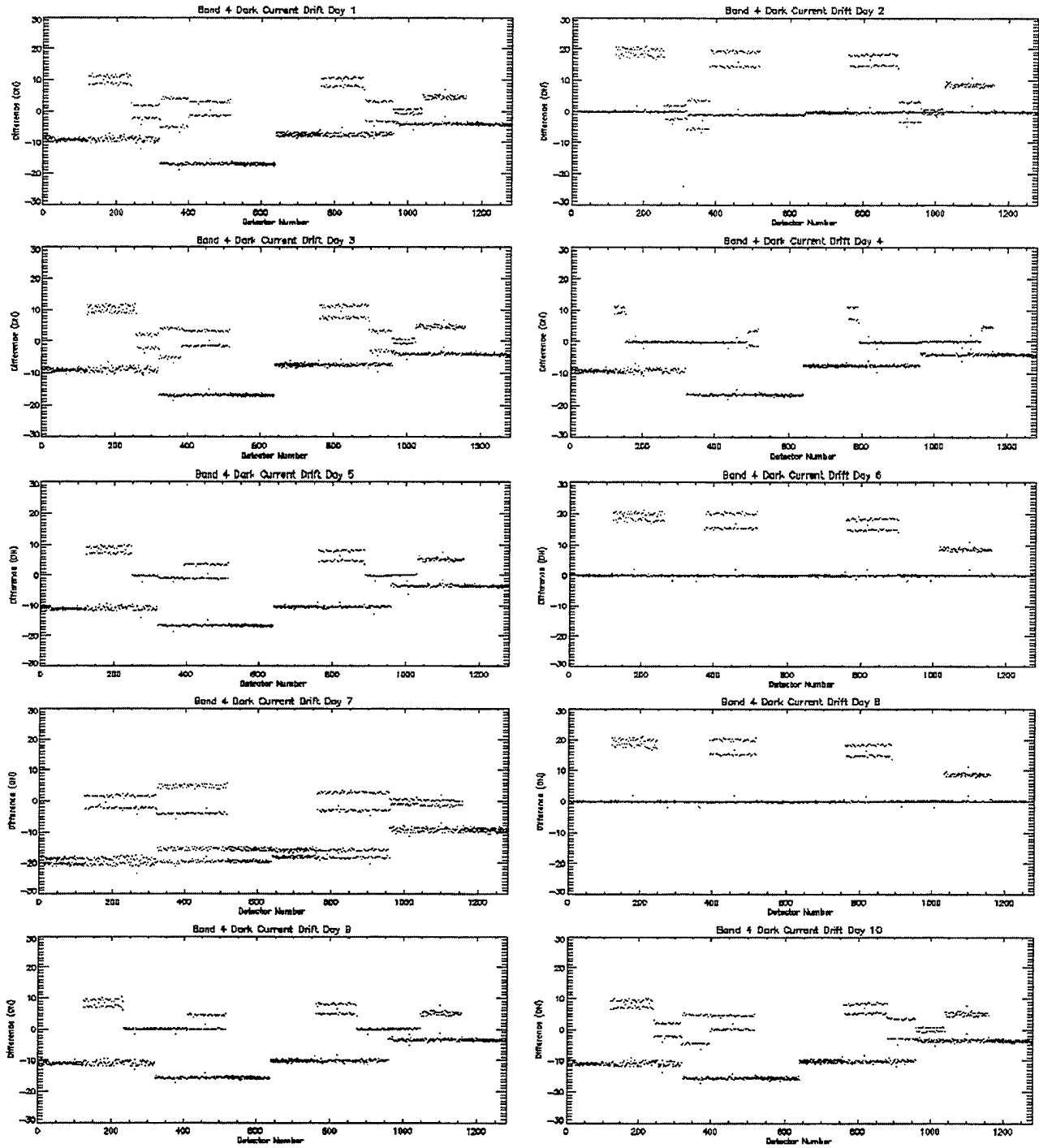


Figure 42. Dark current drifting for Band 4 over 10 day period after an on-orbit bakeout.

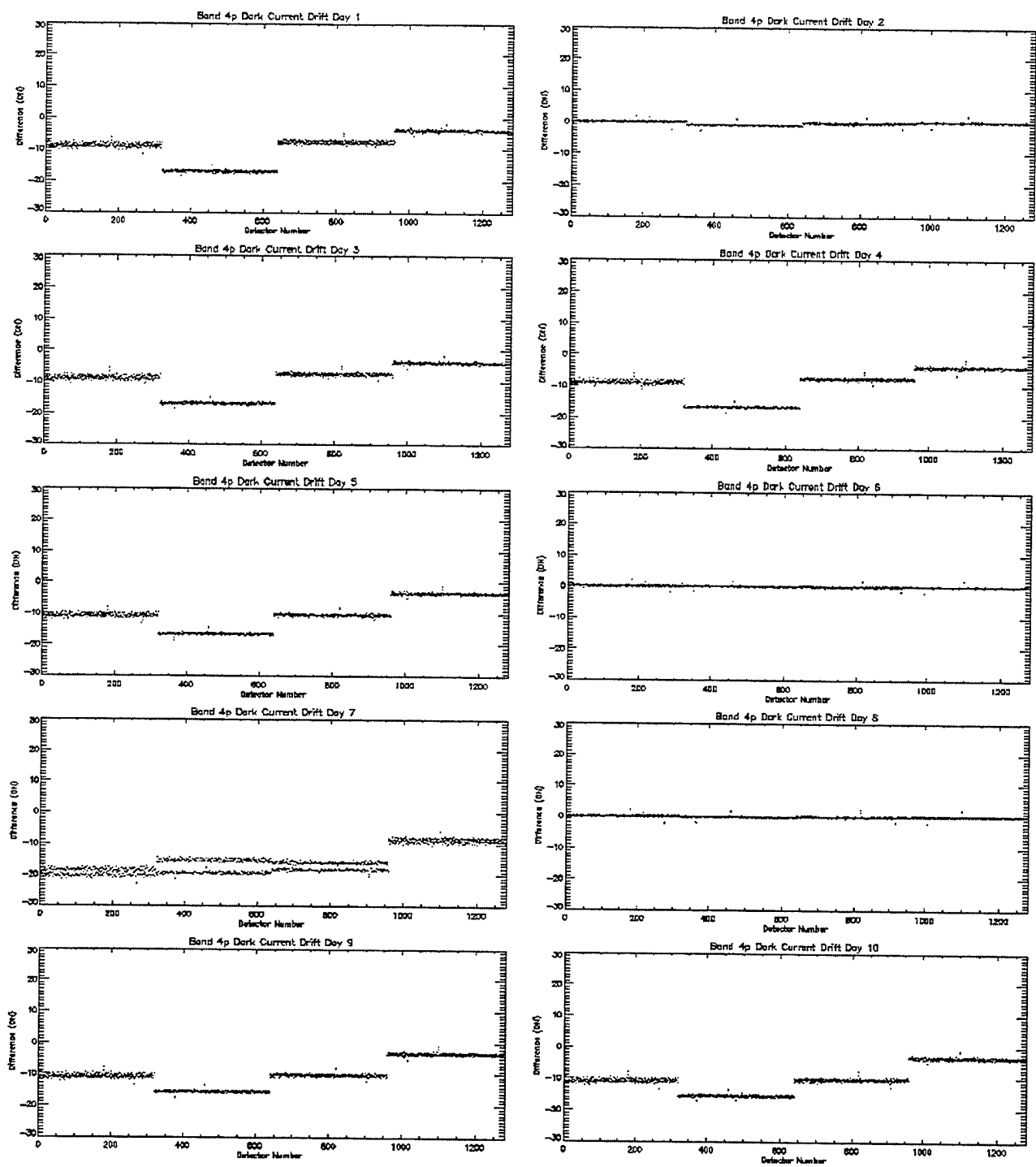


Figure 43. Dark current drifting for Band 4p over 10 day period after an on-orbit bakeout.

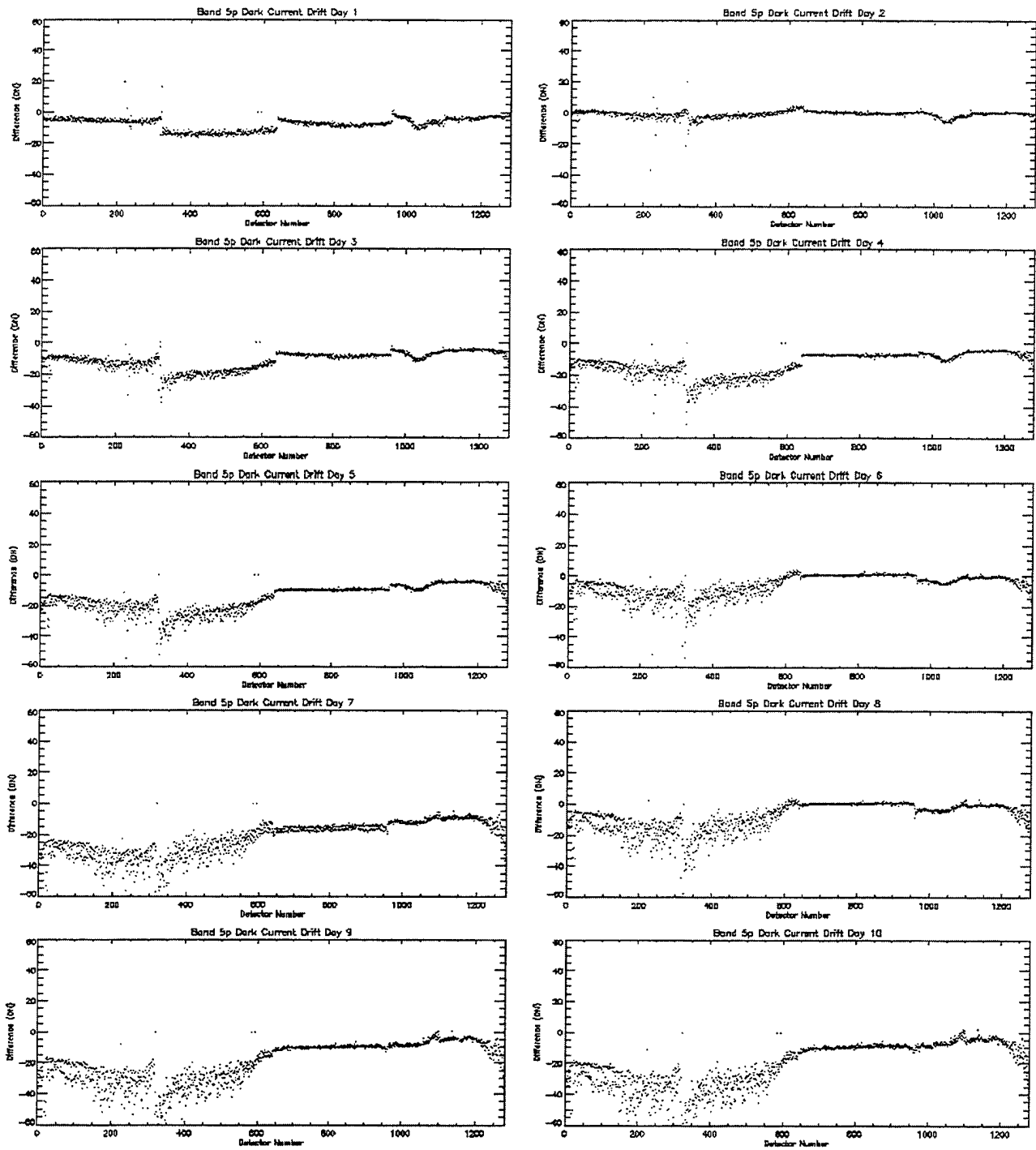


Figure 44. Dark current drifting for Band 5p over 10 day period after an on-orbit bakeout.

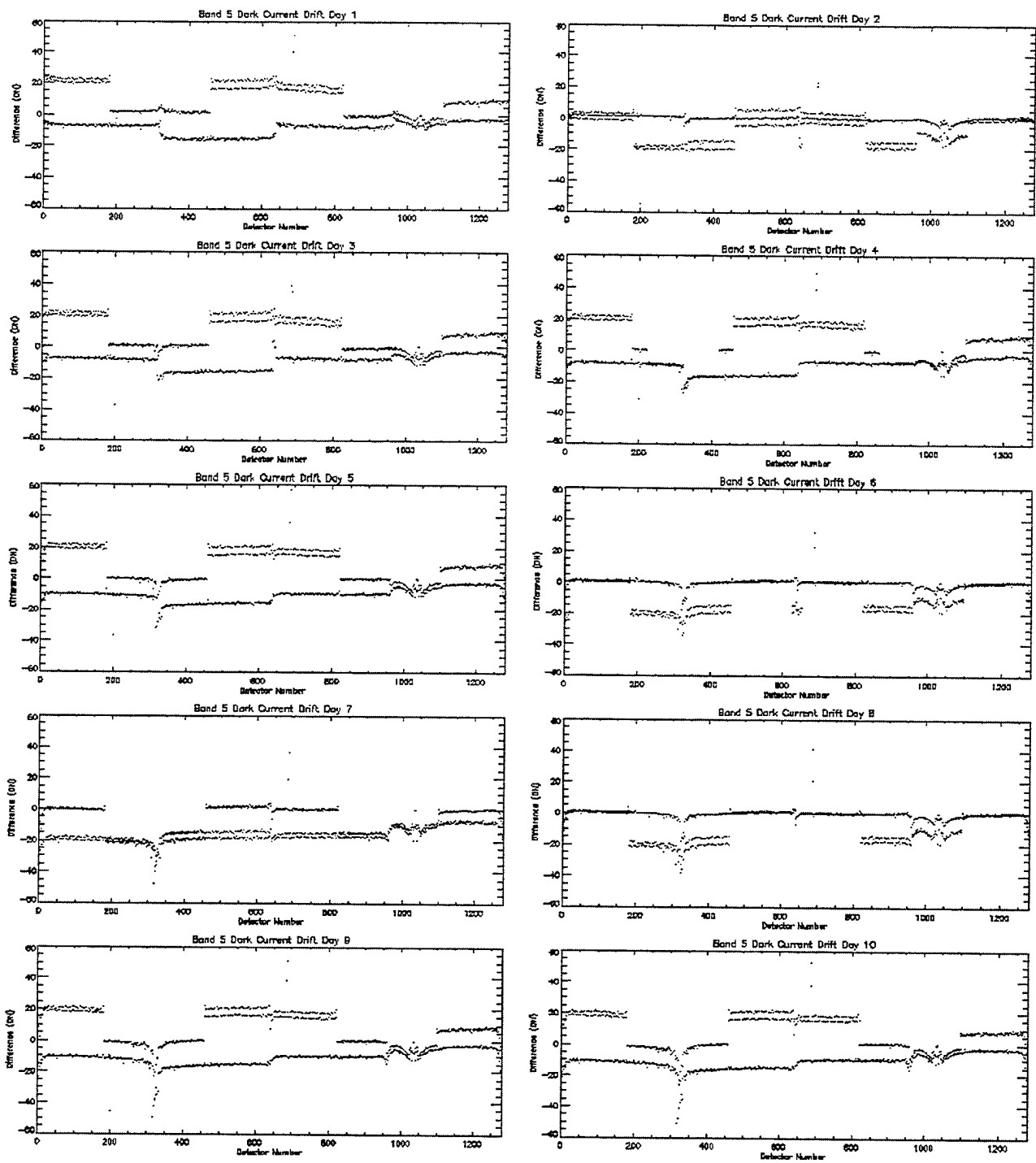


Figure 45. Dark current drifting for Band 5 over 10 day period after an on-orbit bakeout.

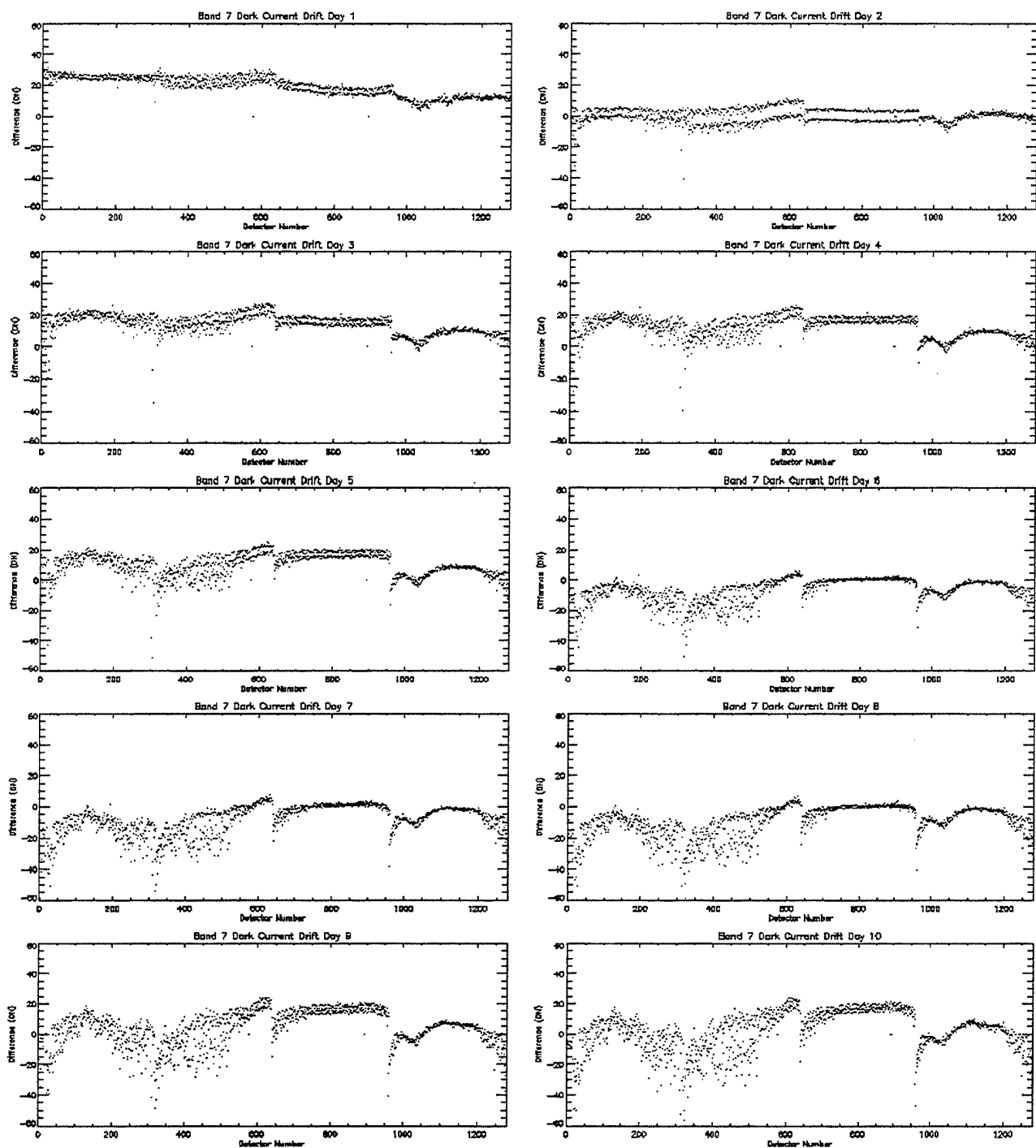


Figure 46. Dark current drifting for Band 7 over 10 day period after an on-orbit bakeout.

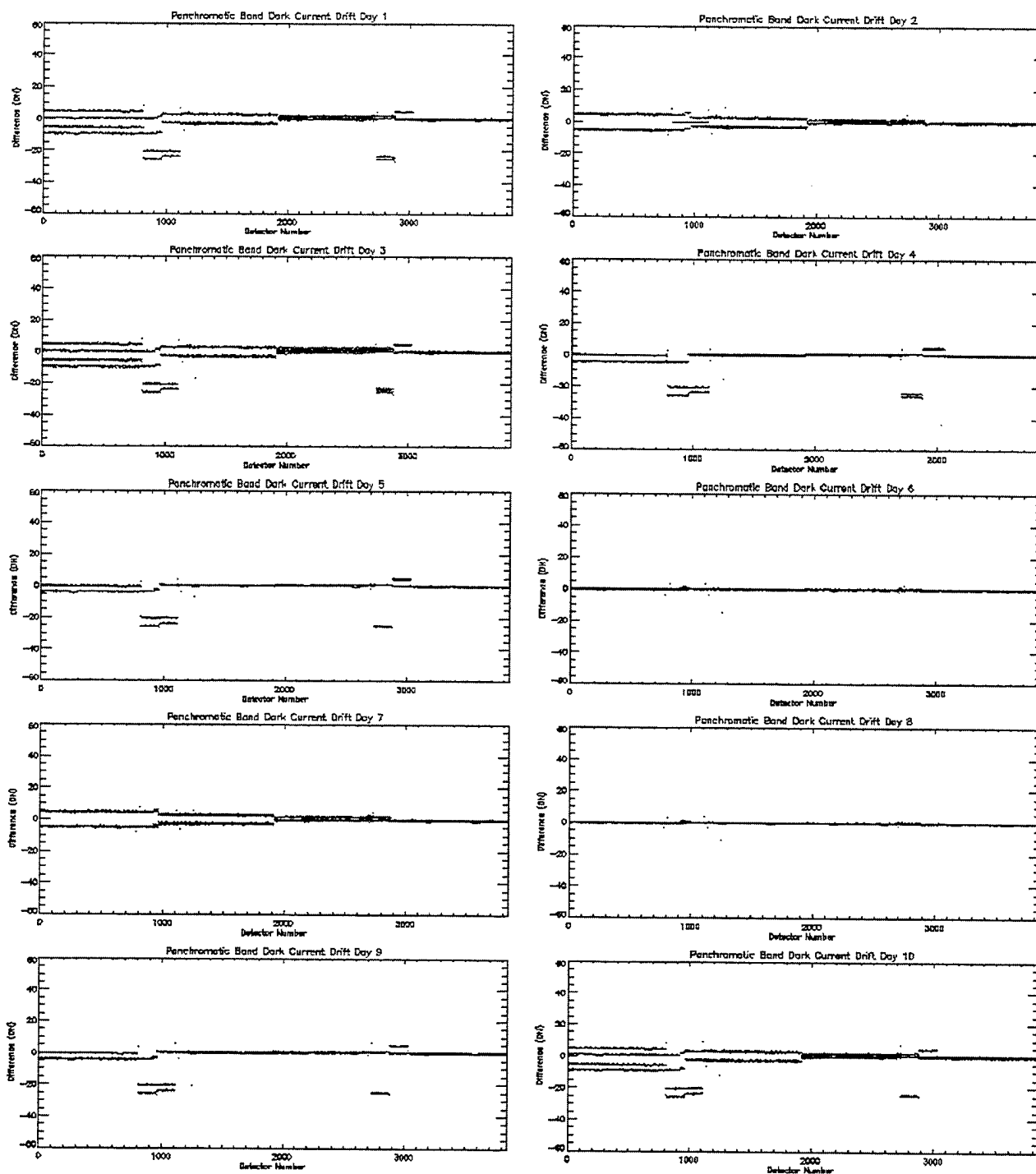


Figure 47. Dark current drifting for the panchromatic band over 10 day period after an on-orbit bakeout.

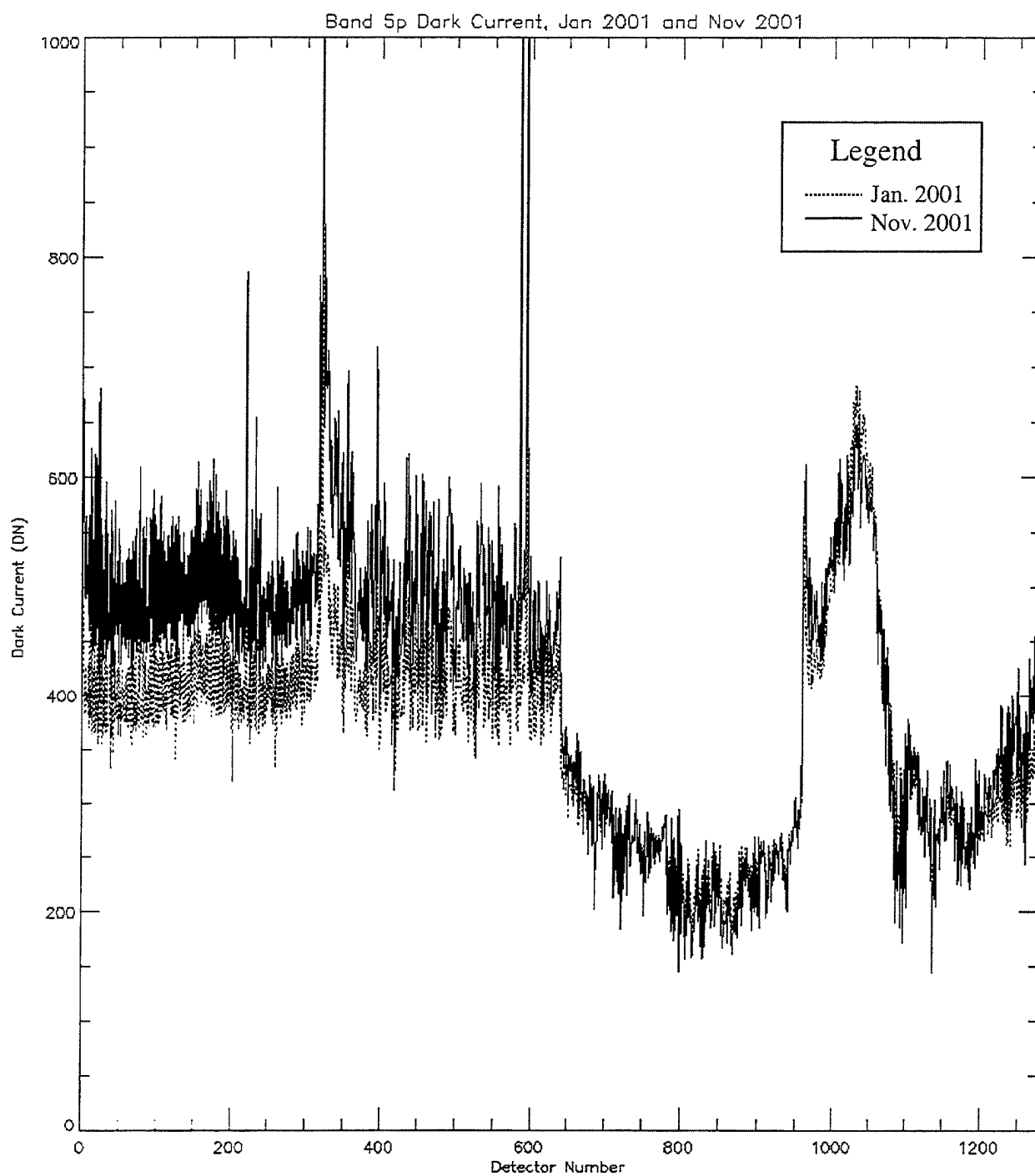


Figure 48. Dark current drifting for Band 5p between Jan. 2001 and Nov. 2001.



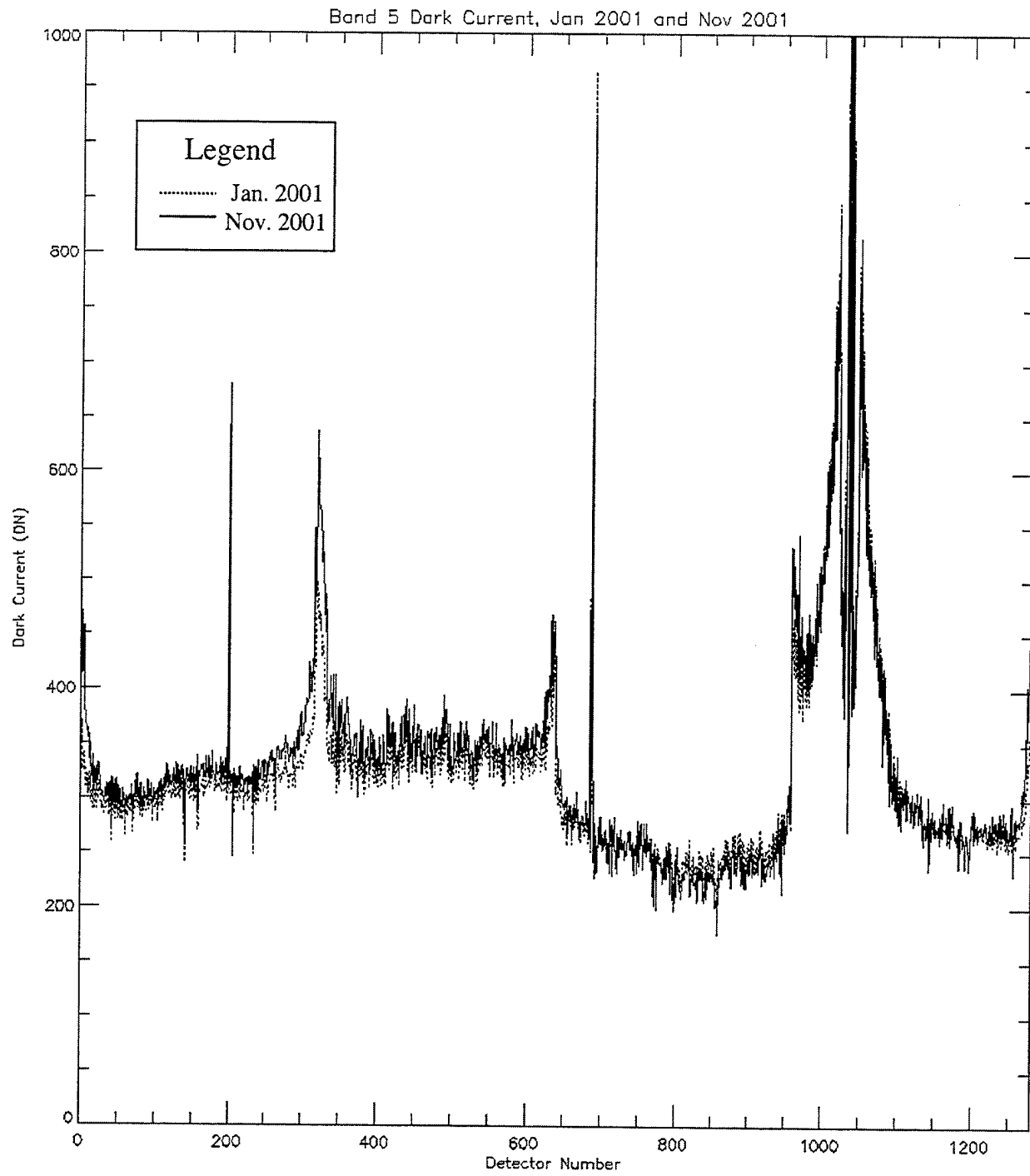


Figure 49. Dark current drifting for Band 5 between Jan. 2001 and Nov. 2001.

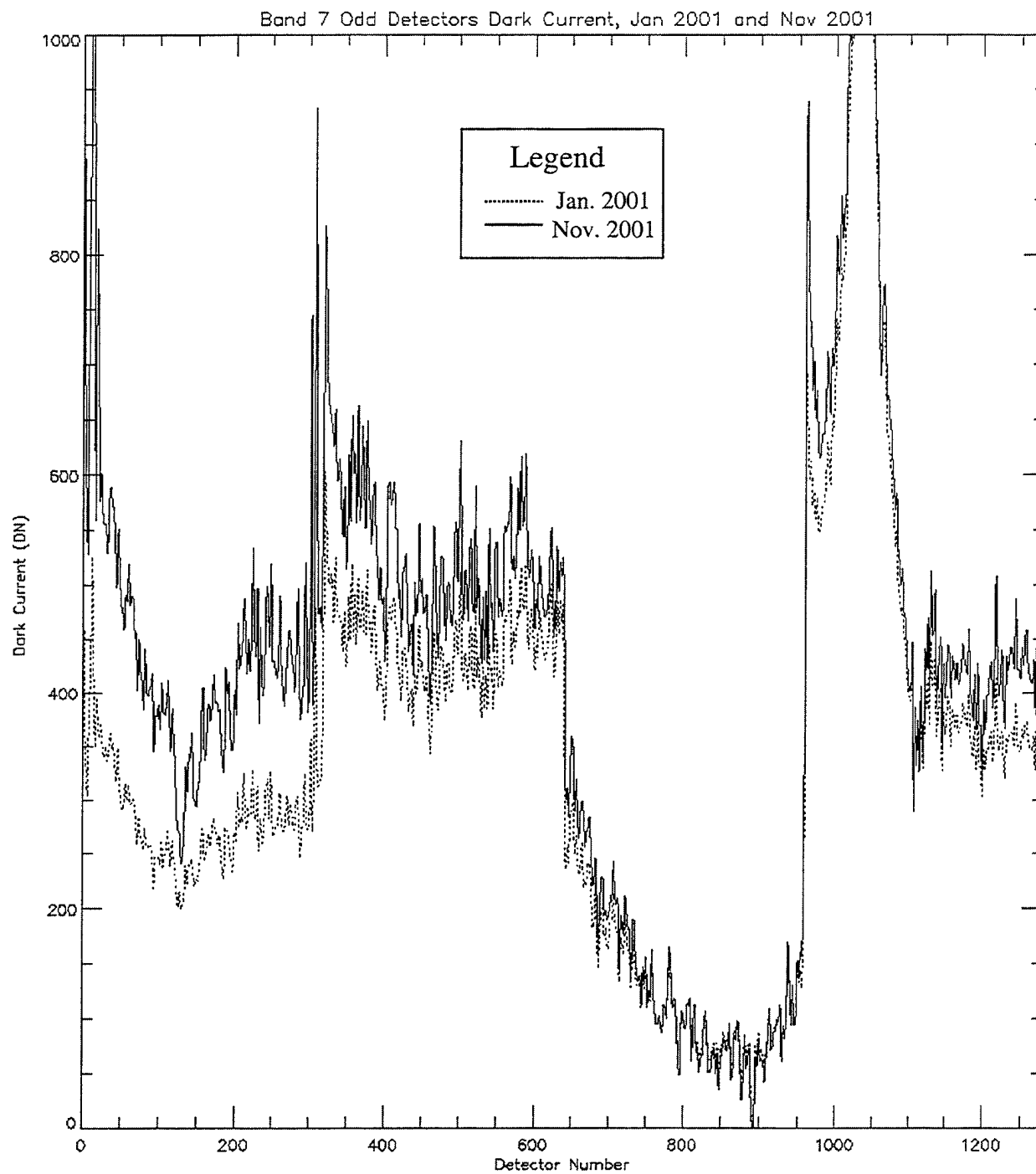
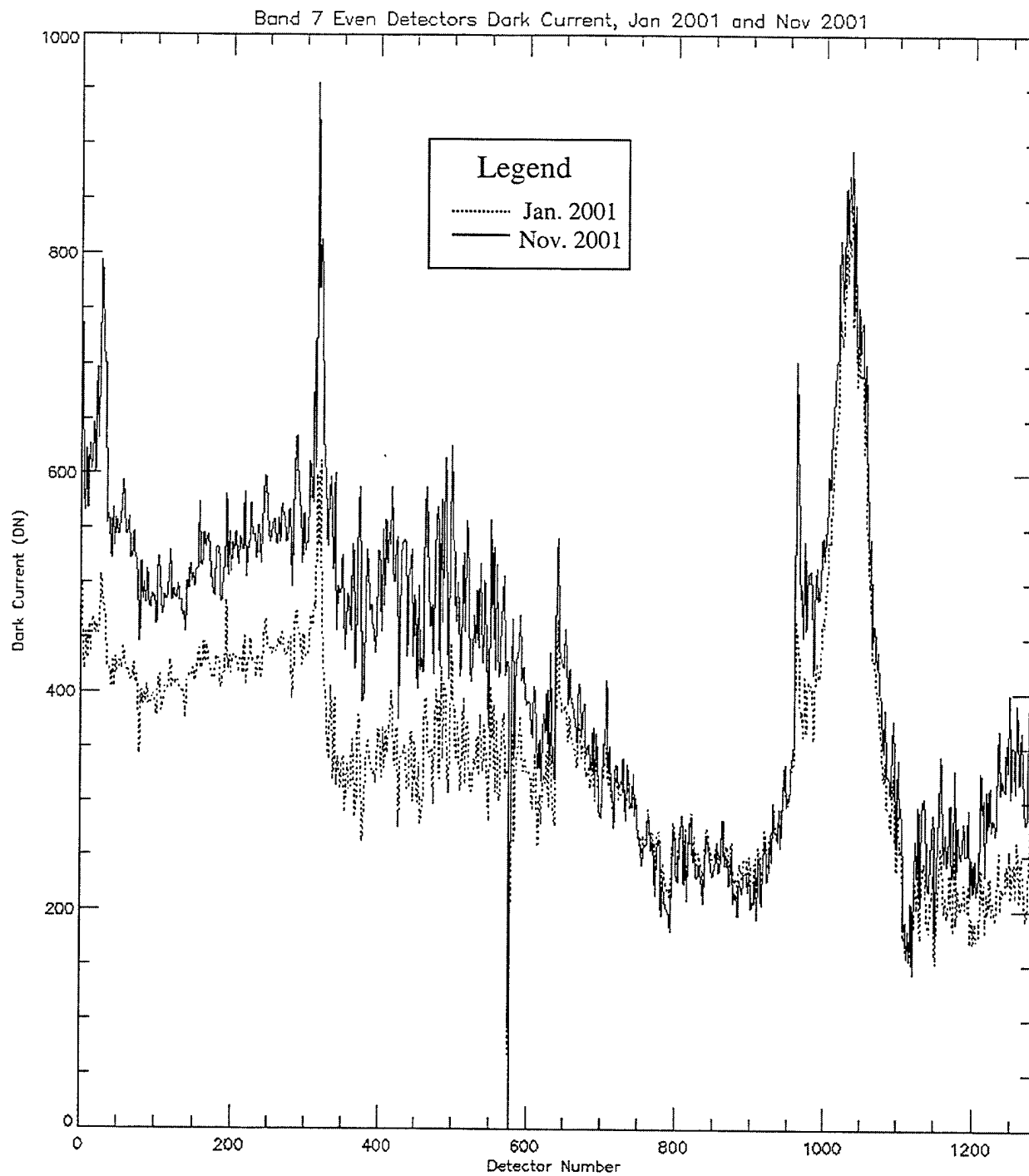


Figure 50. Dark current drifting for Band 7 odd detectors between Jan. 2001 and Nov. 2001.



*Figure 51. Dark current drifting for Band 7 even detectors between Jan. 2001 and Nov. 2001.*

### 3. NOISE

The noise of the Advanced Land Imager has also been trended using dark current data collected as a part of daily Earth scene observations. For each DCE, the data from the second dark period, after the image is collected, is used for the trending in this report. Noise trending is provided for each band and SCA. Noise levels been calculated as the mean of individual detector noise values.

#### 3.1 TRENDING

The results of the ALI focal plane noise trending are provided in Figures 52–71. For each band, two figures are provided. The top figure depicts the noise for each SCA as a function of mission day number. The lower figure is a scatter plot of dark current and noise values for the first year on orbit.

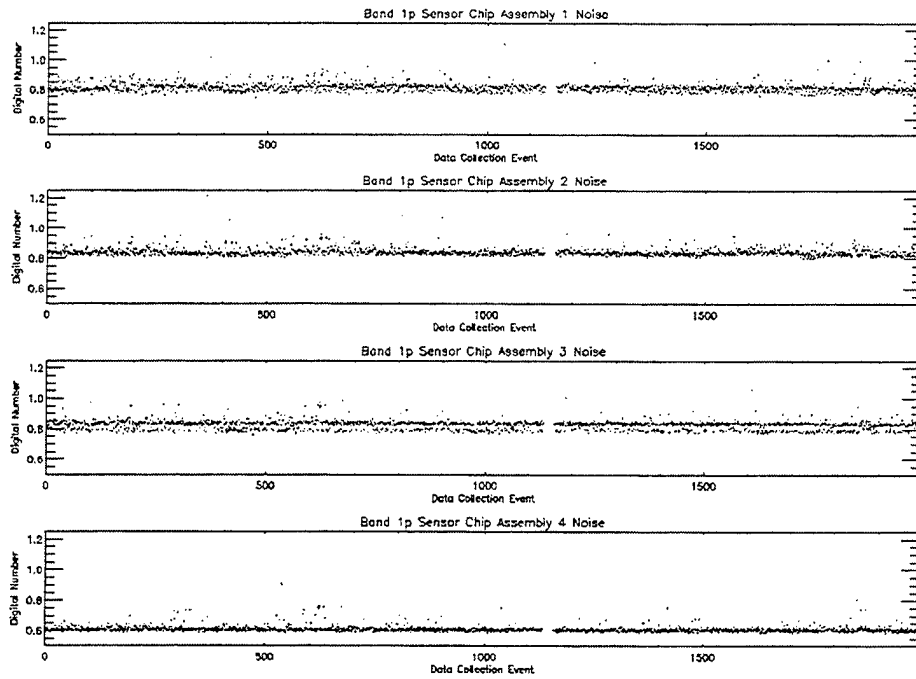


Figure 52. Noise trending for Band 1p.

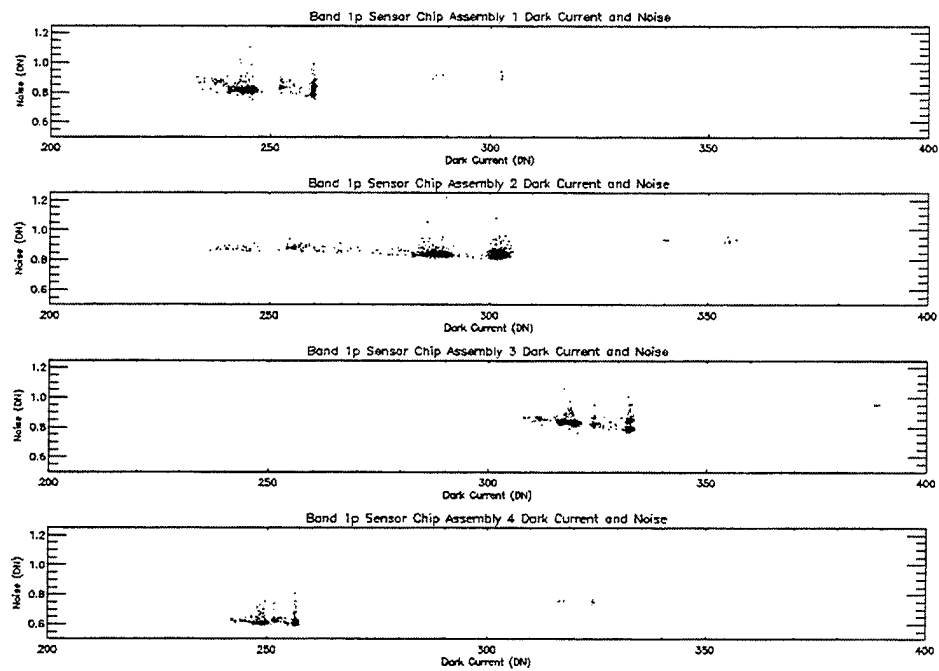


Figure 53. Dark current and noise scatter plot for Band 1p.

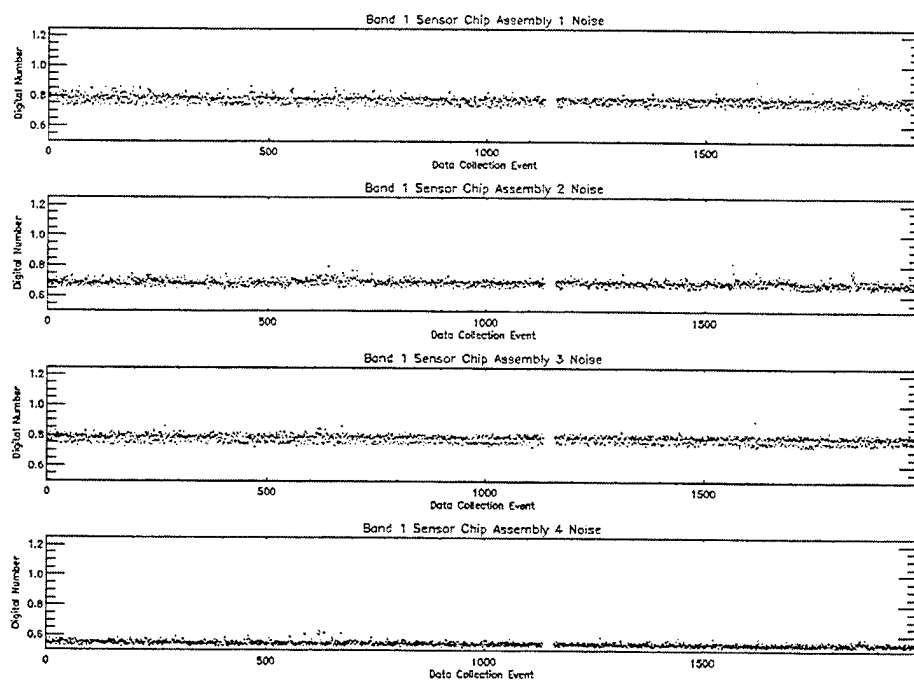


Figure 54. Noise trending for Band 1.

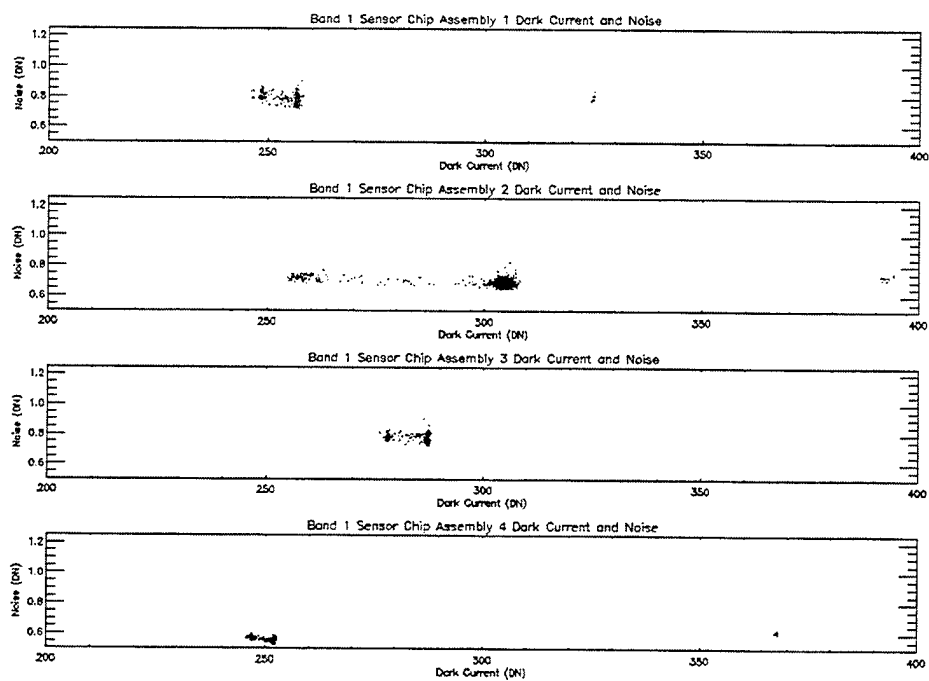


Figure 55. Dark current and noise scatter plot for Band 1.

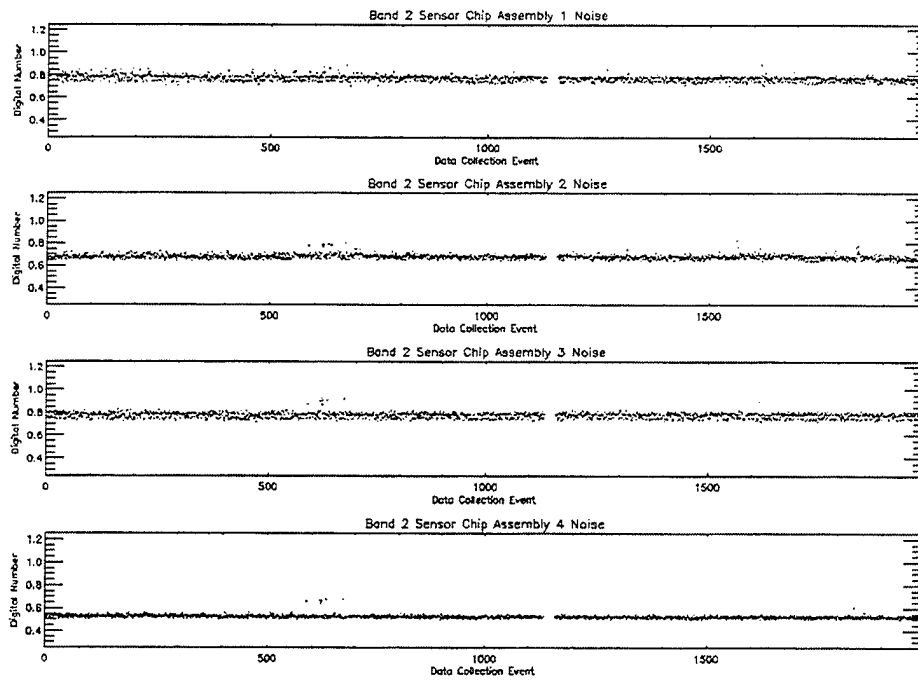


Figure 56. Noise trending for Band 2.

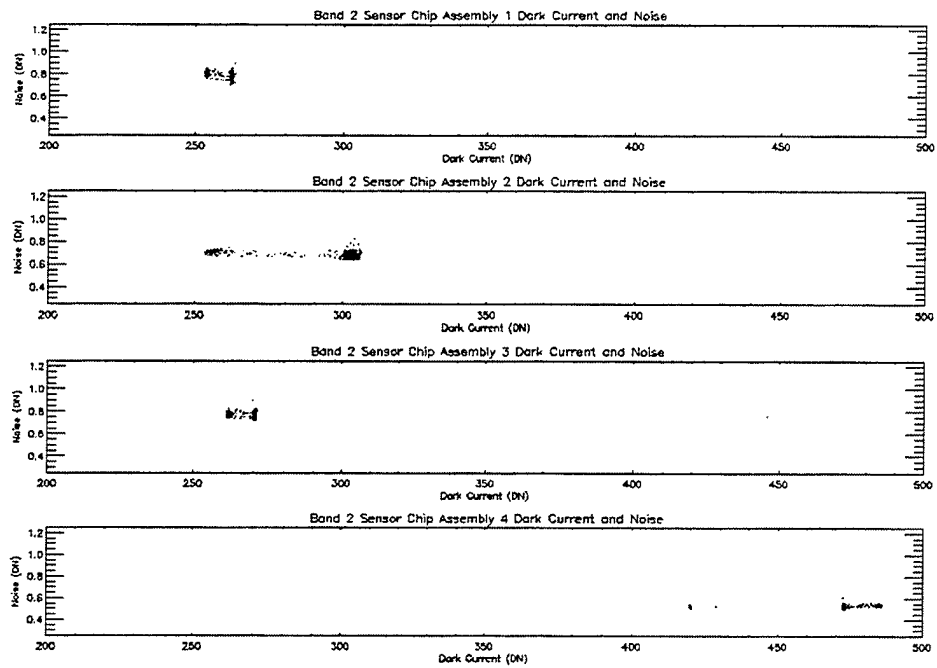


Figure 57. Dark current and noise scatter plot for Band 2.

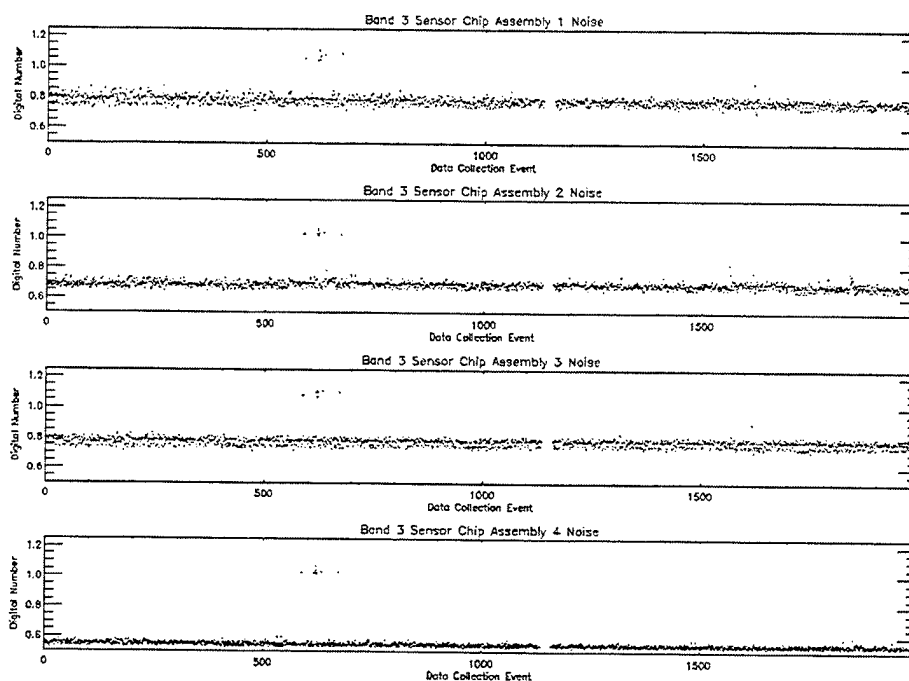


Figure 58. Noise trending for Band 3.

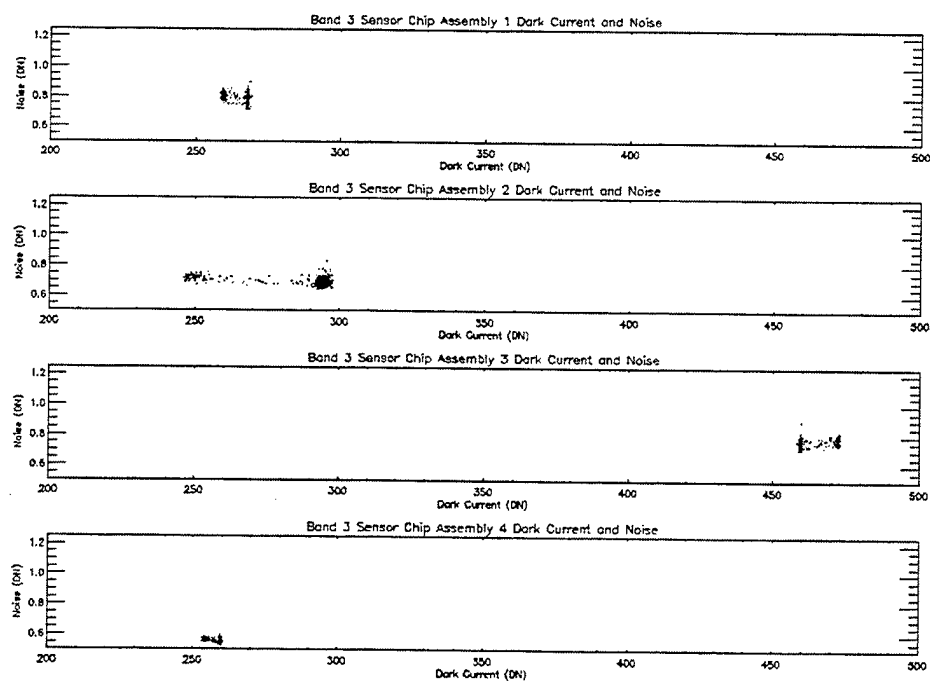


Figure 59. Dark current and noise scatter plot for Band 3.



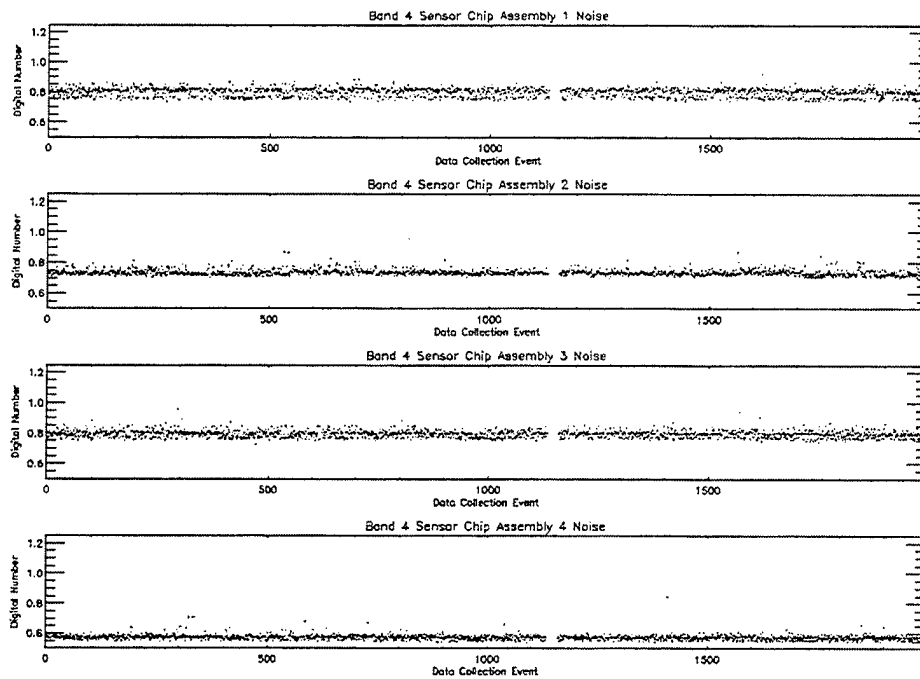


Figure 60. Noise trending for Band 4.

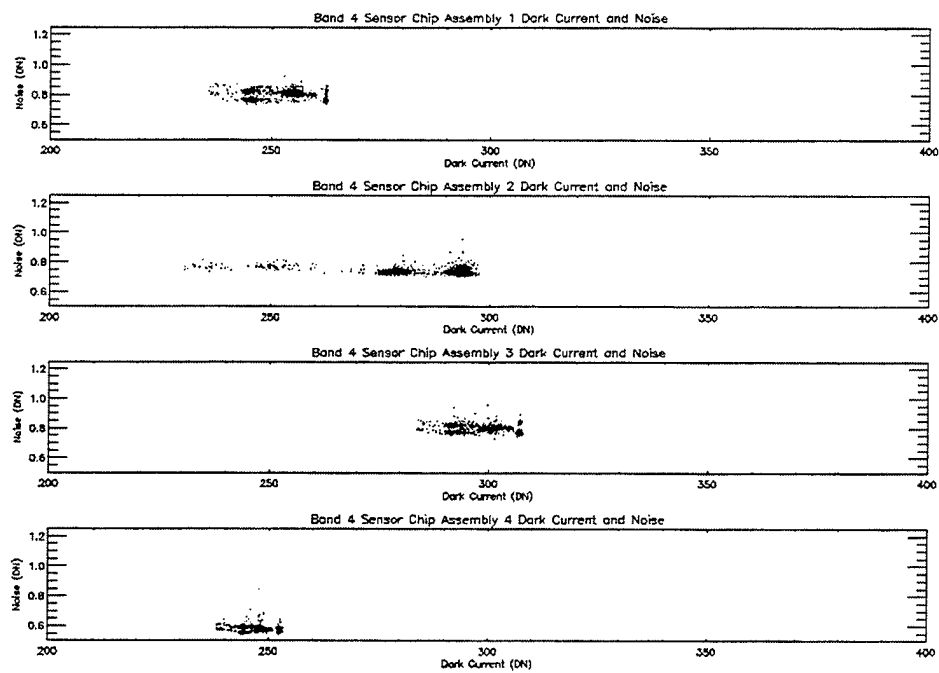


Figure 61. Dark current and noise scatter plot for Band 4.

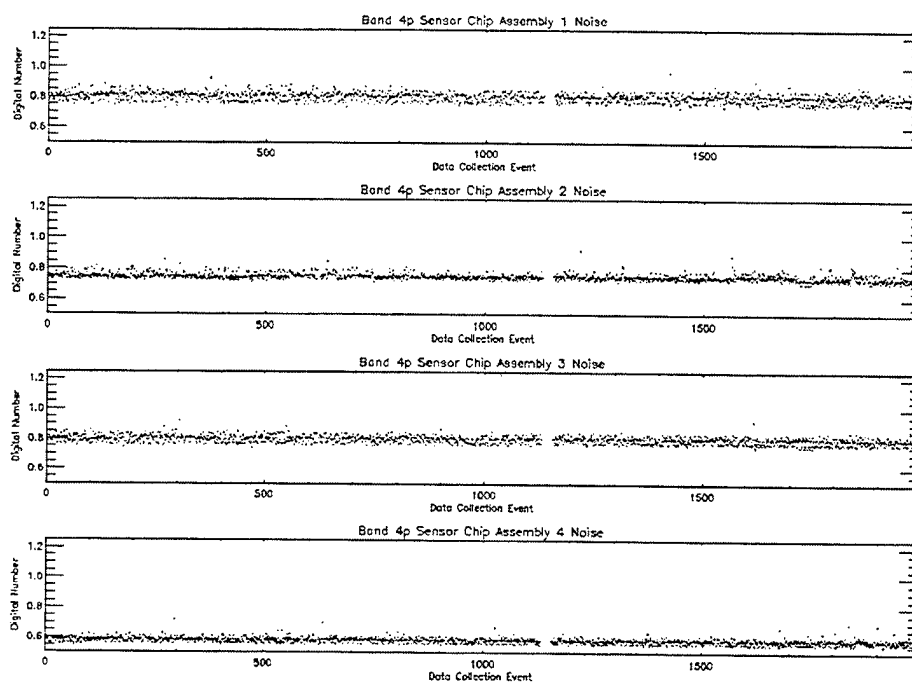


Figure 62. Noise trending for Band 4p.

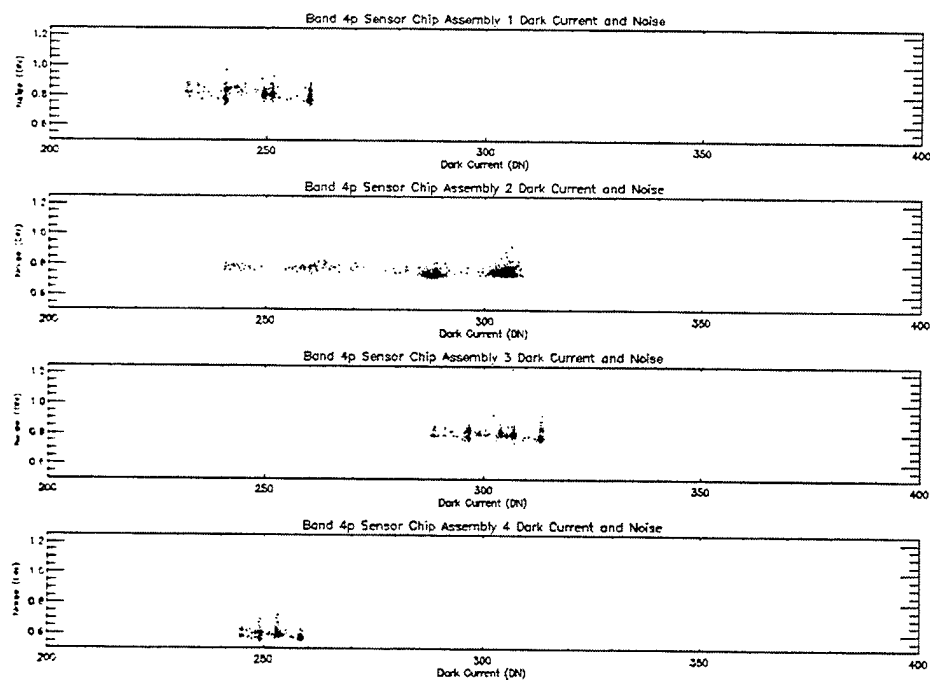


Figure 63. Dark current and noise scatter plot for Band 4p.

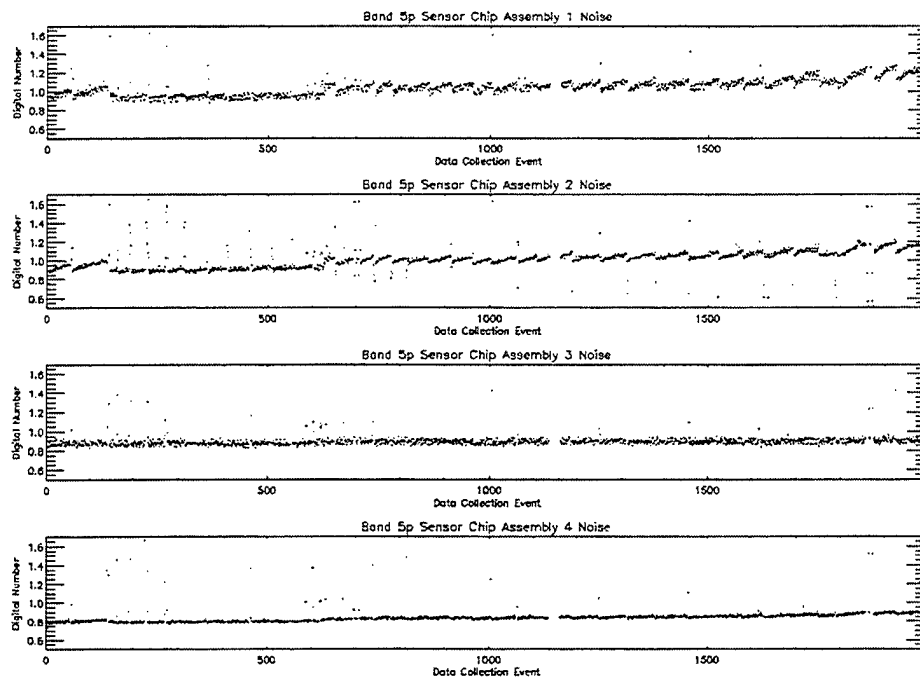


Figure 64. Noise trending for Band 5p.

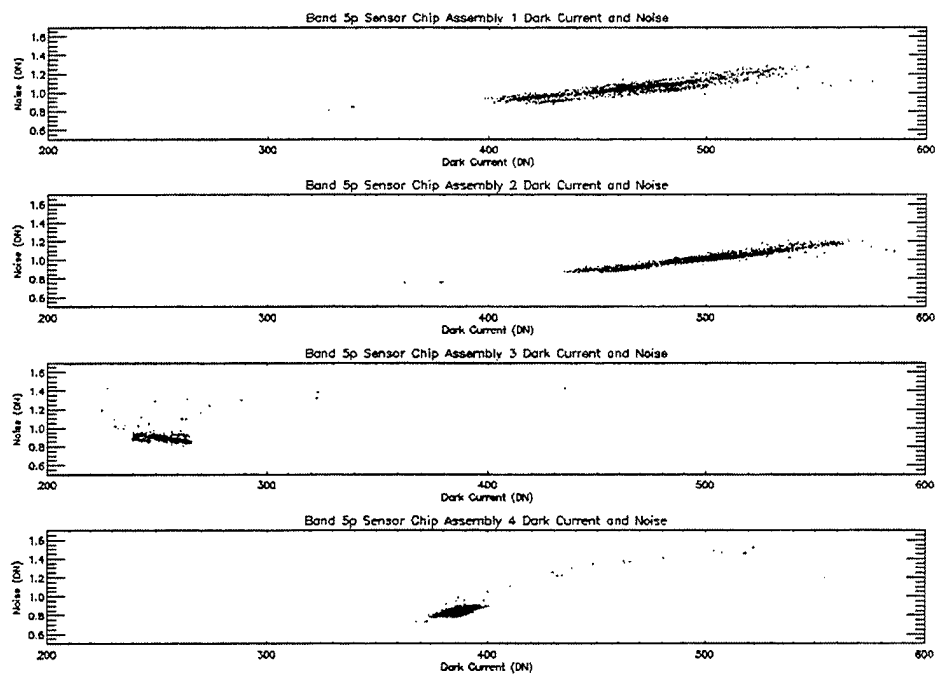


Figure 65. Dark current and noise scatter plot for Band 5p.

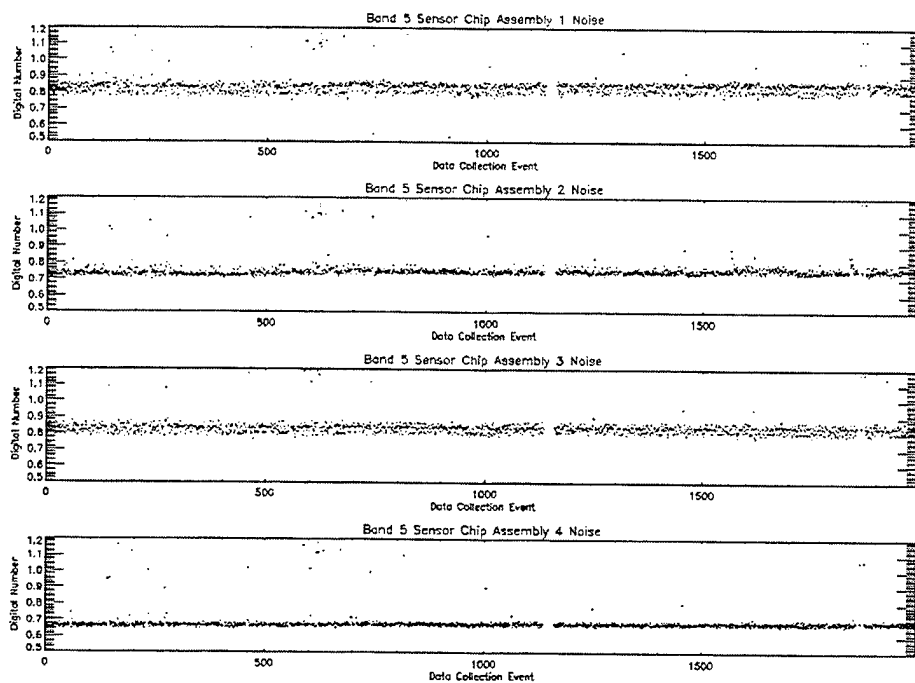


Figure 66. Noise trending for Band 5.

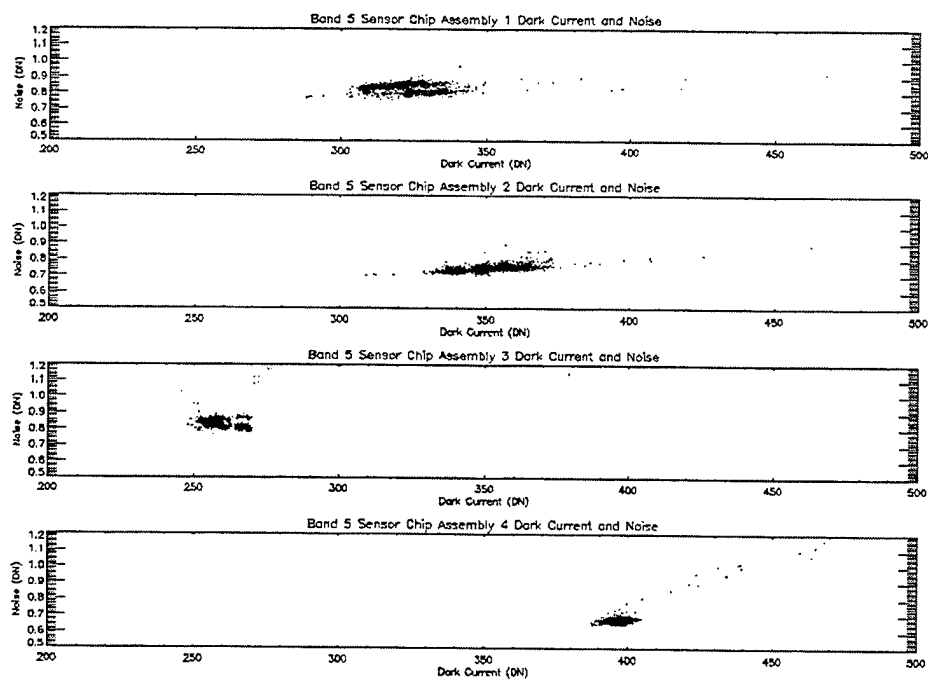


Figure 67. Dark current and noise scatter plot for Band 5.

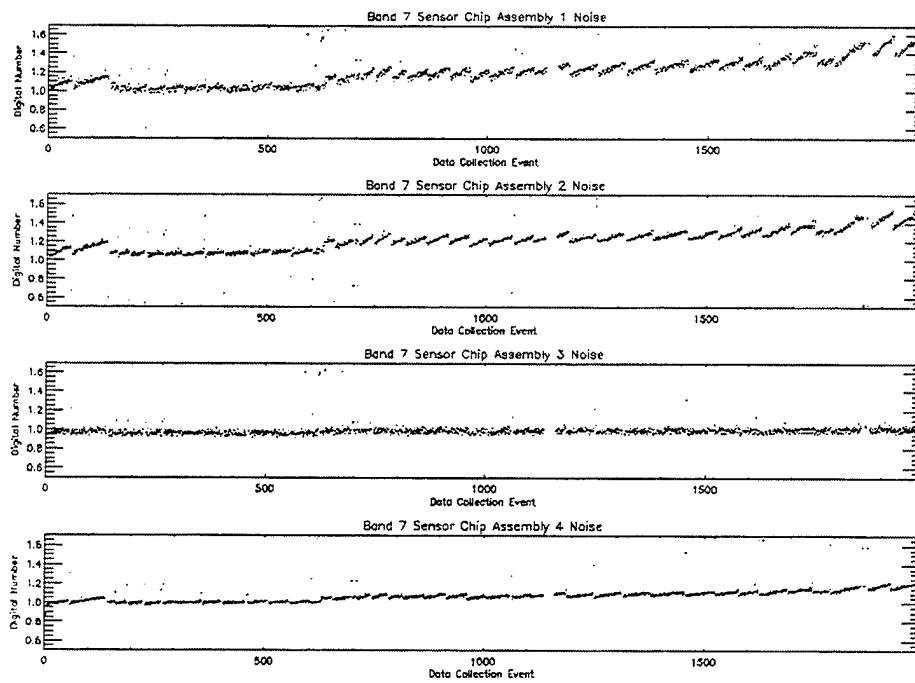


Figure 68. Noise trending for Band 7.

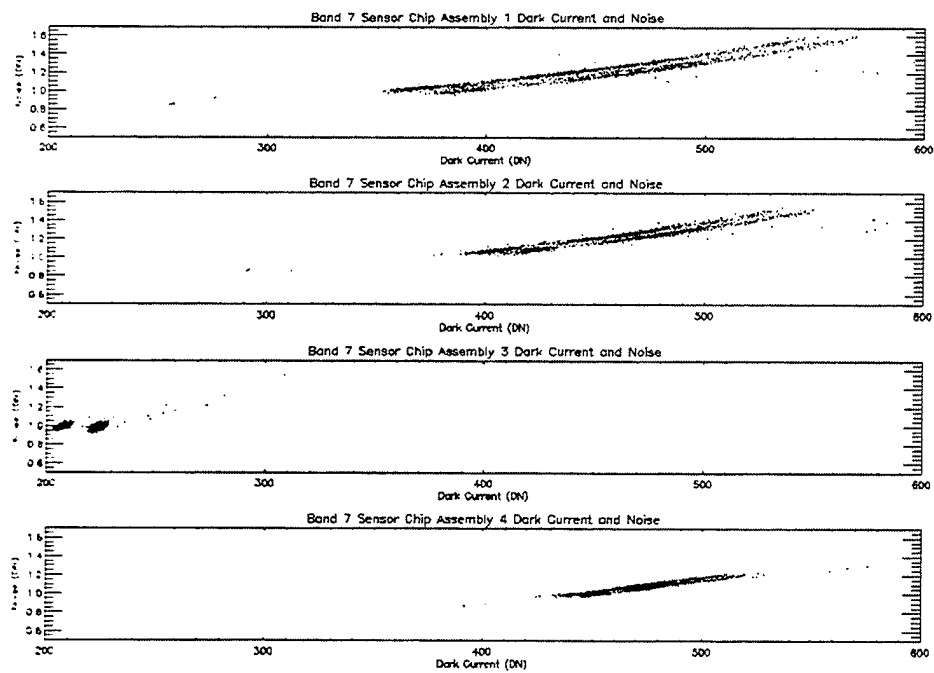


Figure 69. Dark current and noise scatter plot for Band 7.

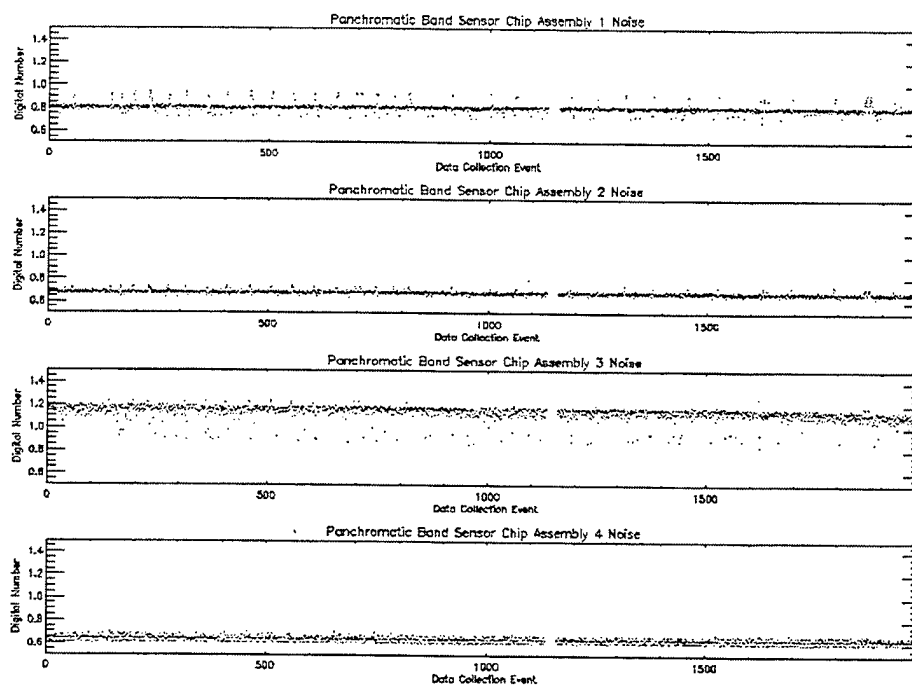


Figure 70. Noise trending for the Panchromatic Band.

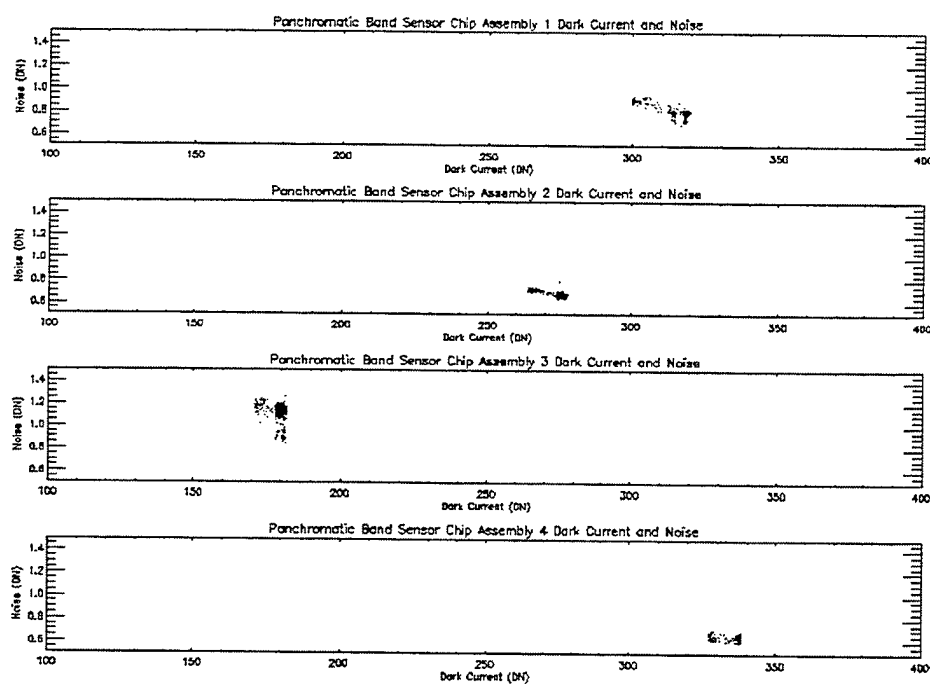


Figure 71. Dark current and noise scatter plot for the Panchromatic Band.

The apparent systematic increase in detector noise across several spectral bands for some particular DCEs is the result of focal plane outgassing performed at the times of those observations. All ALI detectors were heated to 270 K periodically during the first year on-orbit. This heating resulted in increased detector dark current and noise, particularly in the short wave infrared bands (5p, 5, 7).

The noise of the ALI VNIR and panchromatic arrays appears very stable since launch and remained below 1 DN for all bands. Additionally, the scatter plots confirm the different dark current states acquired by the focal plane have been very repeatable.

The noise of Band 5 appears to have remained below 1 DN during the first year, agreeing with the lack of substantial dark current increase during this period. However, the noise levels for SCAs 1 and 2 of Band 5p have tracked the increase in dark current over time in these detectors and have reached between 1.2 and 1.5 DN. Similarly, the noise for SCAs 1 and 2 of Band 7 have tracked rising dark current levels and have reached 1.6 DN. The tracking of dark current and noise in the SWIR bands is clearly evident in the associated scatter plots.

## 4. DISCUSSION

The dark current and noise trending of the ALI focal plane during the first year on orbit have provided insight into the day-to-day stability of the instrument. All data suggest the focal plane assumes between one and four dark current values when powered. Although the source of these multiple discrete values is not understood, their appearance in all the bands, those using Si detectors as well as those using HgCdTe detectors, suggests a likely origin in the FPA/FPE circuitry.

- Dark current and noise data also indicate the VNIR and panchromatic bands have been very stable and changed little during their first year of exposure to the space environment.

- The SWIR detectors of SCAs 1 and 2 of Bands 5p and 7 have shown some increase in dark current levels between bakeouts and over time. The source of this dark current increase is unclear. However, it is interesting to note that contamination build-up on the focal plane filters also appears to increase between bakeouts, only to return to baseline levels after the focal plane is again cooled. Although it is tempting to associate the contamination build-up with elevating dark current levels, reviewing the history of contamination on orbit does not support this hypothesis. First, the rate of Band 7 contamination build-up between bakeouts has decreased over time. If the contaminant was associated with rising dark current levels, one would expect the dark current rate of build-up to decrease over time as well. However, the rate of dark current build-up between bakeouts appears to be increasing with time. Second, long term contamination trending indicates Band 7 has been free of contamination since Day 300. However, the rate of dark current build-up over time appears to be increasing, suggesting it is not associated with contamination rates.

A dark current drift for some SWIR detectors between the first and second dark current reference periods has been observed. This has been attributed to heating of the focal plane by reflected sunlight and has implications on long-term data collection or multiple short-term observations. For nominal EO-1 DCEs, the second dark reference data can be used to effectively remove detector dark current bias. For longer scenes, the SWIR drift may become significant between the beginning and the end of the observation. In this case, interpolation of dark current levels may be required. Additionally, for multiple scenes acquired in sequence over the course of  $\frac{1}{2}$  orbit, intermittent dark reference periods with the cover closed are desirable to ensure proper dark current subtraction. Finally, the observed drift in SWIR dark current levels can be eliminated in future instruments if an active thermal control system, immune to noise, is implemented.

- A small number of detectors on each band of each SCA, covered with an opaque surface, would have been useful as dark current references. These detectors could have been used to track the dark current levels of the focal plane even during the Earth observing portion of a DCE. These detectors would be especially useful in the SWIR. However, the dark current stability of the ALI focal plane has proven non-uniform for these bands, particularly on the SCA level, and the placement of these detectors becomes important.



This report points out certain interesting properties of the ALI focal plane system. However, it is important to note that the system has been performing as it was intended and that the various minor artifacts identified here do not detract from the ability to produce well-calibrated ALI data.

## REFERENCES

1. D.E. Lencioni, C.J. Digenis, W.E. Bicknell, D.R. Hearn, and J.A. Mendenhall, "Design and Performance of the EO-1 Advanced Land Imager," *SPIE Conference on Sensors, Systems, and Next Generation Satellites III*, Florence, Italy, 20 September 1999.
2. J.A. Mendenhall et al., "Earth Observing-1 Advanced Land Imager: Instrument and Flight Operations Overview," MIT Lincoln Laboratory Project Report EO-1-1, 23 June 2000.
3. J.A. Mendenhall and M.D. Gibbs, "Earth Observing-1 Advanced Land Imager Flight Performance Assessment: Noise and Dark Current Trending for the First 60 Days," MIT Lincoln Laboratory Project Report EO-1-7, 1 June 2001.
4. J.A. Mendenhall, "Earth Observing-1 Advanced Land Imager: Dark Current and Noise Characterization and Anomalous Detectors," MIT Lincoln Laboratory Project Report EO-1-5, 7 May 2001.
5. J.A. Mendenhall, "Earth Observing-1 Advanced Land Imager Flight Performance Assessment: Investigating Dark Current Stability Over One-half Orbit Period During the First 60 Days," MIT Lincoln Laboratory Project Report EO-1-6, 1 July 2001.

REPORT DOCUMENTATION PAGE			Form Approved OMB No. 0704-0188	
Public reporting burden for this collection of information is estimated to average 1 hour per response, including the time for reviewing instructions, searching existing data sources, gathering and maintaining the data needed, and completing and reviewing the collection of information. Send comments regarding this burden estimate or any other aspect of this collection of information, including suggestions for reducing this burden, to Washington Headquarters Services, Directorate for Information Operations and Reports, 1215 Jefferson Davis Highway, Suite 1204, Arlington, VA 22202-4302, and to the Office of Management and Budget, Paperwork Reduction Project (0704-0188), Washington, DC 20503.				
1. AGENCY USE ONLY (Leave blank)	2. REPORT DATE 19 August 2002	3. REPORT TYPE AND DATES COVERED Project Report		
4. TITLE AND SUBTITLE  Earth Observing-1 Advanced Land Imager Flight Performance Assessment: Noise and Dark Current Stability During the First Year On Orbit		5. FUNDING NUMBERS  C—F19628-00-C-0002		
6. AUTHOR(S)  J.A. Mendenhall and M.D. Gibbs				
7. PERFORMING ORGANIZATION NAME(S) AND ADDRESS(ES)  Lincoln Laboratory, MIT 244 Wood Street Lexington, MA 02420-9108		8. PERFORMING ORGANIZATION REPORT NUMBER  PR-EO-1-11		
9. SPONSORING/MONITORING AGENCY NAME(S) AND ADDRESS(ES)  NASA/GSFC Mr. Ralph Welsh Building 16, Room 21 MS740.3 Greenbelt, MD 20771		10. SPONSORING/MONITORING AGENCY REPORT NUMBER  ESC-TR-2001-079		
11. SUPPLEMENTARY NOTES  None				
12a. DISTRIBUTION/AVAILABILITY STATEMENT  Approved for public release; distribution is unlimited.			12b. DISTRIBUTION CODE	
13. ABSTRACT (Maximum 200 words)  The noise and dark current stability of the Advanced Land Imager during the first year on orbit (November 21, 2000 – November 21, 2001) are presented. Data have been separated into short-term and long-term periods. The analysis of short-term data indicate some SWIR detectors may drift up to ten digital numbers between the pre and post dark observations of a given data collection event. Analysis of long-term data suggest the VNIR dark current has deviated by less than ten digital numbers and some SCA SWIR dark current have increased by up to 200 digital numbers during the first year on orbit.				
14. SUBJECT TERMS			15. NUMBER OF PAGES 78	
			16. PRICE CODE	
17. SECURITY CLASSIFICATION OF REPORT Unclassified	18. SECURITY CLASSIFICATION OF THIS PAGE Unclassified	19. SECURITY CLASSIFICATION OF ABSTRACT Unclassified	20. LIMITATION OF ABSTRACT Same as Report	